

Random Features for Kernel Approximation: A Survey on Algorithms, Theory, and Beyond

Fanghui Liu, Xiaolin Huang, Yudong Chen, Johan A.K. Suykens

Abstract—Random features is one of the most popular techniques to speed up kernel methods in large-scale problems. Related works have been recognized by the NeurIPS Test-of-Time award in 2017 and the ICML Best Paper Finalist in 2019. The body of work on random features has grown rapidly, and hence it is desirable to have a comprehensive overview on this topic explaining the connections among various algorithms and theoretical results. In this survey, we systematically review the work on random features from the past ten years. First, the motivations, characteristics and contributions of representative random features based algorithms are summarized according to their sampling schemes, learning procedures, variance reduction properties and how they exploit training data. Second, we review theoretical results that center around the following key question: how many random features are needed to ensure a high approximation quality or no loss in the empirical/expected risks of the learned estimator. Third, we provide a comprehensive evaluation of popular random features based algorithms on several large-scale benchmark datasets and discuss their approximation quality and prediction performance for classification. Last, we discuss the relationship between random features and modern over-parameterized deep neural networks (DNNs), including the use of random features in the analysis DNNs as well as the gaps between current theoretical and empirical results. This survey may serve as a gentle introduction to this topic, and as a users’ guide for practitioners interested in applying the representative algorithms and understanding theoretical results under various technical assumptions. We hope that this survey will facilitate discussion on the open problems in this topic, and more importantly, shed light on future research directions.

Index Terms—random features, kernel approximation, generalization properties, over-parameterized neural networks

1 INTRODUCTION

KERNEL methods [1], [2], [3] are one of the most powerful techniques for nonlinear statistical learning problems including classification [4], regression [5], dimension reduction [6], and clustering [7]. The basic idea of kernel methods is as follows. Let $\mathbf{x}, \mathbf{x}' \in \mathcal{X} \subseteq \mathbb{R}^d$ be two samples and $\phi : \mathcal{X} \rightarrow \mathcal{H}$ be a nonlinear feature map transforming each element in \mathcal{X} into a high-dimensional (or even infinite-dimensional) Reproducing Kernel Hilbert Space (RKHS) \mathcal{H} . The inner product between $\phi(\mathbf{x})$ and $\phi(\mathbf{x}')$ in the feature space \mathcal{H} can be computed using a kernel function $k(\cdot, \cdot) : \mathbb{R}^d \times \mathbb{R}^d \rightarrow \mathbb{R}$ as

$$\langle \phi(\mathbf{x}), \phi(\mathbf{x}') \rangle_{\mathcal{H}} = k(\mathbf{x}, \mathbf{x}').$$

In practice, this inner product is given by directly introducing the kernel k without finding the explicit expression of ϕ , which is known as the *kernel trick*. Albeit effective for learning nonlinear structures, kernel methods often suffer from scalability issues in large-scale problems due to high space and time complexities.

This work was supported in part by the European Research Council under the European Union’s Horizon 2020 research and innovation program / ERC Advanced Grant E-DUALITY (787960), in part by the National Natural Science Foundation of China 61977046, in part by the National Key Research and Development Project (No. 2018AAA0100702), in part by National Science Foundation grants CCF-1657420 and CCF-1704828, and in part by SJTU Global Strategic Partnership Fund (2020 SJTU-CORNELL). This paper reflects only the authors’ views and the Union is not liable for any use that may be made of the contained information; Research Council KUL C14/18/068; Flemish Government FWO project GOA4917N; Onderzoeksprogramma Artificiële Intelligentie (AI) Vlaanderen programme.

F. Liu and J.A.K. Suykens are with the Department of Electrical Engineering (ESAT-STADIUS), KU Leuven, B-3001 Leuven, Belgium (email: \{fanghui.liu;johan.suykens\}@esat.kuleuven.be).

X. Huang is with Institute of Image Processing and Pattern Recognition, and also with Institute of Medical Robotics, Shanghai Jiao Tong University, Shanghai 200240, P.R. China (e-mail: xiaolinhuang@sjtu.edu.cn).

Y. Chen is with School of Operations Research and Information Engineering, Cornell University, Ithaca, NY 14850 USA (e-mail: yudong.chen@cornell.edu).

For instance, given n samples in the original d -dimensional space \mathcal{X} , kernel ridge regression (KRR) requires $\mathcal{O}(n^3)$ training time and $\mathcal{O}(n^2)$ space to store the kernel matrix, which is often computationally infeasible when n is large.

To overcome the poor scalability of kernel methods, a series of kernel approximation algorithms have been developed in the past years. A straightforward way is using a divide-and-conquer approach [8], [9], which decomposes the original problem into several smaller sub-problems for more efficient computation. Another representative class of methods compute a low-rank approximation of the kernel matrix, e.g., by random projection; examples include greedy basis selection techniques [10] and Nyström methods [11]. These methods give a data dependent vector representation of the kernel. Random Fourier features (RFF) [12], on the other hand, is a typical data-independent technique to approximate the kernel function using an explicit feature mapping. The work in [13], [14] provides a comparison between Nyström methods and RFF in terms of the construction of approximate functional spaces, eigenvalues of kernel matrices, generalization error bounds, and the final prediction performance potentially with a memory limit.

This survey focuses on RFF [12] and its variants for kernel approximation. RFF applies in particular to shift-invariant (also called “stationary”) kernels that satisfy $k(\mathbf{x}, \mathbf{x}') = k(\mathbf{x} - \mathbf{x}')$. By virtue of the correspondence between a shift-invariant kernel and its Fourier spectral density, the kernel can be approximated by $k(\mathbf{x}, \mathbf{x}') \approx \langle \varphi(\mathbf{x}), \varphi(\mathbf{x}') \rangle$, where the random Fourier feature mapping $\varphi : \mathbb{R}^d \rightarrow \mathbb{R}^s$ is obtained by sampling from a distribution defined by the inverse Fourier transform of k . The number s of random features is generally taken to be larger than the original sample dimension d but much smaller than the sample size n . This approximation strategy hence allows one to train an efficient linear predictor in the transformed space \mathbb{R}^s while retaining the

power of nonlinear kernel methods. In particular, with s random features, this approach applied to KRR only requires $\mathcal{O}(ns^2)$ time and $\mathcal{O}(ns)$ memory, thus achieving a substantial computational saving when $s \ll n$. Indeed, RFF exhibits promising performance for scaling up kernel methods in problems including support vector machines (SVM) [15], regression [16], and nonlinear component analysis [17], [18].

Interestingly, the random features model can be viewed as a class of two-layer neural networks with fixed weights in the first layer. This connection has important theoretical and algorithmic implications. On the one hand, in the *over-parameterized* regime with $s \geq n$, it has been observed that these neural networks exhibit certain intriguing phenomena such as the ability to fit random labels [19] and double descent curves [20]. Theoretical results for random features can be leveraged to explain these phenomena and provide an analysis of two-layer *over-parameterized* neural networks. On the other hand, random features methods may serve as a practical and effective way for implementing the neural tangent kernel (NTK) [21] associated with an infinite wide neural network. Besides, network pruning (as manifested in the lottery ticket hypothesis [22]) can also benefit from the use of random features. Hence, random features is a powerful tool for understanding and improving over-parameterized neural networks [23], [24], [25], [26]. Partly due to its far-reaching repercussions, the seminal work by Rahimi and Recht on RFF [12] won the Test-of-Time Award in the *Thirty-first Advances in Neural Information Processing Systems* (NeurIPS 2017).

RFF spawns a new direction for kernel approximation, and the past ten years has witnessed a flurry of research papers devoted to this topic. On the algorithmic side, subsequent work has focused on improving the kernel approximation quality [36], [52], the time and space complexities [40], [41], and the prediction performance [15], [16], [53]. Implementation of RFF has in fact been taken to the hardware level [54], [55]. On the theoretical side, a series of works aim to address the following two key questions:

- 1) **Approximation:** how many random features are needed to ensure high quality of kernel approximation?
- 2) **Generalization:** how many random features are needed to incur no loss in the empirical risk and expected risk of a learned estimator?

Here “no loss” means achieving a level of performance comparable to an estimator with the exact kernel. For example, considering KRR with an exact kernel as the baseline, one is interested in how large s should be for KRR equipped with s random features to be almost as good as the exact KRR estimator. Much research effort has been devoted to this direction, including analyzing the kernel approximation error (the first question above) [12], [45], and studying the risk and generalization properties (the second question above) [15], [16]. Increasingly refined and general results have been obtained over the years. In the *Thirty-sixth International Conference on Machine Learning* (ICML 2019), Li et al. [16] were recognized by the Honorable Mentions (best paper finalist) for their unified theoretical analysis of RFF.

RFF has proved effective in a broad range of machine learning tasks. Given its remarkable empirical success and the rapid growth of the related literature, we believe it is desirable to have a comprehensive overview on this topic summarizing the progress in algorithm design and applications, and elucidating existing theoretical results and their underlying assumptions. With this goal in mind, in this survey we systematically review the work from the past ten years on the algorithms, theory and applications of random

features methods. Figure 1 gives a schematic overview of the history of the work on random features in recent years, highlighting the differences in existing work in terms of the sampling scheme, learning procedure, use of training data, underlying assumptions, and asymptotic properties.

The main contributions of this survey include:

- 1) We provide an overview of a wide range of random features based algorithms under a unifying framework.
- 2) We summarize existing theoretical results on the kernel approximation error measured in various metrics, as well as results on the empirical risk and generalization risk of kernel estimators. The underlying assumptions in these results are discussed in details.
- 3) We systematically evaluate and compare the empirical performance of representative random features based algorithms under different experimental settings.
- 4) We discuss recent research trends on the connection between random features and over-parameterized neural networks as well as the gaps in existing theoretical analysis. We view this topic as a promising research direction.

The remainder of this paper is organized as follows. In Section 2, after presenting the preliminaries, we provide a taxonomy of random features based algorithms. We review *data-independent* algorithms in Section 3 and *data-dependent* approaches in Section 4. In Section 5, we survey existing theoretical results on kernel approximation and generalization performance. Experimental comparisons of representative random features based methods are given in Section 6. In Section 7, we discuss recent results on the connection between random features and over-parameterized neural networks. The paper is concluded in Section 8 with a discussion on future directions.

2 PRELIMINARIES AND TAXONOMIES

In this section, we introduce the problem setting, the commonly used kernels in random features, and the associated theoretical foundation. We then present a taxonomy of existing random features based algorithms, which sets the stage for the subsequent discussion.

2.1 Notation

We denote vectors using boldface lowercase letters, e.g., \mathbf{a} , and matrices using boldface capital letters, e.g., \mathbf{A} , of which the elements are a_i and A_{ij} , respectively. Sets are denoted by script letters, e.g., \mathcal{A} . The shorthand $[n]$ is used for the set $\{1, 2, \dots, n\}$. Denote by \mathbf{I}_n the $n \times n$ identity matrix, $\mathbf{0}$ the zero matrix or vector with appropriate size, and $\mathbf{1}_n$ the n -dimensional vector of all ones. The unit sphere in the d -dimensional Euclidean space is denoted by $\mathbb{S}^{d-1} := \{\mathbf{x} \in \mathbb{R}^d : \|\mathbf{x}\|_2 = 1\}$.

2.2 Problem settings

Consider the following standard supervised learning setup. Let $\mathcal{X} \subset \mathbb{R}^d$ be a compact metric space of samples, and $\mathcal{Y} = \{-1, 1\}$ (in classification) or $\mathcal{Y} \subseteq \mathbb{R}$ (in regression) be the label space. We assume that a sample set $\{\mathbf{z}_i = (\mathbf{x}_i, y_i)\}_{i=1}^n$ is drawn from a non-degenerate Borel probability measure ρ on $\mathcal{X} \times \mathcal{Y}$. Let \mathcal{H} be a Reproducing Kernel Hilbert Space endowed with a positive definite kernel function $k(\cdot, \cdot)$, and $\mathbf{K} = [k(\mathbf{x}_i, \mathbf{x}_j)]_{i,j=1}^n$ be the kernel matrix associated with the samples. The *target function* of ρ is defined as $f_\rho(\mathbf{x}) = \int_{\mathcal{Y}} y d\rho(y|\mathbf{x})$ for $\mathbf{x} \in \mathcal{X}$, where

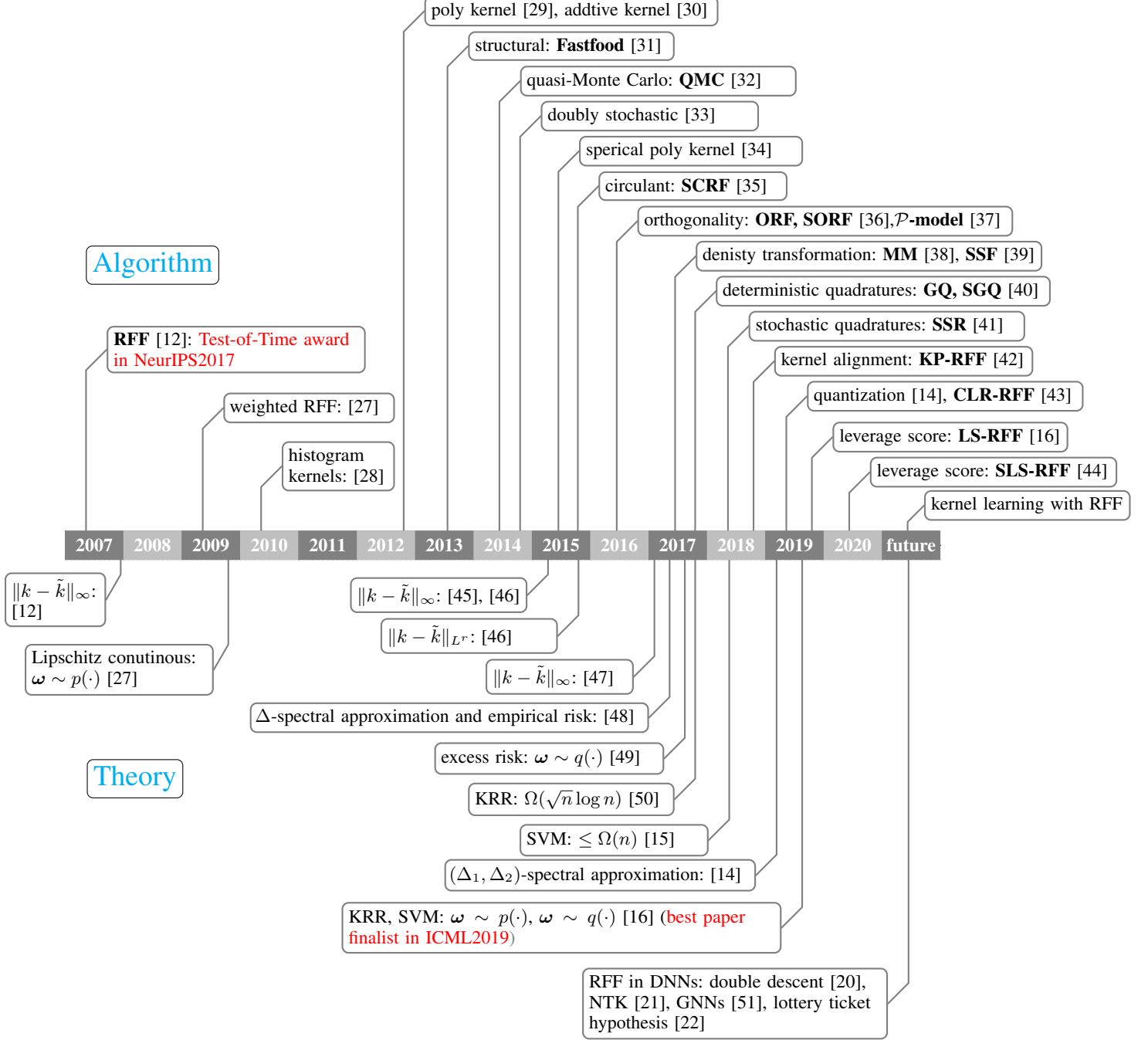


Figure 1. Timeline of representative work on the algorithms and theory of random features.

$\rho(\cdot|\mathbf{x})$ is the conditional distribution of y given \mathbf{x} . We consider the functional empirical risk minimization problem regularized by the norm associated with the RKHS \mathcal{H} :

$$f_{\mathbf{z}, \lambda} := \operatorname{argmin}_{f \in \mathcal{H}} \left\{ \frac{1}{n} \sum_{i=1}^n \ell(y_i, f(\mathbf{x}_i)) + \lambda \|f\|_{\mathcal{H}}^2 \right\}, \quad (1)$$

where $\ell : \mathcal{Y} \times \mathcal{Y} \rightarrow \mathbb{R}$ is a loss function and $\lambda \equiv \lambda(n) > 0$ is a regularization parameter that may depend on the sample size. Typically one assumes that $\lim_{n \rightarrow \infty} \lambda(n) = 0$ and adopts the scaling $\lambda = n^{-\alpha}$ with $\alpha \in (0, 1]$, as suggested by standard learning theory. Different choices for λ may lead to different convergence rates of generalization error. For example, Li et al. [16] choose $\lambda := n^{-1/2}$ in KRR and $\lambda := 1/n$ in SVM,

which achieves an $\mathcal{O}(n^{-1/2})$ learning rate. We will detail this in Section 5.

The loss $\ell(y, f(\mathbf{x}))$ measures the quality of the prediction $f(\mathbf{x})$ at $\mathbf{x} \in \mathcal{X}$ with respect to the observed response y . Popular choices of ℓ include the squared loss $\ell(y, f(\mathbf{x})) = (y - f(\mathbf{x}))^2$ in KRR and the hinge loss $\ell(y, f(\mathbf{x})) = \max(0, 1 - yf(\mathbf{x}))$ in SVM, etc. For a given ℓ , the empirical risk functional on the sample set is defined as $\mathcal{E}_{\mathbf{z}}(f) = \frac{1}{n} \sum_{i=1}^n \ell(y_i, f(\mathbf{x}_i))$, and the corresponding expected risk is defined as $\mathcal{E}(f) = \int_{\mathcal{X} \times \mathcal{Y}} \ell(y, f(\mathbf{x})) d\rho$. The statistical theory of supervised learning aims to understand the generalization property of $f_{\mathbf{z}, \lambda}$ as an approximation of the true target function f_ρ , which can be quantified by the excess risk $\mathcal{E}(f_{\mathbf{z}, \lambda}) - \mathcal{E}(f_\rho)$, or the estimation error $\|f_{\mathbf{z}, \lambda} - f_\rho\|^2$ in an

appropriate norm $\|\cdot\|$.

Using an explicit randomized feature mapping $\varphi : \mathbb{R}^d \rightarrow \mathbb{R}^s$, one may approximate the kernel function $k(\mathbf{x}, \mathbf{x}')$ by $\tilde{k}(\mathbf{x}, \mathbf{x}') = \langle \varphi(\mathbf{x}), \varphi(\mathbf{x}') \rangle$. In this case, the approximate kernel $\tilde{k}(\cdot, \cdot)$ defines an RKHS $\tilde{\mathcal{H}}$ (not necessarily contained in the RKHS \mathcal{H} associated with the original kernel function k). With the above approximation, one solves the following approximate version of problem (1):

$$\widetilde{f}_{\mathbf{z}, \lambda} := \operatorname{argmin}_{f \in \tilde{\mathcal{H}}} \left\{ \frac{1}{n} \sum_{i=1}^n \ell(y_i, f(\mathbf{x}_i)) + \lambda \|f\|_{\tilde{\mathcal{H}}}^2 \right\}. \quad (2)$$

By virtue of the Representer Theorem [1], the above problem can be rewritten as a finite-dimensional empirical risk minimization problem. For example, in least squares regression where ℓ is the squared loss, problem (2) is equivalent to

$$\beta_\lambda := \operatorname{argmin}_{\beta \in \mathbb{R}^s} \frac{1}{n} \|\mathbf{y} - \mathbf{Z}\beta\|_2^2 + \lambda \|\beta\|_2^2, \quad (3)$$

where $\mathbf{y} = [y_1, y_2, \dots, y_n]^\top$ is the label vector and $\mathbf{Z} = [\varphi(\mathbf{x}_1), \dots, \varphi(\mathbf{x}_n)]^\top \in \mathbb{R}^{n \times s}$ is the random feature matrix. Problem (3) is a linear ridge regression problem in the space spanned by the random features, with the optimal prediction given by $f_{\mathbf{z}, \lambda}(\mathbf{x}') = \beta_\lambda^\top \varphi(\mathbf{x}')$ for a new data point \mathbf{x}' , where β_λ has the explicit expression $\beta_\lambda = (\mathbf{Z}^\top \mathbf{Z} + n\lambda \mathbf{I})^{-1} \mathbf{Z}^\top \mathbf{y}$. Note that problem (3) also corresponds to fixed-size kernel methods with feature map approximation (related to Nyström approximation) and estimation in the primal [2].

2.3 Commonly used kernels

Random features based algorithms often consider the following kernels:

i) Gaussian kernel: Arguably the most important member of shift-invariant kernels, the Gaussian kernel is given by

$$k(\mathbf{x}, \mathbf{x}') = \exp \left(-\frac{\|\mathbf{x} - \mathbf{x}'\|_2^2}{2\sigma^2} \right),$$

where $\sigma > 0$ is the kernel width. The density (see Theorem 1) associated with the Gaussian kernel is Gaussian $\omega \sim \mathcal{N}(0, \sigma^{-2} \mathbf{I}_d)$.

ii) arc-cosine kernels: These kernels are rotation-invariant but not shift-invariant. Following [56], we define the b -order arc-cosine kernel by

$$k(\mathbf{x}, \mathbf{x}') = \frac{1}{\pi} \|\mathbf{x}\|_2^b \|\mathbf{x}'\|_2^b J_b(\theta),$$

where $\theta = \cos^{-1} \left(\frac{\mathbf{x}^\top \mathbf{x}'}{\|\mathbf{x}\|_2 \|\mathbf{x}'\|_2} \right)$ and

$$J_b(\theta) = (-1)^b (\sin \theta)^{2b+1} \left(\frac{1}{\sin \theta} \frac{\partial}{\partial \theta} \right)^b \left(\frac{\pi - \theta}{\sin \theta} \right).$$

Most common in practice are the zeroth order ($b = 0$) and first order ($b = 1$) arc-cosine kernels. The zeroth order kernel is given explicitly by

$$k(\mathbf{x}, \mathbf{x}') = 1 - \frac{\theta}{\pi},$$

and the first order kernel is

$$k(\mathbf{x}, \mathbf{x}') = \frac{1}{\pi} \|\mathbf{x}\|_2 \|\mathbf{x}'\|_2 (\sin \theta + (\pi - \theta) \cos \theta).$$

iii) Polynomial kernel: This is a widely used family of non-stationary kernels given by

$$k(\mathbf{x}, \mathbf{x}') = (1 + \langle \mathbf{x}, \mathbf{x}' \rangle)^b,$$

where b is the order of the polynomial.

Besides the aforementioned, other kernels considered in random features approximation include additive kernels [57], polynomial kernels on the unit sphere [34], and indefinite (real, symmetric, but not positive definite) kernels [58].

2.4 Theoretical foundation of random features

The theoretical foundation of RFF builds on Bochner's celebrated characterization of positive definite functions.

Theorem 1 (Bochner's Theorem [59]). *A continuous and shift-invariant function $k : \mathbb{R}^d \times \mathbb{R}^d \rightarrow \mathbb{R}$ is positive definite if and only if it can be represented as*

$$k(\mathbf{x} - \mathbf{x}') = \int_{\mathbb{R}^d} \exp(i\omega^\top (\mathbf{x} - \mathbf{x}')) \mu_k(d\omega),$$

where μ_k is a positive finite measure on the frequencies ω .

According to Bochner's theorem, the spectral distribution μ_k of a stationary kernel k is the finite measure induced by a Fourier transform. By setting $k(0) = 1$, we may normalize μ_k to a probability density p (the Fourier transform associated with k), hence

$$\begin{aligned} k(\mathbf{x} - \mathbf{x}') &= \int_{\mathbb{R}^d} p(\omega) \exp(i\omega^\top (\mathbf{x} - \mathbf{x}')) d\omega \\ &= \mathbb{E}_{\omega \sim p(\cdot)} [\exp(i\omega^\top \mathbf{x}) \exp(i\omega^\top \mathbf{x}')^*], \end{aligned} \quad (4)$$

where \mathbf{z}^* denotes the complex conjugate of \mathbf{z} . The kernels used in practice are typically real-valued and thus the imaginary part in Eq. (4) can be discarded. Based on the integral representation (4), RFF makes use of the standard Monte Carlo sampling scheme to approximate $k(\mathbf{x}, \mathbf{x}')$. In particular, one uses the approximation

$$k(\mathbf{x}, \mathbf{x}') = \mathbb{E}_{\omega \sim p(\cdot)} [\varphi_p(\mathbf{x})^\top \varphi_p(\mathbf{x}')] \approx \tilde{k}_p(\mathbf{x}, \mathbf{x}') := \varphi_p(\mathbf{x})^\top \varphi_p(\mathbf{x}')$$

with the explicit feature mapping¹

$$\varphi_p(\mathbf{x}) := \frac{1}{\sqrt{s}} [\exp(-i\omega_1^\top \mathbf{x}), \dots, \exp(-i\omega_s^\top \mathbf{x})]^\top, \quad (5)$$

where $\{\omega_i\}_{i=1}^s$ are sampled from $p(\cdot)$ independently of the training set. Consequently, the original kernel matrix $\mathbf{K} = [k(\mathbf{x}_i, \mathbf{x}_j)]_{n \times n}$ can be approximated by $\mathbf{K} \approx \tilde{\mathbf{K}}_p = \mathbf{Z}_p \mathbf{Z}_p^\top$ with $\mathbf{Z}_p = [\varphi_p(\mathbf{x}_1), \dots, \varphi_p(\mathbf{x}_n)]^\top \in \mathbb{R}^{n \times s}$. It is convenient to introduce the shorthand $z_p(\omega_i, \mathbf{x}_j) := \exp(-i\omega_i^\top \mathbf{x}_j)$ such that $\varphi_p(\mathbf{x}) = 1/\sqrt{s}[z_p(\omega_1, \mathbf{x}), \dots, z_p(\omega_s, \mathbf{x})]^\top$. With this notation, the approximate kernel $\tilde{k}_p(\mathbf{x}, \mathbf{x}')$ can be rewritten as

$$\tilde{k}_p(\mathbf{x}, \mathbf{x}') = \frac{1}{s} \sum_{i=1}^s z_p(\omega_i, \mathbf{x}) z_p(\omega_i, \mathbf{x}').$$

This equation suggests that the above approximation principle can be further generalized to the class of kernel functions [49] admitting the decomposition

$$k(\mathbf{x}, \mathbf{x}') = \int_{\mathbb{R}^d} z(\omega, \mathbf{x}) z(\omega, \mathbf{x}') p(\omega) d\omega, \quad (6)$$

where $z(\omega, \mathbf{x})$ is a continuous and bounded function satisfying $|z(\omega, \mathbf{x})| \leq z_0$. Note that the above kernel class need not be shift-invariant as required by Bochner's theorem, and the function $z(\omega, \mathbf{x})$ is not limited to $\exp(-i\omega^\top \mathbf{x})$ as in Eq. (6). Therefore, the RFF approach can be extended to other kernels including,

1. The subscript in \tilde{k}_p and φ_p emphasizes the dependence on the sampling distribution $p(\cdot)$.

in particular, rotation-invariant kernels, which we briefly discuss below.

Rotation-invariant kernels [56], [60], [61], typically defined on the hyper-sphere $\mathcal{X} = \mathbb{S}^{d-1}$, are kernels whose values depend only on the inner product between the samples, i.e., $k(\mathbf{x}, \mathbf{x}') \equiv k(\langle \mathbf{x}, \mathbf{x}' \rangle)$. These kernels are among the most general family of kernels used in practice and include the aforementioned arc-cosine kernels. Rotation-invariant kernels do not satisfy the shift invariant condition of Bochner's theorem, but one may extend Bochner's theorem by using the Fourier basis functions given by *spherical harmonics*. These functions are a countably infinite family of complex polynomials that form an orthogonal basis for square-integrable functions mapping \mathcal{X} to the complex numbers \mathbb{C} .

Theorem 2 ([62], [63]). *A rotation-invariant continuous function $k : \mathbb{S}^{d-1} \times \mathbb{S}^{d-1} \rightarrow \mathbb{R}$ is positive definite if and only if it has a symmetric non-negative expansion into spherical harmonics $Y_{\ell,m}^d$, that is,*

$$k(\langle \mathbf{x}, \mathbf{x}' \rangle) = \sum_{j=0}^{\infty} \sum_{\ell=1}^{N(d,\ell)} p(\ell, m) Y_{\ell,m}^d(\mathbf{x}) \overline{Y_{\ell,m}^d(\mathbf{x}')}, \quad (7)$$

for some $p(\omega) \geq 0$ satisfying $p(\omega) = p(-\omega)$ for all valid index pairs $\omega = (\ell, m) \in \mathbb{S}^{d-1} \times \mathbb{S}^{d-1}$. Here $N(d, \ell) := \binom{d-1+\ell}{\ell} - \binom{d-1+\ell}{\ell-2}$ and we assume that $\int_{\mathbb{S}^{d-1}} |Y_{\ell,m}^d(\mathbf{x})|^2 d\mathbf{x} = 1$.

We remark that the above mentioned Gaussian and arc-cosine kernels both admit the following unified integration representation [39], [41]

$$k(\mathbf{x}, \mathbf{x}') = \int_{\mathbb{R}^d} g(\omega) \mathcal{N}(\omega; \mathbf{0}, \mathbf{I}_d) d\omega, \quad (8)$$

where $g(\omega) = \phi(\omega^\top \mathbf{x})^\top \phi(\omega^\top \mathbf{x}')$ and $\mathcal{N}(\omega; \mathbf{0}, \mathbf{I}_d)$ is the density function of $\mathcal{N}(\mathbf{0}, \mathbf{I}_d)$. The Gaussian kernel, which is both shift-invariant and rotation-invariant, corresponds to $\phi(x) = [\cos(x), \sin(x)]^\top$. The first order arc-cosine kernel corresponds to $\phi(x) = \max\{0, x\}$. The zeroth order arc-cosine kernel corresponds to $\phi(x) = \Xi(x) := \frac{1}{2}(1 + \text{sign}(x))$, the Heaviside step function.

2.5 Taxonomy of random features based algorithms

The key step in a random features based algorithm is constructing the mapping

$$\varphi(\mathbf{x}) := \frac{1}{\sqrt{s}} [a_1 \exp(-i\omega_1^\top \mathbf{x}), \dots, a_s \exp(-i\omega_s^\top \mathbf{x})]^\top \quad (9)$$

so as to uniformly approximate the integral in Eq. (4). Existing algorithms differ in how they select the points ω_i and weights a_i . Figure 2 presents a taxonomy of some representative random features based algorithms. They can be grouped into two categories, *data-independent* algorithms and *data-dependent* algorithms, based on whether or not the selection of ω_i and a_i is independent of the training data.

Data-independent random features based algorithms can be further categorized into three classes according to their sampling strategy:

i) *Monte Carlo sampling*: The points $\{\omega_i\}_{i=1}^s$ are sampled from the distribution $p(\cdot)$ in Eq. (4) (see the red box in Figure 2). In particular, to approximate the Gaussian kernel by RFF [12], these points are sampled from the Gaussian distribution

$p = \mathcal{N}(0, \sigma^{-2} \mathbf{I}_d)$, with the weights being equal, i.e., $a_i \equiv 1$ in Eq. (9). To reduce the storage and time complexity, one may replace the dense Gaussian matrix in RFF by structural matrices; see, e.g., Fastfood [31] using Hadamard matrices as well as its general version \mathcal{P} -model [37]. An alternative approach is using circulant matrices; see, e.g., Signed Circulant Random Features (SCRF) [35]. To improve the approximation quality, a simple and effective approach is to use an ℓ_2 -normalization scheme, which leads to Normalized RFF (NRFF) [64]. Another powerful technique for variance reduction is Orthogonal Random Features (ORF) [36], which incorporates an orthogonality constraint to the random Gaussian matrix. The transformation matrix \mathbf{W} in ORF can be efficiently computed and stored by using structural matrices, as in, e.g., Structural ORF (SORF) [36], [73]. The structural orthogonal property of random features is further exploited in Random Orthogonal Embeddings (ROM) [65] for rotation-invariant kernels.

ii) *Quasi-Monte Carlo sampling*: The convergence of Monte-Carlo sampling used in RFF and ORF can be significantly improved by quasi-Monte Carlo sampling (QMC) [52], which makes use of a low-discrepancy² sequence $\mathbf{t}_1, \mathbf{t}_2, \dots, \mathbf{t}_s \in [0, 1]^d$ over the unit cube to construct the sample points; see the integral representation in the green box in Figure 2. Based on this representation, Lyu [39] proposes Spherical Structural Features (SSF), which generates asymptotically uniformly distributed points on the sphere \mathbb{S}^{d-1} to achieve better convergence rate and approximation quality. The Moment Matching (MM) scheme [38] is based on the same integral representation but uses a d -dimensional refined uniform sampling sequence $\{\mathbf{t}_i\}_{i=1}^s$ instead of a low discrepancy sequence. Strictly speaking, SSF and MM go beyond the quasi-Monte Carlo framework. Nevertheless, these methods share the same integration formulation with QMC over the unit cube and thus we include them here for a streamlined presentation.

iii) *Quadrature based methods*: Numerical integration techniques can be used to approximate the integral representation in Eq. (4). These techniques may involve *deterministic* selection of the points and weights, e.g., by using Gaussian Quadrature (GQ) [40] and Sparse Grids Quadrature (SGQ) [40] over each dimension (their integration formulation can be found in the first blue box in Figure 2). The selection can also be *randomized*. For example, in the work [41], the d -dimensional integration in Eq. (4) is transformed to a double integral, which is then approximated by using the Stochastic Spherical-Radial (SSR) rule (see the second blue box in Figure 2).

Data-dependent algorithms use the training data to guide the selection of points and weights in the random features for better approximation quality and/or generalization performance. These algorithms can be grouped into three classes according to how the random features are generated.

i) *Leverage score sampling*: Built upon the importance sampling framework, this class of algorithm replaces the original distribution $p(\omega)$ by a carefully chosen distribution $q(\omega)$ constructed using leverage scores [48], [49] (see the yellow box in Figure 2). The representative approach in this class is Leverage Score based RFF (LS-RFF) [16], which can be further accelerated by using Surrogate Leverage Score based RFF (SLS-RFF) [44].

2. A low-discrepancy sequence has values close to being uniformly distributed.

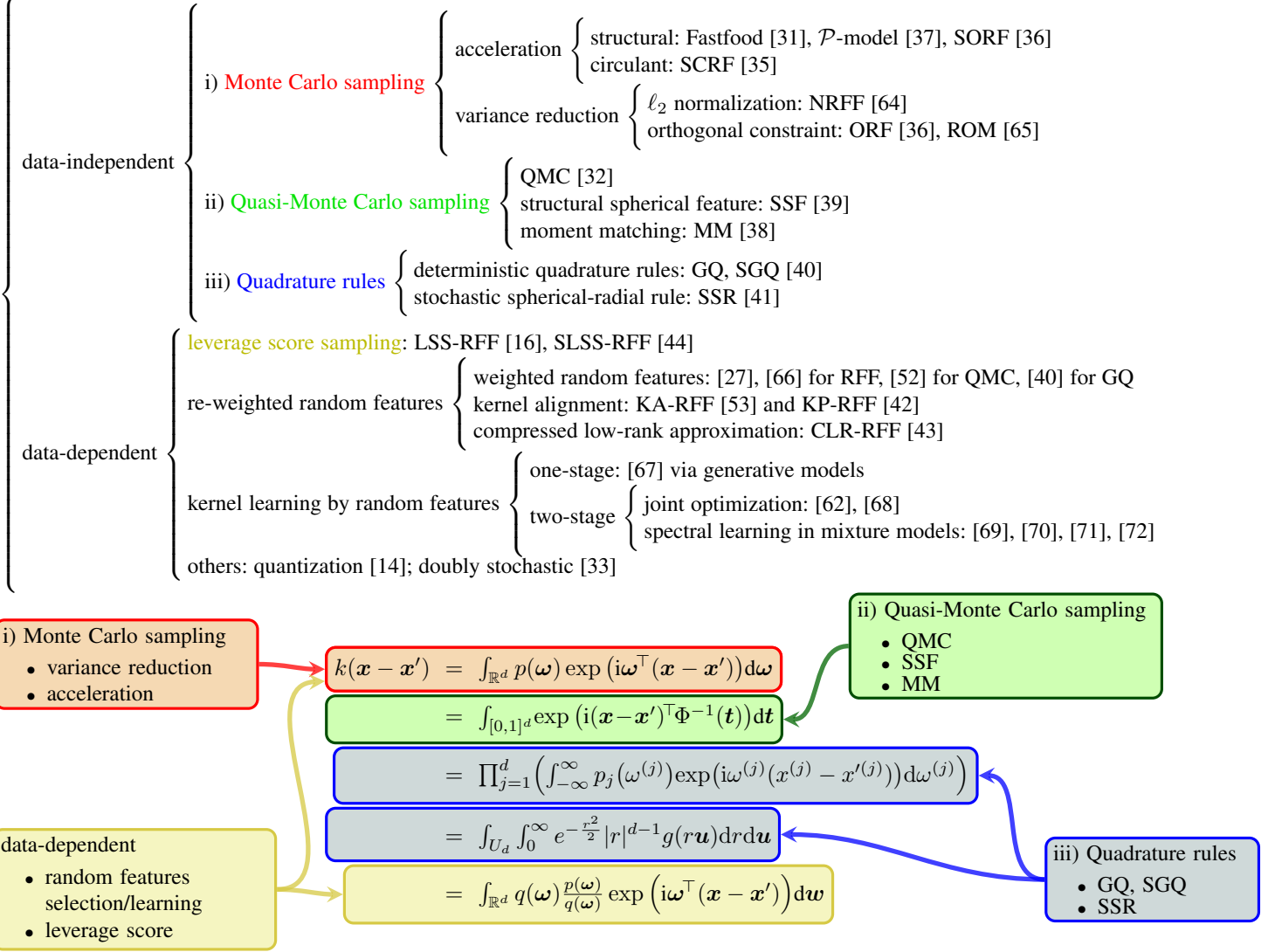


Figure 2. A taxonomy of representative random features based algorithms.

ii) *Re-weighted random feature selection*: Here the basic idea is to re-weight the random features by solving a constrained optimization problem. Examples of this approach include weighted RFF [27], [66], weighted QMC [52], and weighted GQ [40]. Note that these algorithms directly learn the weights of pre-given random features. Another line of methods re-weight the random features using a two-step procedure: i) “up-projection”: first generate a large set of random features $\{\omega_i\}_{i=1}^J$; ii) “compression”: then reduce these features to a small number of weighted features in a data-dependent manner, e.g., by using kernel alignment [53], kernel polarization [42], or compressed low-rank approximation [43].

iii) *Kernel learning by random features*: This class of methods aim to learn the spectral distribution of kernel *from the data* so as to achieve better similarity representation and prediction. Note that these methods learn both the weights and the distribution of the features, and hence differ from the other random features selection methods mentioned above, which assume that the candidate features are generated from a pre-given distribution and only learn the weights of these features. Representative approaches for kernel learning involve a *one-stage* [67] or *two-stage* procedure [62], [68], [69], [70], [71], [72]. From a more general point of view, the

aforementioned *re-weighted random features selection* methods can also be classified into this class. Since these methods belong to the broad area of kernel learning instead of kernel approximation, we do not detail them in this survey.

Besides the above three main categories, other data-dependent approaches include the following. i) Quantization random features [14]: Given a memory budget, this method quantizes RFF for approximation of the Gaussian kernel. A key observation from this work is that random features based algorithms achieve better generalization performance than Nyström approximation [13] under the same budget constraint. ii) Doubly stochastic random features [33]: This method uses two sources of stochasticity, one from sampling data points by stochastic gradient descent (SGD), and the other from using RFF to approximate the kernel. This doubly stochastic scheme has been used for Kernel PCA approximation [17], and can be further extended to triply stochastic scheme for multiple kernel approximation [74].

In the next two sections, we provide the details for representative data-independent and data-dependent algorithms, respectively.

Table 1
Comparison of different kernel approximation methods on space and time complexities to obtain $\mathbf{W}\mathbf{x}$.

Method	Kernels	Extra Memory	Time	Lower variance than RFF
Random Fourier Features (RFF) [12]	shift-invariant kernels	$\mathcal{O}(sd)$	$\mathcal{O}(sd)$	-
Quasi-Monte Carlo (QMC) [32]	shift-invariant kernels	$\mathcal{O}(sd)$	$\mathcal{O}(sd)$	Yes
Normalized RFF (NRFF) [64]	Gaussian kernel	$\mathcal{O}(sd)$	$\mathcal{O}(sd)$	Yes
Moment matching (MM) [38]	shift-invariant kernels	$\mathcal{O}(sd)$	$\mathcal{O}(sd)$	Yes
Orthogonal Random Feature (ORF) [36]	Gaussian kernel	$\mathcal{O}(sd)$	$\mathcal{O}(sd)$	Yes
Fastfood [31]	Gaussian kernel	$\mathcal{O}(s)$	$\mathcal{O}(s \log d)$	No
Spherical Structured Features (SSF) [39]	shift and rotation-invariant kernels	$\mathcal{O}(s)$	$\mathcal{O}(s \log d)$	Yes
Structured ORF (SORF) [36], [73]	shift and rotation-invariant kernels	$\mathcal{O}(s)$	$\mathcal{O}(s \log d)$	Unknown
Signed Circulant (SCRF) [35]	shift-invariant kernels	$\mathcal{O}(s)$	$\mathcal{O}(s \log d)$	The same
\mathcal{P} -model [37]	shift and rotation-invariant kernels	$\mathcal{O}(s)$	$\mathcal{O}(s \log d)$	No
Random Orthogonal Embeddings (ROM) [65]	rotation-invariant kernels	$\mathcal{O}(d)$	$\mathcal{O}(d \log d)$	Yes
Gaussian Quadrature (GQ), Sparse Grids Quadrature (SGQ) [40]	shift invariant kernels	$\mathcal{O}(d)$	$\mathcal{O}(d \log d)$	Yes
Stochastic Spherical-Radial rules (SSR) [41]	shift and rotation-invariant kernels	$\mathcal{O}(d)$	$\mathcal{O}(d \log d)$	Yes

3 DATA-INDEPENDENT ALGORITHMS

In this section, we discuss data-independent algorithms in a unified framework based on the transformation matrix $\mathbf{W} := [\omega_1, \omega_2, \dots, \omega_s]^\top \in \mathbb{R}^{s \times d}$, for which we recall that $\{\omega_i\}$ are the frequency points for constructing the mapping $\varphi(\cdot)$ in Eq. (9). The matrix \mathbf{W} plays an important role in determining how well the estimated kernel converges to the actual kernel. Table 1 reports various random features based algorithms in terms of the class of kernels they apply to as well as their space and time complexities for computing the feature mapping $\mathbf{W}\mathbf{x}$ for a given $\mathbf{x} \in \mathcal{X}$. In Table 1, we also summarize the *variance reduction* properties of these algorithms, i.e., whether the variance of the resulting kernel estimator is smaller than the standard RFF.

Before proceeding, we introduce some notations and definitions. When discussing a shift-invariant kernel function $k(\mathbf{x}, \mathbf{x}') = k(\mathbf{x} - \mathbf{x}')$, we use the convenient shorthands $\tau := \mathbf{x} - \mathbf{x}'$ and $\tau := \|\tau\|_2$. For a random features algorithm A with frequencies $\{\omega_i\}_{i=1}^s$ sampled from a distribution $\mu(\cdot)$, we define its expectation $\mathbb{E}(A) := \mathbb{E}[k(\tau)] = \mathbb{E}_{\omega \sim \mu} [1/s \sum_{i=1}^s \cos(\omega_i^\top \tau)]$ and variance $\mathbb{V}[A] := \mathbb{V}[k(\tau)] = \mathbb{V} [\frac{1}{s} \sum_{i=1}^s \cos(\omega_i^\top \tau)]$ (it is implicit that both of them depend on τ).

3.1 Monte Carlo sampling based approaches

We describe several representative data-independent algorithms based on Monte Carlo sampling, using the Gaussian kernel $k(\mathbf{x}, \mathbf{x}') = k(\tau) = \exp(-\frac{\|\tau\|_2^2}{2\sigma^2})$ as an example. Note that these algorithms often apply to more general classes of kernels, as summarized in Table 1.

RFF [12]: For Gaussian kernels, RFF samples the frequencies from a Gaussian distribution: $\{\omega_i\}_{i=1}^s \sim p(\omega)$. In particular, the corresponding transformation matrix is

$$\mathbf{W}_{\text{RFF}} = \frac{1}{\sigma} \mathbf{G}, \quad (10)$$

where $\mathbf{G} \in \mathbb{R}^{s \times d}$ is a (dense) Gaussian matrix with each entry sampled independently from the standard normal distribution. For other shift-invariant kernels, the associated $p(\cdot)$ corresponds to the specific distribution given by the Bochner's Theorem. For example, the Laplacian kernel $k(\tau) = \exp(-\|\tau\|_1/\sigma)$ is associated with a Cauchy distribution.

RFF is unbiased, i.e., $\mathbb{E}[\text{RFF}] = \exp(-\frac{\|\tau\|_2^2}{2\sigma^2})$, with the corresponding variance $\mathbb{V}[\text{RFF}] = \frac{(1-e^{-\tau^2})^2}{2s}$ as shown in [36].

Fastfood [31]: It makes use of Hadamard matrices to speed up the construction of dense Gaussian matrices in RFF. In particular, the transformation matrix used in Eq. (10) is substituted by

$$\mathbf{W}_{\text{Fastfood}} = \frac{1}{\sigma} \mathbf{B}_1 \mathbf{H} \mathbf{G} \mathbf{T} \mathbf{H} \mathbf{B}_2, \quad (11)$$

where \mathbf{H} is the Walsh-Hadamard matrix admitting fast multiplication in $\mathcal{O}(d \log d)$ time, and $\mathbf{\Gamma} \in \{0, 1\}^{d \times d}$ is a permutation matrix that decorrelates the eigen-systems of two Hadamard matrices. The three *diagonal* random matrices \mathbf{G} , \mathbf{B}_1 and \mathbf{B}_2 are specified as follows: \mathbf{G} has independent Gaussian entries drawn from $\mathcal{N}(0, 1)$; \mathbf{B}_1 is a random scaling matrix with $(\mathbf{B}_1)_{ii} = \|\omega_i\|_2/\|\mathbf{G}\|_F$, which encodes the spectral properties of the associated kernel; \mathbf{B}_2 is a binary decorrelation matrix with independent random $\{\pm 1\}$ entries. FastFood is also an unbiased estimator, but may have a larger variance than RFF:

$$\mathbb{V}[\text{Fastfood}] \leq \mathbb{V}[\text{RFF}] + \frac{6\tau^4}{s} \left(e^{-\tau^2} + \frac{\tau^2}{3} \right),$$

where the second right hand side term converges at an $\mathcal{O}(1/s)$ rate.

\mathcal{P} -model [37]: A general version of Fastfood, the \mathcal{P} -model constructs the transformation matrix as

$$\mathbf{W}_{\mathcal{P}} = [\mathbf{g}^\top \mathbf{P}_1, \mathbf{g}^\top \mathbf{P}_2, \dots, \mathbf{g}^\top \mathbf{P}_s]^\top \in \mathbb{R}^{s \times d},$$

where \mathbf{g} is a Gaussian random vector of length t and $\mathcal{P} = \{\mathbf{P}_i\}_{i=1}^s$ is a sequence of t -by- d matrices each with unit ℓ_2 norm columns. Fastfood can be viewed as a special case of the \mathcal{P} -model: the matrix $\mathbf{H}\mathbf{G}$ in Eq. (11) can be constructed by using a fixed budget of randomness in \mathbf{g} and letting each \mathbf{P}_i be a random diagonal matrix with diagonal entries of the form $H_{i1}, H_{i2}, \dots, H_{id}$. The \mathcal{P} -model is unbiased and its variance is close to that of RFF with an $\mathcal{O}(1/d)$ convergence rate:

$$|\mathbb{V}[\mathcal{P}\text{-model}] - \mathbb{V}[\text{RFF}]| = \mathcal{O}(1/d).$$

SCRF [35]: It accelerates the construction of random features by using circulant matrices. The transformation matrix is

$$\mathbf{W}_{\text{SCRF}} = [\boldsymbol{\nu} \otimes \mathcal{C}(\omega_1), \boldsymbol{\nu} \otimes \mathcal{C}(\omega_2), \dots, \boldsymbol{\nu} \otimes \mathcal{C}(\omega_t)]^\top \in \mathbb{R}^{td \times d},$$

where $\nu = [\nu_1, \nu_2, \dots, \nu_d]$ is a Rademacher vector with $\mathbb{P}(\nu_i = 1) = \mathbb{P}(\nu_i = -1) = 1/2$, and $\mathcal{C}(\mathbf{w}_i) \in \mathbb{R}^{d \times d}$ is a circulant matrix generated by the vector $\omega_i \sim \mathcal{N}(0, \sigma^{-2} \mathbf{I}_d)$. Thanks to the circulant structure, we only need $\mathcal{O}(s)$ space to store the feature mapping matrix \mathbf{W}_{SCRF} with $s = td$. Note that $\mathcal{C}(\mathbf{w}_i)$ can be diagonalized using the Discrete Fourier Transform (DFT) for any generating vector ω_i . SCRF is unbiased and has the same variance as RFF.

The above approaches are designed to accelerate the computation of RFF. We next overview representative methods that aim for variance reduction.

NRFF [64]: It normalizes the input data to have unit ℓ_2 norm before constructing the random Fourier features. With normalized data, the Gaussian kernel can be computed as

$$k(\mathbf{x}, \mathbf{x}') = \exp\left(-\frac{1}{\sigma^2}\left(1 - \frac{\mathbf{x}^\top \mathbf{x}'}{\|\mathbf{x}\|_2 \|\mathbf{x}'\|_2}\right)\right),$$

which is related to the normalized linear kernel [34], [64]. Albeit simple, NRFF is effective in variance reduction and in particular satisfies

$$\mathbb{V}[\text{NRFF}] = \mathbb{V}[\text{RFF}] - \frac{1}{4s}e^{-\tau^2}(3 - e^{-2\tau^2}).$$

ORF [36]: It imposes orthogonality on random features for the Gaussian kernel and has the transformation matrix

$$\mathbf{W}_{\text{ORF}} = \frac{1}{\sigma} \mathbf{S} \mathbf{Q},$$

where \mathbf{Q} is a uniformly distributed random orthogonal matrix, and \mathbf{S} is a diagonal matrix with diagonal entries sampled *i.i.d* from the χ -distribution with d degrees of freedom. This orthogonality constraint is useful in reducing the approximation error in random features. It is also considered in [75] for unifying orthogonal Monte Carlo methods. ORF is unbiased and with variance bounded by

$$\mathbb{V}[\text{ORF}] - \mathbb{V}[\text{RFF}] \leq \frac{1}{s} \left(\frac{g(\tau)}{d} - \frac{(d-1)e^{-\tau^2}\tau^4}{2d} \right),$$

where we have $g(\tau) = e^{\tau^2}(\tau^8 + 6\tau^6 + 7\tau^4 + \tau^2)/4 + e^{\tau^2}\tau^4(\tau^6 + 2\tau^4)/2d$. It can be seen that the variance reduction property $\text{Var}[\text{ORF}] < \text{Var}[\text{RFF}]$ holds under some conditions, e.g., when d is large and τ is small. For a large d , the ratio of the variances of ORF and RFF can be approximated by

$$\frac{\mathbb{V}[\text{ORF}]}{\mathbb{V}[\text{RFF}]} \approx 1 - \frac{(s-1)e^{-\tau^2}\tau^4}{d(1-e^{-\tau^2})^2}. \quad (12)$$

Choromanski et al. [76] further improve the variance bound to

$$\begin{aligned} \mathbb{V}[\text{RFF}] - \mathbb{V}[\text{ORF}] &= \\ &= \frac{s-1}{s} \mathbb{E}_{R_1, R_2} \left[\frac{J_{\frac{d}{2}-1}(\sqrt{R_1^2 + R_2^2}\tau) \Gamma(d/2)}{(\sqrt{R_1^2 + R_2^2}\tau/2)^{\frac{d}{2}-1}} \right] \\ &\quad - \frac{s-1}{s} \mathbb{E}_{R_1} \left[\frac{J_{\frac{d}{2}-1}(R_1\tau) \Gamma(d/2)}{(R_1\tau/2)^{\frac{d}{2}-1}} \right]^2, \end{aligned} \quad (13)$$

where J_d is the Bessel function of the first kind of degree d , and R_1 and R_2 are two independent scalar random variables satisfying $\omega_1 = R_1 \mathbf{v}$ and $\omega_2 = R_2 \mathbf{v}$ with $\omega_1, \omega_2 \sim \mathcal{N}(0, \sigma^{-2} \mathbf{I}_d)$ and $\mathbf{v} \sim \text{Unif}(\mathcal{S}^{d-1})$. According to Eq. (13), the property $\mathbb{V}[\text{ORF}] < \mathbb{V}[\text{RFF}]$ holds asymptotically in cases: i) a fixed d and a small

enough τ with $\mathbb{E}[\|\omega\|_2^4] \leq \infty$; ii) a fixed $\tau < \frac{1}{4\sqrt{c}}$ with some constant c and a large d , in which case we have

$$\mathbb{V}[\text{RFF}] - \mathbb{V}[\text{ORF}] = \frac{s-1}{s} \left(\frac{1}{2d} \frac{\tau^4}{\sigma^2} e^{-\frac{\tau^2}{\sigma^2}} + \mathcal{O}\left(\frac{1}{d}\right) \right).$$

SORF [36], [73]: It replaces the random orthogonal matrices used in ORF by a class of structured matrices akin to those in Fastfood. The transformation matrix of SORF is given by

$$\mathbf{W}_{\text{SORF}} = \frac{\sqrt{d}}{\sigma} \mathbf{H} \mathbf{D}_1 \mathbf{H} \mathbf{D}_2 \mathbf{H} \mathbf{D}_3, \quad (14)$$

where \mathbf{H} is the normalized Walsh-Hadamard matrix and $\mathbf{D}_i \in \mathbb{R}^{d \times d}$, $i = 1, 2, 3$ are diagonal sign-flipping matrices, of which each diagonal entry is sampled from the Rademacher distribution. Bojarski et al. [73] consider more general structures for the three blocks of matrices $\mathbf{H} \mathbf{D}_i$ in Eq. (14). Note that each block plays a different role. The first block $\mathbf{H} \mathbf{D}_1$ satisfies $\Pr\left[\|\mathbf{H} \mathbf{D}_1 \mathbf{x}\|_\infty > \frac{\log d}{\sqrt{d}}\right] \leq 2de^{-\frac{\log^2 d}{8}}$ for any $\mathbf{x} \in \mathbb{R}^d$ with $\|\mathbf{x}\|_2 = 1$, termed as $(\log d, 2de^{-\frac{\log^2 d}{8}})$ -balanced, hence no dimension carries too much of the ℓ_2 norm of the vector \mathbf{x} . The second block $\mathbf{H} \mathbf{D}_2$ ensures that vectors are close to orthogonal. The third block $\mathbf{H} \mathbf{D}_3$ controls the capacity of the entire structured transform by providing a vector of parameters. SORF is not an unbiased estimator of the Gaussian kernel, but it satisfies an asymptotic unbiased property

$$\left| \mathbb{E}[\text{SORF}] - e^{-\tau^2/2} \right| \leq \frac{6\tau}{\sqrt{d}}.$$

ROM [65]: It generalizes SORF to the form

$$\mathbf{W}_{\text{ROM}} = \frac{\sqrt{d}}{\sigma} \prod_{i=1}^t \mathbf{H} \mathbf{D}_i,$$

where \mathbf{H} can be the normalized Hadamard matrix or the Walsh matrix, and \mathbf{D}_i is the Rademacher matrix as defined in SORF. Theoretical results in [65] show that the ROM estimator achieves variance reduction compared to RFF. Interestingly, odd values of t yield better results than even t . This provides an explanation for why SORF chooses $t = 3$.

3.2 Quasi-Monte Carlo sampling

Here we briefly review methods based on quasi-Monte Carlo sampling (QMC) [32], spherical structured feature (SSF) [39], and moment matching (MM) [38]. These three methods achieve a lower variance or approximation error than RFF.

Classical Monte Carlo sampling generates a sequence of samples randomly and independently, which may lead to an undesired clustering effect and empty spaces between the samples [77]. Instead of fully random samples, QMC [32] outputs low-discrepancy sequences. A typical QMC sequence has a hierarchical structure: the initial points are sampled on a coarse scale whereas the subsequent points are sampled more finely. For approximating a high-dimensional integral, QMC achieves an asymptotic error convergence rate of $\epsilon = \mathcal{O}((\log s)^d/s)$, which is faster than the $\mathcal{O}(s^{-1/2})$ rate of Monte Carlo. Note however that QMC often requires s to be exponential in d for the improvement to manifest.

QMC [32]: It assumes that $p(\cdot)$ factorizes with respect to the dimensions, i.e., $p(\mathbf{x}) = \prod_{j=1}^d p_j(x_j)$, where each $p_j(\cdot)$ is a univariate density function. The QMC method generally transforms an integral on \mathbb{R}^d to one on the unit cube $[0, 1]^d$. In particular, by

a change of variables, the integral in Eq. (4) can be equivalently written as

$$k(\mathbf{x} - \mathbf{x}') = \int_{[0,1]^d} \exp(i(\mathbf{x} - \mathbf{x}')^\top \Phi^{-1}(\mathbf{t})) d\mathbf{t}, \quad (15)$$

where

$$\Phi^{-1}(\mathbf{t}) = (\Phi_1^{-1}(t_1), \dots, \Phi_d^{-1}(t_d)) \in \mathbb{R}^d,$$

with Φ_j being the cumulative distribution function (CDF) of p_j . Accordingly, by generating a low *discrepancy* sequence³ $\mathbf{t}_1, \mathbf{t}_2, \dots, \mathbf{t}_s \in [0,1]^d$, the random frequencies can be constructed by $\omega_i = \Phi^{-1}(\mathbf{t}_i)$ for $i \in [s]$. The corresponding transformation matrix for QMC is

$$\mathbf{W}_{\text{QMC}} = [\Phi^{-1}(\mathbf{t}_1), \Phi^{-1}(\mathbf{t}_2), \dots, \Phi^{-1}(\mathbf{t}_s)]^\top \in \mathbb{R}^{s \times d}. \quad (16)$$

SSF [39]: It improves the space and time complexities of QMC for approximating shift- and rotation-invariant kernels. SSF generates points $\{\mathbf{v}_1, \mathbf{v}_2, \dots, \mathbf{v}_s\}$ asymptotically uniformly distributed on the sphere \mathbb{S}^{d-1} , and construct the transformation matrix as

$$\mathbf{W}_{\text{SSF}} = [\Phi^{-1}(\mathbf{t}) \mathbf{v}_1, \Phi^{-1}(\mathbf{t}) \mathbf{v}_2, \dots, \Phi^{-1}(\mathbf{t}) \mathbf{v}_s]^\top \in \mathbb{R}^{s \times d},$$

where $\Phi^{-1}(\mathbf{t})$ uses the one-dimensional QMC point. The structure matrix $\mathbf{V} := [\mathbf{v}_1, \mathbf{v}_2, \dots, \mathbf{v}_s] \in \mathbb{S}^{(d-1) \times s}$ has the form

$$\mathbf{V} = \frac{1}{\sqrt{d/2}} \begin{bmatrix} \text{Re } \mathbf{F}_\Lambda & -\text{Im } \mathbf{F}_\Lambda \\ \text{Im } \mathbf{F}_\Lambda & \text{Re } \mathbf{F}_\Lambda \end{bmatrix} \in \mathbb{R}^{d \times s},$$

where $\mathbf{F}_\Lambda \in \mathbb{C}^{\frac{d}{2} \times \frac{s}{2}}$ consists of a subset of the rows of the discrete Fourier matrix $\mathbf{F} \in \mathbb{C}^{\frac{s}{2} \times \frac{s}{2}}$. The selection of $\frac{d}{2}$ rows from \mathbf{F} is done by minimizing the discrete Riesz 0-energy [78] such that the points spread as evenly as possible on the sphere.

MM [38]: It also uses the transformation matrix in Eq. (16), but generates a d -dimensional uniform sampling sequence $\{\mathbf{t}_i\}_{i=1}^s$ by a moment matching scheme instead of using a low discrepancy sequence as in QMC. In particular, the transformation matrix of MM is

$$\mathbf{W}_{\text{MM}} = [\tilde{\Phi}^{-1}(\mathbf{t}_1), \tilde{\Phi}^{-1}(\mathbf{t}_2), \dots, \tilde{\Phi}^{-1}(\mathbf{t}_s)]^\top \in \mathbb{R}^{s \times d}, \quad (17)$$

where one uses moment matching to construct the vectors

$$\tilde{\Phi}^{-1}(\mathbf{t}_i) = \tilde{\mathbf{A}}^{-1}(\Phi^{-1}(\mathbf{t}_i) - \tilde{\boldsymbol{\mu}}),$$

with $\tilde{\boldsymbol{\mu}} = \frac{1}{s} \sum_{i=1}^s \Phi^{-1}(\mathbf{t}_i)$ being the sample mean and $\tilde{\mathbf{A}}$ the square root of the sample covariance matrix, i.e., $\tilde{\mathbf{A}} \tilde{\mathbf{A}}^\top = \text{Cov}(\Phi^{-1}(\mathbf{t}_i) - \tilde{\boldsymbol{\mu}})$.

3.3 Quadrature based methods

Quadrature based methods build on a long line of work on numerical quadrature for estimating integrals. The equivalence between kernel quadrature and random features is elucidated in [49]. In these methods, the weights are often non-uniform, and the points are usually selected using *deterministic* rules including Gaussian quadrature (GQ) [40], [79] and sparse grids quadrature (SGQ) [40]. Deterministic rules can be extended to their stochastic versions. For example, Munkhoeva et al. [41] explore the stochastic spherical-radial (SSR) rule [80] in kernel approximation. Below we briefly review these methods.

3. Four types of sequences are considered: Halton, Sobol', Lattice rules, and digital nets.

GQ [40]: It assumes that the kernel function k factorizes with respect to the dimensions and the corresponding distribution $p(\boldsymbol{\omega}) = p([\omega^{(1)}, \omega^{(2)}, \dots, \omega^{(d)}]^\top)$ in Eq. (4) is sub-Gaussian. Therefore, the d -dimensional integral in Eq. (4) can be factorized as

$$k(\mathbf{x} - \mathbf{x}') = \prod_{j=1}^d \left(\int_{-\infty}^{\infty} p_j(\omega^{(j)}) \exp(i\omega^{(j)}(x^{(j)} - x'^{(j)})) d\omega^{(j)} \right). \quad (18)$$

Since each of the factors is a one-dimensional integral, we can approximate them using a one-dimensional quadrature rule. For example, one may use Gaussian quadrature [79] with orthogonal polynomials:

$$\int_{-\infty}^{\infty} p(\omega) \exp(i\omega(x - x')) d\omega \approx \sum_{j=1}^L a_j \exp(i\gamma_j^\top (x - x')), \quad (19)$$

where L is the accuracy level and each γ_j is a univariate point associated with the weight a_j . For a third-point rule with the points $\{-\hat{p}_1, 0, \hat{p}_1\}$ and their associated weights $(\hat{a}_1, \hat{a}_0, \hat{a}_1)$, the transformation matrix $\mathbf{W}_{\text{GQ}} \in \mathbb{R}^{s \times d}$ has entries W_{ij} following the distribution

$$\Pr(W_{ij} = \pm \hat{p}_1) = \hat{a}_1, \quad \Pr(W_{ij} = 0) = \hat{a}_0, \quad \forall i \in [s], j \in [d].$$

In general, the univariate Gaussian quadrature with L quadrature points is exact for polynomials up to $(2L - 1)$ degrees. The multivariate Gaussian quadrature is exact for all polynomials of the form $\omega_1^{i_1} \omega_2^{i_2} \cdots \omega_d^{i_d}$ with $1 \leq i_j \leq 2L - 1$; however the total number of points $s = L^d$ scales exponentially with the dimension d and thus this method suffers from the curse of dimensionality.

SGQ [40]: To alleviate the curse of dimensionality, SGQ uses the Smolyak rule [81] to decrease the needed number of points. Here we consider the third-degree SGQ using the symmetric univariate quadrature points $\{-\hat{p}_1, 0, \hat{p}_1\}$ with weights $(\hat{a}_1, \hat{a}_0, \hat{a}_1)$:

$$k(\mathbf{x}, \mathbf{x}') \approx (1 - d + d\hat{a}_0) g(\mathbf{0}) + \hat{a}_1 \sum_{j=1}^d [g(\hat{p}_1 \mathbf{e}_j) + g(-\hat{p}_1 \mathbf{e}_j)],$$

where the function g is defined in Eq. (8), and \mathbf{e}_i is the d -dimensional standard basis vector with the i -th element being 1. The corresponding transformation matrix is

$$\mathbf{W}_{\text{SGQ}} = [\mathbf{0}_d, \hat{p}_1 \mathbf{e}_1, \dots, \hat{p}_1 \mathbf{e}_d, -\hat{p}_1 \mathbf{e}_1, \dots, -\hat{p}_1 \mathbf{e}_d]^\top \in \mathbb{R}^{(2d+1) \times d},$$

which leads to the explicit feature mapping

$$\varphi(\mathbf{x}) = [\hat{a}_0 g(\mathbf{0}), \hat{a}_1 g(\mathbf{w}_2^\top \mathbf{x}), \dots, g(\mathbf{w}_{2d+1}^\top \mathbf{x})],$$

where \mathbf{w}_i is the i -th row of \mathbf{W}_{SGQ} . Note that SGQ generates $2d + 1$ points. To obtain a *dimension-adaptive* feature mapping, Dao et al. [40] propose to subsample the points according to the distribution determined by their weights such that the mapping feature dimension is equal to s .

SSR [41]: It transforms the d -dimensional integral in Eq. (8) to a double integral over a hypersphere and the real line. Let $\boldsymbol{\omega} = r\mathbf{u}$ with $\mathbf{u}^\top \mathbf{u} = 1$ for $r \in [0, \infty]$, we have

$$k(\mathbf{x} - \mathbf{x}') = \frac{1}{2} \int_{\mathbb{S}^{d-1}} \int_{-\infty}^{\infty} e^{-\frac{r^2}{2}} |r|^{d-1} g(r\mathbf{u}) dr d\mathbf{u}, \quad (20)$$

where the integrand g is given in Eq. (8). The inner integral in Eq. (20) can be approximated by stochastic *radial* rules of

degree $2l + 1$, i.e., $R(g) = \sum_{i=0}^l \hat{w}_i \frac{g(\rho_i) + g(-\rho_i)}{2}$. The outer integral over the d -sphere in Eq. (20) can be approximated by stochastic *spherical* rules: $S_Q(g) = \sum_{j=1}^q \tilde{w}_j g(Q\mathbf{v}_j)$, where Q is a random orthogonal matrix and \tilde{w}_j are stochastic weights whose distributions are such that the rule is exact for polynomials of degree q and gives unbiased estimate for other functions. Combining the above two rules, we have the SSR rule

$$k(\mathbf{x}, \mathbf{x}') \approx g(\mathbf{0}) \left(1 - \frac{d}{\vartheta^2}\right) + \frac{d}{d+1} \sum_{j=1}^{d+1} \frac{g(-\vartheta Q\mathbf{v}_j) + g(\vartheta Q\mathbf{v}_j)}{2\vartheta^2},$$

where $\vartheta \sim \chi(d+2)$ and $\{\mathbf{v}_j\}$ are the vertices of a unit regular d -simplex, which is randomly rotated by Q . Accordingly, the transformation matrix of SSR is

$$\mathbf{W}_{\text{SSR}} = \vartheta \otimes \begin{bmatrix} (\mathbf{Q}\mathbf{V})^\top \\ -(\mathbf{Q}\mathbf{V})^\top \end{bmatrix} \in \mathbb{R}^{2(d+1) \times d},$$

with $\vartheta = [\vartheta_1, \vartheta_2, \dots, \vartheta_s]$ and $\mathbf{V} = [\mathbf{v}_1, \mathbf{v}_2, \dots, \mathbf{v}_{d+1}]$. To get s features, one may stack $s/(2d+3)$ independent copies of \mathbf{W} as suggested by [41]. Finally, the feature mapping by SSR is given by

$$\varphi(\mathbf{x}) = [a_0 g(\mathbf{0}), a_1 g(\mathbf{w}_1^\top \mathbf{x}), \dots, g(\mathbf{w}_s^\top \mathbf{x})],$$

where $a_0 = \sqrt{1 - \sum_{j=1}^{d+1} \frac{d}{\rho_j^2}}$, $a_j = \frac{1}{\rho_j} \sqrt{\frac{d}{2(d+1)}}$ for $j \in [s]$, and w_j is the j -th element of the stacked \mathbf{W} .

4 DATA-DEPENDENT ALGORITHMS

Data-dependent approaches aim to design/learn the random features using the training data so as to achieve better approximation quality or generalization performance. Based on how the random features are generated, we can group these algorithms into three classes: *leverage score sampling*, *random features selection*, and *kernel learning by random features*.

4.1 Leverage score based sampling

Leverage score based approaches [16], [44], [82] are built on the *importance sampling* framework. Here one samples $\{\mathbf{w}_i\}_{i=1}^s$ from a distribution $q(\mathbf{w})$ that needs to be designed, and then uses the following feature mapping in Eq. (5):

$$\varphi_q(\mathbf{x}) = \frac{1}{\sqrt{s}} \left(\sqrt{\frac{p(\mathbf{w}_1)}{q(\mathbf{w}_1)}} e^{-i\mathbf{w}_1^\top \mathbf{x}}, \dots, \sqrt{\frac{p(\mathbf{w}_s)}{q(\mathbf{w}_s)}} e^{-i\mathbf{w}_s^\top \mathbf{x}} \right)^\top. \quad (21)$$

Consequently, we have the approximation

$$\begin{aligned} k(\mathbf{x}, \mathbf{x}') &= \mathbb{E}_{\mathbf{w} \sim q} [\varphi_q(\mathbf{x})^\top \varphi_q(\mathbf{x}')] \\ &\approx \tilde{k}_q(\mathbf{x}, \mathbf{x}') = \sum_{i=1}^s z_q(\mathbf{w}_i, \mathbf{x}) z_q(\mathbf{w}_i, \mathbf{x}'), \end{aligned}$$

where $z_q(\mathbf{w}_i, \mathbf{x}_j) := \sqrt{p(\mathbf{w}_i)/q(\mathbf{w}_i)} z_p(\mathbf{w}_i, \mathbf{x}_j)$. Thus, the kernel matrix \mathbf{K} can be approximated by $\mathbf{K}_q = \mathbf{Z}_q \mathbf{Z}_q^\top$, where $\mathbf{Z}_q := [\varphi_q(\mathbf{x}_1), \dots, \varphi_q(\mathbf{x}_n)]^\top \in \mathbb{R}^{n \times s}$. Denoting by $\mathbf{z}_{q, \mathbf{w}_i}(\mathbf{X})$ the i -th column of \mathbf{Z}_q , we have $\mathbf{K} = \mathbb{E}_{\mathbf{w} \sim p} [\mathbf{z}_{p, \mathbf{w}}(\mathbf{X}) \mathbf{z}_{p, \mathbf{w}}^\top(\mathbf{X})] = \mathbb{E}_{\mathbf{w} \sim q} [\mathbf{z}_{q, \mathbf{w}}(\mathbf{X}) \mathbf{z}_{q, \mathbf{w}}^\top(\mathbf{X})]$.

To design the distribution q , one makes use of the ridge leverage function [48], [49] in KRR:

$$l_\lambda(\mathbf{w}_i) = p(\mathbf{w}_i) \mathbf{z}_{p, \mathbf{w}_i}^\top(\mathbf{X}) (\mathbf{K} + n\lambda \mathbf{I})^{-1} \mathbf{z}_{p, \mathbf{w}_i}(\mathbf{X}), \quad (22)$$

where λ is the KRR regularization parameter. Define

$$d_K^\lambda := \int_{\mathbb{R}^d} l_\lambda(\mathbf{w}) d\mathbf{w} = \text{Tr} [\mathbf{K} (\mathbf{K} + n\lambda \mathbf{I})^{-1}]. \quad (23)$$

The quantity $d_K^\lambda \ll n$ determines the number of independent parameters in a learning problem and hence is referred to as the *number of effective degrees of freedom* [83]. With the above notation, the distribution q designed in [48] is given by

$$q(\mathbf{w}) := \frac{l_\lambda(\mathbf{w})}{\int l_\lambda(\mathbf{w}) d\mathbf{w}} = \frac{l_\lambda(\mathbf{w})}{d_K^\lambda}. \quad (24)$$

Compared to standard Monte Carlo sampling for RFF, leverage score sampling requires fewer Fourier features and enjoys nice theoretical guarantees [16], [48] (see the next section for details).

LS-RFF (Leverage Score-RFF) [16]: It uses a subset of data to approximate the matrix \mathbf{K} in Eq. (23) so as to compute d_K^λ :

$$\text{Tr}(\mathbf{K}(\mathbf{K} + n\lambda \mathbf{I}_n)^{-1}) \approx \text{Tr}(\mathbf{Z}^\top \mathbf{Z} (\mathbf{Z}^\top \mathbf{Z} + n\lambda \mathbf{I}_s)^{-1}),$$

where $\mathbf{Z} \in \mathbb{R}^{n \times s}$ is the feature matrix sampled from $q(\mathbf{w})$. LS-RFF needs $\mathcal{O}(ns^2 + s^3)$ time to generate refined random features, which can be used in KRR [16] and SVM [15] for prediction.

SLS-RFF (Surrogate Leverage Score-RFF) [44]: To avoid inverting an $s \times s$ matrix in LS-RFF, SLS-RFF designs a simple but effective surrogate leverage function

$$L_\lambda(\mathbf{w}) = p(\mathbf{w}) \mathbf{z}_{p, \mathbf{w}}^\top(\mathbf{X}) \left(\frac{1}{n^2 \lambda} (\mathbf{y} \mathbf{y}^\top + n\mathbf{I}) \right) \mathbf{z}_{p, \mathbf{w}}(\mathbf{X}), \quad (25)$$

where the additional term $n\mathbf{I}$ and the coefficient $1/(n^2 \lambda)$ in Eq. (25) ensure that L_λ is a *surrogate* function that upper bounds the function l_λ in Eq. (22). One then samples random features from the *surrogate* distribution $Q(\mathbf{w}) = \frac{L_\lambda(\mathbf{w})}{\int L_\lambda(\mathbf{w}) d\mathbf{w}}$, which has the same time complexity $\mathcal{O}(ns^2)$ as RFF. SLS-RFF and can be applied to KRR [44] and Canonical Correlation Analysis [82].

We mention that Yamasaki et al. [84] develop a quantum algorithm for sampling the optimized random features from $q(\mathbf{w})$. This algorithm achieves the same time complexity as the standard RFF [12]. Note that here the used optimized distribution $q(\mathbf{w})$ is defined by the integral operator [49] rather than the Gram matrix used above. One often does not strictly distinguish these two cases.

4.2 Re-weighted random features

Here we briefly review three re-weighted methods: KA-RFF [53] by kernel alignment, KP-RFF [42] by kernel polarization, and CLR-RFF [43] by compressed low-rank approximation.

KA-RFF (Kernel Alignment-RFF) [53]: It pre-computes a large number of random features that are generated by RFF, and then select a subset of them by solving a simple optimization problem based on kernel alignment [85]. In particular, the optimization problem is

$$\max_{\mathbf{a} \in \mathcal{P}_J} \sum_{i, j=1}^n y_i y_j \sum_{t=1}^J a_t z_p(\mathbf{x}_i, \mathbf{w}_t) z_p(\mathbf{x}_j, \mathbf{w}_t), \quad (26)$$

where $J > s$ is the number of the candidate random features by RFF, and \mathbf{a} is the weight vector. Here the maximization is over the set of distributions $\mathcal{P}_J := \{\mathbf{a} : D_f(\mathbf{a} \| \mathbf{1}/J) \leq c\}$, where $c > 0$ is a pre-specified constant and $D_f(P \| Q) := \int f(\frac{dP}{dQ}) dQ$ with $f(t) = t^2 - 1$ is the χ^2 -divergence between the distributions P and Q (a special case of the f -divergence). Solving the problem (26) learns a (sparse) weight vector \mathbf{a} of the candidate random features, so that the kernel matrix matches the target kernel $\mathbf{y} \mathbf{y}^\top$. Problem (26) can be efficiently solved via bisection over a scalar dual variable, and an ϵ -suboptimal solution can be found in $\mathcal{O}(J \log(1/\epsilon))$ time.

KP-RFF (Kernel Polarization-RFF) [42]: It first generates a large number of random features by RFF and then selects a subset from them using an energy-based scheme

$$\tilde{S}(\omega) = \frac{1}{n} \sum_{i=1}^n y_i z_p(\mathbf{x}_i, \omega).$$

Further, the quantity $(1/J) \sum_{i=1}^J \tilde{S}^2(\omega_j)$ can be associated with kernel polarization for $\{\mathbf{w}_i\}_{i=1}^J$ sampled from $p(\omega)$. Accordingly, the top s random features with the top $|\tilde{S}(\cdot)|$ values are selected as the refined random features. This algorithm can in fact be regarded as a version of the kernel alignment method for generating random features.

CLR-RFF (Compression Low Rank-RFF) [43]: It first generates a large number of random features and then selects a subset from them by approximately solving the optimization problem

$$\begin{aligned} \min_{\mathbf{a} \in \mathbb{R}^J: \|\mathbf{a}\|_0 \leq s} \frac{1}{n^2} \left\| \mathbf{Z}_J \mathbf{Z}_J^\top - \tilde{\mathbf{Z}}_J(\mathbf{a}) \tilde{\mathbf{Z}}_J(\mathbf{a})^\top \right\|_{\text{F}}^2 = \\ \mathbb{E}_{i, j \stackrel{\text{i.i.d.}}{\sim} [J]} \left[\varphi_p(\mathbf{x}_i)^\top \varphi_p(\mathbf{x}_j) - \tilde{\varphi}_p(\mathbf{x}_i)^\top \tilde{\varphi}_p(\mathbf{x}_j) \right], \end{aligned} \quad (27)$$

where $\varphi_p(\mathbf{x}) \in \mathbb{R}^J$ uses J random features, and $\tilde{\varphi}_p(\mathbf{x})$ is

$$\tilde{\varphi}_p(\mathbf{x}) := \frac{1}{\sqrt{J}} [a_1 \exp(-i\omega_1^\top \mathbf{x}), \dots, a_J \exp(-i\omega_J^\top \mathbf{x})]^\top,$$

which leads to $\tilde{\mathbf{Z}}_J(\mathbf{a}) = [\tilde{\varphi}_p(\mathbf{x}_1), \tilde{\varphi}_p(\mathbf{x}_2), \dots, \tilde{\varphi}_p(\mathbf{x}_n)] \in \mathbb{R}^{n \times J}$. We can construct a Monte-Carlo estimate of the optimization objective function in Eq. (27) by sampling some pairs $i, j \stackrel{\text{i.i.d.}}{\sim} [J]$. Therefore, this scheme focuses on a subset of pairs, instead of the all data pairs, by seeking a sparse weight vector \mathbf{a} with only s nonzero elements. The problem of building a small, weighted subset of the data that approximates the full dataset, is known as the *Hilbert coresset construction problem*. It can be approximately solved by greedy iterative geodesic ascent [86] or Frank-Wolfe based methods [87]. Another way to obtain the compact random features is using Johnson-Lindenstrauss random projection [88] instead of the above data-dependent optimization scheme.

4.3 Kernel learning by random features

This class of approaches construct random features using sophisticated learning techniques, e.g., by learning the spectral distribution of kernel from the data.

Representative approaches in this class often involve a *one-stage* or *two-stage* process. The two-stage scheme is common when using random features. It first learns the random features, and then incorporates them into kernel methods for prediction. Actually, the above-mentioned *leverage sampling* and *random features selection* based algorithms employ this scheme. The algorithm proposed in [67] is a typical method for kernel learning by random features. This method first learns a spectral distribution of a kernel via an implicit generative model, and then trains a linear model by these learned features.

One-stage algorithms aim to simultaneously learn the spectral distribution of a kernel and the prediction model by solving a single joint optimization problem or using a spectral inference scheme. For example, Yu et al. [68] propose to jointly optimize the nonlinear feature mapping matrix \mathbf{W} and the linear model with the hinge loss. The associated optimization problem can be solved in an alternating fashion with SGD. In [62], the kernel alignment approach in the Fourier domain and SVM are combined

into a unified framework, which can be also solved using an alternating scheme by Langevin dynamics and projection gradient descent. Wilson and Adams [69] construct stationary kernels as the Fourier transform of a Gaussian mixture based on Gaussian process frequency functions. This approach can be extended to learning with Fastfood [70], non-stationary spectral kernel generalization [61], [89], and the harmonizable mixture kernel [71]. Moreover, Oliva et al. [72] propose a nonparametric Bayesian model, in which $p(\omega)$ is modeled as a mixture of Gaussians with a Dirichlet process prior. The parameters of the Gaussian mixture and the classifier/regressor model are inferred using MCMC.

4.4 Algorithms for non-stationary kernels

The above methods are usually suitable for shift-invariant and rotation-invariant kernels. Here we briefly review approximation algorithms for non-stationary kernels.

In [29], the authors consider positive definite kernels of the form $k(\mathbf{x}, \mathbf{x}') = f(\langle \mathbf{x}, \mathbf{x}' \rangle)$, where f admits a Maclaurin expansion. The polynomial kernel $k(\mathbf{x}, \mathbf{x}') = (\langle \mathbf{x}, \mathbf{x}' \rangle)^b$ and the Hellinger's kernel $k(\mathbf{x}, \mathbf{x}') = \sqrt{\langle \mathbf{x}, \mathbf{x}' \rangle}$ [30] are two dot-product kernels of this form. The coefficients of the Maclaurin's expansion can be regarded as a positive measure, and thus one can sample from this distribution to construct estimators for each individual term of the expansion. In their algorithm implementation, an exponential tail distribution is used to ensure a sufficient amount randomness for estimating higher order terms. In [90], a feature hashing technique called Count Sketch [91] is used as a random projection scheme in a high dimensional space by simple independent hash functions. This method can be accelerated in the Fourier domain to achieve an $\mathcal{O}(nr(d + s \log s))$ time complexity and an $\mathcal{O}(rd \log s)$ space complexity. For polynomial kernels over a unit sphere, which are indefinite (real, symmetric, but not positive definite), and one can use Gaussian mixtures via RFF to approximate such kernels [34]. Approximation of more general indefinite kernels are considered in [58], which uses infinite Gaussian mixtures in a double-variational Bayesian framework. The authors of [3] introduce a new concomitant rank order kernel to approximate the Gaussian kernel on the unit sphere by the discrete cosine transform.

Besides, Li et al. [28] consider the extension of shift-invariant kernels to general locally compact groups, e.g., the χ^2 kernel. Histogram intersection kernels are investigated in the work [92] and are further generalized to a class of additive homogeneous kernels in [30].

5 THEORETICAL ANALYSIS

In this section, we review a range of theoretical results that center around the two questions mentioned in the introduction and restated below:

- 1) **Approximation:** how many random features are needed to ensure a high quality estimator in kernel approximation?
- 2) **Generalization:** how many random features are needed to incur no loss of empirical risk and expected risk in a learning estimator?

Figure 3 provides a taxonomy of representative work on these two questions.

For the approximation error, existing work focuses on the error metrics $\|k - \tilde{k}\|_\infty$ [12], [45], [46], $\|k - \tilde{k}\|_{L^r}$ with $1 \leq r < \infty$ [46], Δ -spectral approximation [48], [76], and (Δ_1, Δ_2) -spectral approximation [14]. For the empirical risk under the fixed design

approximation error	$\left\{ \begin{array}{l} \ k - \tilde{k}\ _\infty: [12], [45], [46], [47] \\ \ k - \tilde{k}\ _{L^r}: [46] \\ \Delta\text{-spectral approximation: [48], [76]} \\ (\Delta_1, \Delta_2)\text{-spectral approximation: [14]} \end{array} \right.$
empirical risk: [14], [48]	
expected risk	$\left\{ \begin{array}{l} \text{squared loss} \left\{ \begin{array}{l} \omega \sim p(\omega): [16], [50] \\ \omega \sim q(\omega): [16] \end{array} \right. \\ \text{Lipschitz continuous} \left\{ \begin{array}{l} \omega \sim p(\omega): [16], [93] \\ \omega \sim q(\omega): [15], [16], [49] \end{array} \right. \end{array} \right.$

Figure 3. Taxonomy of theoretical results on random features.

setting, existing work provides guarantees on the expected in-sample predication error of the KRR estimator based on Δ -spectral approximation bounds [48] and (Δ_1, Δ_2) -spectral approximation bounds [14]. For the expected risk, a series of works investigate the generalization properties of methods based on $p(\omega)$ -sampling (i.e., random features are sampled from the distribution p given by Bochner's Theorem) or $q(\omega)$ -sampling (i.e., random features are sampled from the leverage score based distribution q). These results cover loss functions with/without Lipschitz continuity and apply to e.g. KRR [16], [50] and SVM [15], [27], [49] under different assumptions.

More specifically, Rahimi and Recht [27] provide the earliest result on learning with RFF with Lipschitz continuous loss functions. Their results imply that $\Omega(n)$ random features are sufficient to incur no loss of learning accuracy. This result is improved in [16], which shows that $\Omega(\sqrt{n} \log n)$ random features or even less suffice for the Gaussian kernel. When using the data-dependent sampling $\{\omega_i\}_{i=1}^s \sim q(\omega)$, the above results are further improved in [15], [16], [49] under various settings. Note that some results above do not directly apply to the squared loss in KRR, whose Lipschitz parameter is unbounded. For squared losses, Rudi et al. [50] show that $\Omega(\sqrt{n} \log n)$ random features by RFF suffice to achieve a minimax optimal learning rate $\mathcal{O}(1/\sqrt{n})$. A more refined analysis is given in [16] under the $p(\omega)$ -sampling and $q(\omega)$ -sampling settings.

Below we discuss the above theoretical work in more details.

5.1 Approximation error

Table 2 summarizes representative theoretical results on the convergence rates, the upper bound of the growing diameter, and the resulting sample complexity under different metrics. Here sample complexity means the number of random features sufficient for achieving a maximum approximation error at most ϵ .

The first result of this kind is given by Rahimi and Recht [12], who use a covering number argument to derive a uniform convergence guarantee as follows. For a compact subset \mathcal{S} of \mathbb{R}^d , let $|\mathcal{S}| := \sup_{\mathbf{x}, \mathbf{x}' \in \mathcal{S}} \|\mathbf{x} - \mathbf{x}'\|_2$ be its diameter and consider the L^∞ error $\|k - \tilde{k}\|_\infty := \sup_{\mathbf{x}, \mathbf{x}' \in \mathcal{S}} |k(\mathbf{x}, \mathbf{x}') - \tilde{k}(\mathbf{x}, \mathbf{x}')|$.

Theorem 3 (Uniform convergence of RFF [12], [45]). *Let \mathcal{S} be a compact subset of \mathbb{R}^d with diameter $|\mathcal{S}|$. Then, for a shift-invariant kernel k and its approximated kernel \tilde{k} obtained by RFF, we have*

$$\Pr \left[\|k - \tilde{k}\|_\infty \geq \epsilon \right] \leq C_d \left(\frac{\sigma_p |\mathcal{S}|}{\epsilon} \right)^{\frac{2d}{d+2}} \exp \left(-\frac{s\epsilon^2}{4(d+2)} \right),$$

where $\sigma_p^2 = \mathbb{E}_p[\omega^\top \omega] = \text{Tr} \nabla^2 k(0) \in \mathcal{O}(d)$ is the second moment of the Fourier transform of k , and $C_d := 2^{\frac{6d+2}{d+2}} \left(\left(\frac{2}{d} \right)^{\frac{d}{d+2}} + \left(\frac{d}{2} \right)^{\frac{2}{d+2}} \right)$ satisfies $C_d \leq 256$ in [12] and is further improved to $C_d \leq 66$ in [45].

According to the above theorem, with $s := \Omega(\epsilon^{-2} d \log(1/\epsilon\delta))$ random features, one can ensure an ϵ uniform approximation error with probability greater than $1 - \delta$. This result also applies to dot-product kernels by random Maclaurin feature maps (see Theorem 8 in [29]).

Sriperumbudur and Szabó [46] revisit the above bound by using a Rademacher complexity approach instead of covering numbers.

Theorem 4 (Theorem 1 in [46]). *Under the same assumption of Theorem 3, we have*

$$\Pr \left[\|k - \tilde{k}\|_\infty \geq \frac{h(d, |\mathcal{S}|, \sigma_p) + \sqrt{2\epsilon}}{\sqrt{s}} \right] \leq e^{-\epsilon},$$

where $h(d, |\mathcal{S}|, \sigma_p)$ is an appropriately defined function of d , $|\mathcal{S}|$, and σ_p . For better comparison, the above inequality can be rewritten as [47]

$$\Pr \left[\|k - \tilde{k}\|_\infty \geq \epsilon \right] \leq [(\sigma_p + 1)(2|\mathcal{S}| + 1)]^{1024d} \exp \left(-\frac{s\epsilon^2}{2} + \frac{256d}{\log(2|\mathcal{S}| + 1)} \right).$$

Theorem 4 shows that \tilde{k} is a consistent estimator of k in the topology of compact convergence as $s \rightarrow \infty$ with the convergence rate $\mathcal{O}_p(\sqrt{s^{-1} \log |\mathcal{S}|})$. Consequently, $\mathcal{O}(\epsilon^{-2} \log |\mathcal{S}|)$ random features suffice to achieve an ϵ approximation accuracy. This sample complexity bound scales logarithmically with $|\mathcal{S}|$, which improves upon the $\mathcal{O}(\epsilon^{-2} |\mathcal{S}|^2 \log(|\mathcal{S}|/\epsilon))$ bound that follows from [12], [45] (cf. Theorem 3).

For the Gaussian kernel, the approximation guarantee can be further improved. In particular, the following theorem gives a probability bound independent of d .

Theorem 5 (Theorem 1 in [47]). *Under the same assumption of Theorem 3, for the Gaussian kernel k and its approximation \tilde{k} by RFF, we have*

$$\Pr \left[\|k - \tilde{k}\|_\infty \geq \epsilon \right] \leq \frac{3}{s^{1/3}} \left(\frac{|\mathcal{S}|}{\epsilon} \right)^{2/3} \exp \left(-\frac{s\epsilon^2}{12} \right).$$

When translated to a guarantee for approximating the n -by- n kernel matrix \mathbf{K} , the above three results require $\Omega(n)$ random features [16]. Based on the L^∞ error bound in Theorem 4, the authors of [46] further derive bounds on the L^r error $\|k - \tilde{k}\|_{L^r} := \int_{\mathcal{S}} \int_{\mathcal{S}} |k(\mathbf{x}, \mathbf{x}') - \tilde{k}(\mathbf{x}, \mathbf{x}')| d\mathbf{x} d\mathbf{x}'$ for $1 \leq r < \infty$; see Table 2 for a summary.

Avron et al. [48] argue that the above point-wise distances $\|k - \tilde{k}\|_\infty$ or $\|k - \tilde{k}\|_{L^r}$ are not sufficient to accurately measure the approximation quality. Instead, they focus on the following spectral approximation criterion.

Definition 1 (Δ -spectral approximation [48]). *For $0 \leq \Delta < 1$, a symmetric matrix \mathbf{A} is a Δ -spectral approximation of another symmetric matrix \mathbf{B} , if $(1 - \Delta)\mathbf{B} \preceq \mathbf{A} \preceq (1 + \Delta)\mathbf{B}$.*

According to this definition, $\mathbf{Z}\mathbf{Z}^\top + \lambda\mathbf{I}_n$ is Δ -spectral approximation of $\mathbf{K} + \lambda\mathbf{I}_n$ if

$$(1 - \Delta)(\mathbf{K} + \lambda\mathbf{I}_n) \preceq \mathbf{Z}\mathbf{Z}^\top + \lambda\mathbf{I}_n \preceq (1 + \Delta)(\mathbf{K} + \lambda\mathbf{I}_n).$$

Table 2
Comparison of convergence rates and required random features for kernel approximation error.

Metric	Results	Convergence rate	Upper bound of $ \mathcal{S} $	Required random features s
$\ k - \tilde{k}\ _\infty$	Theorem 3 ([12], [45])	$\mathcal{O}_p\left(\mathcal{S} \sqrt{\frac{\log s}{s}}\right)$	$ \mathcal{S} \leq \Omega\left(\sqrt{\frac{s}{\log s}}\right)$	$s \geq \Omega\left(d\epsilon^{-2} \log \frac{ \mathcal{S} }{\epsilon}\right)$
	Theorem 4 (Theorem 1 in [46])	$\mathcal{O}_p\left(\sqrt{\frac{\log \mathcal{S} }{s}}\right)$	$ \mathcal{S} \leq \Omega(s^c)^1$	$s \geq \Omega(d\epsilon^{-2} \log \mathcal{S})$
	Theorem 5 (Theorem 1 in [47])	$\mathcal{O}_p\left(\sqrt{\frac{\log \mathcal{S} }{s}}\right)$	$ \mathcal{S} \leq \Omega(s^c)$	$s \geq \Omega(\epsilon^{-2} \log \mathcal{S})$
$\ k - \tilde{k}\ _{L^r}$ ($1 \leq r < \infty$)	(Corollary 2 in [46])	$\mathcal{O}_p\left(\mathcal{S} ^{\frac{2d}{r}} \sqrt{\frac{\log \mathcal{S} }{s}}\right)$	$ \mathcal{S} \leq \Omega\left(\left(\frac{s}{\log s}\right)^{\frac{r}{4d}}\right)$	$s \geq \Omega(d\epsilon^{-2} \log \mathcal{S})$
$\ k - \tilde{k}\ _{L^r}$ ($2 \leq r < \infty$)	(Theorem 3 in [46])	$\mathcal{O}_p\left(\mathcal{S} ^{\frac{2d}{r}} \sqrt{\frac{1}{s}}\right)$	$ \mathcal{S} \leq \Omega\left(s^{\frac{r}{4d}}\right)$	$s \geq \Omega(d\epsilon^{-2} \log \mathcal{S})$
Δ -spectral approximation	Theorem 6 (Theorem 7 in [48])	$\mathcal{O}_p\left(\sqrt{\frac{n\lambda}{s}}\right)$	-	$s \geq \Omega(n_\lambda \log d_K^\lambda)$
	Theorem 7 (Theorem 5.4 in [76])	$\mathcal{O}_{\text{RFF/ORF}}\left(\frac{1}{s\lambda^2}\right)$	-	$s \geq \Omega(n^{2\alpha})$
	Theorem 8 (Lemma 6 in [48])	$\mathcal{O}_q\left(\sqrt{\frac{d_K^\lambda}{s}}\right)$	-	$s \geq \Omega(d_K^\lambda \log d_K^\lambda)$
(Δ_1, Δ_2) -spectral approximation	Theorem 9 (Theorem 2 in [14])	$\mathcal{O}_{\text{LP}}\left(\sqrt{\frac{n\lambda}{s}}\right)^2$	-	$s \geq \Omega(n_\lambda \log d_K^\lambda)$

¹ c is some constant satisfying $0 < c < 1$.

² LP denotes that $\{\omega_i\}_{i=1}^s$ are obtained by RFF and then are quantized to a Low-Precision b -bit representation; see [14].

The follow theorem gives the number of random features s that are sufficient to guarantee Δ -spectral approximation.

Theorem 6 (Theorem 7 in [48]). *Let k be a shift-invariant kernel and its associated probability distribution $p(\omega)$ (i.e., the Fourier transform of k), $\Delta \leq 1/2$, $\delta \in (0, 1)$, and $n_\lambda := n/\lambda$. Assume that $\|\mathbf{K}\|_2 \geq \lambda$ and $\{\omega_i\}_{i=1}^s \sim p(\omega)$. If the total number of random features satisfies*

$$s \geq \frac{8}{3} \Delta^{-2} n_\lambda \log\left(16d_K^\lambda/\delta\right),$$

then

$$\begin{aligned} \Pr\left[(1-\Delta)(\mathbf{K} + \lambda\mathbf{I}_n) \preceq \mathbf{Z}\mathbf{Z}^\top + \lambda\mathbf{I}_n \preceq (1+\Delta)(\mathbf{K} + \lambda\mathbf{I}_n)\right] \\ \geq 1 - 16d_K^\lambda \exp\left(\frac{-3s\Delta^2}{8n_\lambda}\right) \geq 1 - \delta. \end{aligned}$$

Theorem 6 shows that for standard random Fourier features, $\Omega(n)$ features suffice for spectral approximation, which similar to the sample complexity for point-wise approximation. Further, Choromanski et al. [76] present a non-asymptotic comparison result between RFF and ORF for spectral approximation.

Theorem 7 (Theorem 5.4 in [76]). *For the Gaussian kernel, let $\tilde{\Delta}$ be the smallest positive number such that $\tilde{\mathbf{K}} + \lambda n\mathbf{I}_n$ is a $\tilde{\Delta}$ -spectral approximation of $\mathbf{K} + \lambda n\mathbf{I}_n$, where $\tilde{\mathbf{K}}$ is an approximate kernel matrix obtained by RFF or ORF. Then, for any $\epsilon > 0$ we have*

$$\Pr[\tilde{\Delta} > \epsilon] \leq \frac{B}{\epsilon^2 \sigma_{\min}^2},$$

where $B := \mathbb{E}[\|\tilde{\mathbf{K}} - \mathbf{K}\|_{\text{F}}^2]$ and σ_{\min}^2 is the smallest singular value of $\mathbf{K} + \lambda n\mathbf{I}_n$. In particular, letting B^{ORF} denotes the value of B for the estimator ORF and B^{RFF} for RFF, we have

$$B^{\text{RFF}} - B^{\text{ORF}} = \frac{s-1}{s} \left(\frac{1}{2d} \sum_{i,j=1}^n \frac{\|\mathbf{x}_i - \mathbf{x}_j\|_2^4}{\sigma^2} e^{-\frac{\|\mathbf{x}_i - \mathbf{x}_j\|_2^2}{\sigma^2}} + \mathcal{O}\left(\frac{1}{d}\right) \right).$$

Theorem 7 shows that $B^{\text{RFF}} > B^{\text{ORF}}$ always holds for the Gaussian kernel. To better understand the above upper bound on $\Pr[\tilde{\Delta} > \epsilon]$, we note that both $\mathbb{V}[\text{RFF}]$ and $\mathbb{V}[\text{ORF}]$ are $\mathcal{O}(1/s)$, hence $B = \mathcal{O}(n^2/s)$. Moreover, since the Gaussian kernel has exponentially decaying eigenvalues (see Assumption 4), we have $\sigma_{\min}^2 = \Omega(n^2 \lambda^2)$. Therefore, the upper bound of $\Pr[\tilde{\Delta} > \epsilon]$ is on the order of $\mathcal{O}(\frac{1}{s\lambda^2})$. With the standard scaling of the regularization parameter $\lambda = n^{-\alpha}$, $\alpha \in (0, 1]$, we need $s := \Omega(n^{2\alpha})$ to get a non-trivial upper bound on the probability. When $\alpha = 1/2$, these results for RFF and ORF require $\Omega(n)$ random Fourier features, which is somewhat unsatisfactory [16].

The results in Theorem 6 can be improved if we consider data-dependent sampling, i.e., $\{\omega_i\}_{i=1}^s$ are sampled from the empirical ridge leverage score distribution $q(\omega) = l_\lambda(\omega)/d_K^\lambda$ in Eq. (24) instead of the standard $p(\omega)$.

Theorem 8 (Lemma 6 in [48]). *Let k be a shift-invariant kernel associated with the empirical ridge leverage score distribution $q(\omega)$ in Eq. (24), $\Delta \leq 1/2$ and $\delta \in (0, 1)$. Assume that $\|\mathbf{K}\|_2 \geq \lambda$ and $\{\omega_i\}_{i=1}^s \sim q(\omega)$. If the total number of random features satisfies*

$$s \geq \frac{8}{3} \Delta^{-2} d_K^\lambda \log\left(16d_K^\lambda/\delta\right),$$

then

$$\begin{aligned} \Pr\left[(1-\Delta)(\mathbf{K} + \lambda\mathbf{I}_n) \preceq \mathbf{Z}\mathbf{Z}^\top + \lambda\mathbf{I}_n \preceq (1+\Delta)(\mathbf{K} + \lambda\mathbf{I}_n)\right] \\ \geq 1 - 16d_K^\lambda \exp\left(\frac{-3s\Delta^2}{8d_K^\lambda}\right) \geq 1 - \delta. \end{aligned}$$

Theorem 8 shows that if we sample using the ridge leverage function, then $\Omega(d_K^\lambda \log d_K^\lambda)$ random features, which is less than $\Omega(n_\lambda \log d_K^\lambda)$, suffice for spectral approximation of \mathbf{K} .

The authors of [14] generalize the notion of Δ -spectral approximation to (Δ_1, Δ_2) -spectral approximation.

Definition 2 $((\Delta_1, \Delta_2)$ -spectral approximation [14]). *For $\Delta_1, \Delta_2 \geq 0$, a symmetric matrix \mathbf{A} is a (Δ_1, Δ_2) -*

spectral approximation of another symmetric matrix \mathbf{B} , if $(1 - \Delta_1)\mathbf{B} \preceq \mathbf{A} \preceq (1 + \Delta_2)\mathbf{B}$.

This definition is motivation by the argument that the quantities Δ_1 and Δ_2 in the upper and lower bounds may have different impact on the generalization performance. Using this definition, Zhang et al. [14] derive the following approximation guarantees when one quantizes each random Fourier feature ω_i to a low-precision b -bit representation, which allows more features to be stored in the same amount of space.

Theorem 9 (Theorem 2 in [14]). *Let $\tilde{\mathbf{K}}$ be an s -features b -bit LP-RFF approximation of a kernel matrix \mathbf{K} and $\delta \in (0, 1)$. Assume that $\|\mathbf{K}\|_2 \geq \lambda \geq \delta_b^2 = 2/(2^b - 1)^2$ and define $a := 8 \operatorname{Tr}(\mathbf{K} + \lambda \mathbf{I}_n)^{-1}(\mathbf{K} + \delta_b^2 \mathbf{I}_n)$. For $\Delta_1 \leq 3/2$ and $\Delta_2 \in [\frac{\delta_b^2}{\lambda}, \frac{3}{2}]$, if the total number of random features satisfies*

$$s \geq \frac{8}{3} n_\lambda \max \left\{ \frac{2}{\Delta_1}, \frac{2}{\Delta_2 - \delta_b^2/\lambda} \right\} \log \left(\frac{a}{\delta} \right),$$

then

$$\begin{aligned} \Pr \left[(1 - \Delta_1)(\mathbf{K} + \lambda \mathbf{I}_n) \preceq \tilde{\mathbf{K}} + \lambda \mathbf{I}_n \preceq (1 + \Delta_2)(\mathbf{K} + \lambda \mathbf{I}_n) \right] \\ \geq 1 - a \left[\exp \left(\frac{-3s\Delta_1^2}{4n_\lambda(1+2/3\Delta_1)} \right) \right. \\ \left. + \exp \left(\frac{-3s(\Delta_2 - \delta_b^2/\lambda)^2}{4n_\lambda(1+2/3(\Delta_2 - \delta_b^2/\lambda))} \right) \right]. \end{aligned}$$

Theorem 9 shows that when the quantization noise is small relative to the regularization parameter, using low precision has minimal impact on the number of features required for the (Δ_1, Δ_2) -spectral approximation. In particular, as $s \rightarrow \infty$, Δ_1 converges to zero for any precision b , whereas Δ_2 converges to a value upper bounded by δ_b^2/λ . If $\delta_b^2/\lambda \ll \Delta_2$, using b -bit precision has negligible effect on the number of features required to attain this Δ_2 .

5.2 Risk and generalization property

The above results on approximation error are a means to an end. More directly related to the learning performance is understanding the expected risk and generalization properties of random features based algorithms. To this end, a series of research works investigate the generalization properties of algorithms based on $p(\omega)$ -sampling and $q(\omega)$ -sampling. Under different assumptions, theoretical results have been obtained for loss functions with/without Lipschitz continuity and for learning tasks including KRR [16], [50] and SVM [15], [27], [49].

5.2.1 Assumptions

Before we detail these theoretical results, we summarize the standard assumptions imposed in existing work. Some assumptions are technical, and thus familiarity with statistical learning theory (see Section 2.2) would be helpful. We organize these assumptions in four categories as shown in Figure 4, including i) the existence of f_ρ (Assumption 1) and its stronger version (Assumption 8); ii) quality of random features (Assumptions 2, 6, 7); iii) noise conditions (Assumptions 3, 9, 10); iv) eigenvalue decay (Assumptions 4, 5).

We first state three basic assumptions, which are needed in all of the results to be presented.

Assumption 1 (Existence [50]). *We assume that the target function f_ρ exists almost surely.*

Note that since we consider a potentially infinite dimensional RKHS \mathcal{H} , possibly universal [94], the existence of the target function f_ρ is not automatic. However, if we restrict to a bounded subspace of \mathcal{H} , i.e., $\mathcal{H}_R = \{f \in \mathcal{H} : \|f\| \leq R\}$ with $R < \infty$ fixed a prior, then a minimizer of the risk $\mathcal{E}(f)$ always exists as long as \mathcal{H}_R is not universal. If f_ρ exists, then it must lie in a ball of some radius $R_{\rho, \mathcal{H}}$. The results in this section do not require prior knowledge of $R_{\rho, \mathcal{H}}$ and they hold for any finite radius.

Assumption 2 (Random features are bounded and continuous). *For the shift-invariant kernel k , we assume that $z(\omega, \mathbf{x})$ in Eq. (6) is continuous in both variables and bounded, i.e., there exists $\kappa \geq 1$ such that $|z(\omega, \mathbf{x})| < \kappa$ for all $\mathbf{x} \in \mathcal{X}$ and $\omega \in \mathbb{R}^d$.*

Assumption 3 (Output condition on y). *For any $\mathbf{x} \in \mathcal{X}$,*

$$\mathbb{E} [|y|^t | \mathbf{x}] \leq \frac{1}{2} t! \sigma^2 B^{t-2}, \quad \forall t = 2, 3, 4, \dots$$

The last assumption, sometimes called the Bernstein's condition [95], is weaker than boundedness on y . It is satisfied when y is bounded, sub-Gaussian, or sub-exponential. In particular, if $y \in [-\frac{b}{2}, \frac{b}{2}]$ almost surely with $b > 0$, then Assumption 3 is satisfied with $\sigma = B = b$.

The above three assumptions are needed in all theoretical results presented in this section, so we omit them when stating these results. We next introduce several additional assumptions, which are needed in some of the theoretical results.

Eigenvalue Decay Assumptions: The following assumption, which characterizes the “size of the RKHS \mathcal{H} of interest, is required in many results for random features based algorithms. We write $u_i = \Theta(v_i)$, if there exist two strictly positive constants A and B such that $Au_i \leq v_i \leq Bu_i$ for all $i = 1, 2, \dots, n$.

Assumption 4 (Eigenvalue decays [49], [83]). *Assume that the eigenvalues of a kernel matrix \mathbf{K} have the form $\lambda_i = \Theta(nv_i)$, $i = 1, 2, \dots, n$, so $\operatorname{Tr}(\mathbf{K}) = \Theta(n \sum_i v_i)$. We consider the following three types of eigenvalue decays:*

- Geometric/exponential decay: $v_i = \mathcal{O}(\exp(-i^{1/c}))$ for some $c > 0$, which means $\lambda_i \propto n \exp(-i^{1/c})$. This condition holds for the Gaussian kernel with a sub-Gaussian marginal distribution $\rho_{\mathcal{X}}$. In this case, we have $d_{\mathbf{K}}^\lambda \leq \log(R_0/\lambda)$, where $R_0^2 := \mathbb{E} k(\mathbf{x}, \mathbf{x})$.
- Polynomial decay: $v_i = \mathcal{O}(i^{-2t})$ for some $t > \frac{1}{2}$, which means $\lambda_i \propto ni^{-2t}$. This condition holds when, e.g., \mathcal{H} is a Sobolev space. In this case we have $d_{\mathbf{K}}^\lambda \leq (1/\lambda)^{1/2t}$.
- Slowest polynomial decay: $v_i = \mathcal{O}(1/i)$, which means $\lambda_i \propto n/i$. In this case we have $d_{\mathbf{K}}^\lambda \leq (1/\lambda)$.

We give some remarks on the above assumption. For shift-invariant kernels, if the RKHS is small, the eigenvalues of the kernel matrix \mathbf{K} often admit a fast decay. Consequently, functions in the RKHS are smooth enough that a good prediction performance can be achieved. On the other hand, if the RKHS is large and the eigenvalues decay slowly, then functions in the RKHS are not smooth, which would lead to a sub-optimal error rate for prediction.

To make the above description precise, we introduce a key quantity, namely the integral operator [49], [50] defined by the kernel k and the marginal distribution $\rho_{\mathcal{X}}$. In particular, define the integral operator $\Sigma : L_{\rho_{\mathcal{X}}}^2 \rightarrow L_{\rho_{\mathcal{X}}}^2$ as

$$(\Sigma g)(\mathbf{x}) = \int_{\mathcal{X}} k(\mathbf{x}, \mathbf{x}') g(\mathbf{x}') d\rho_{\mathcal{X}}(\mathbf{x}'), \quad \forall g \in L_{\rho_{\mathcal{X}}}^2.$$

Since $\int_{\mathcal{X}} k(\mathbf{x}, \mathbf{x}) d\rho(\mathbf{x})$ is finite, the operator Σ is self-adjoint, positive definite, and trace-class. This operator can be represented

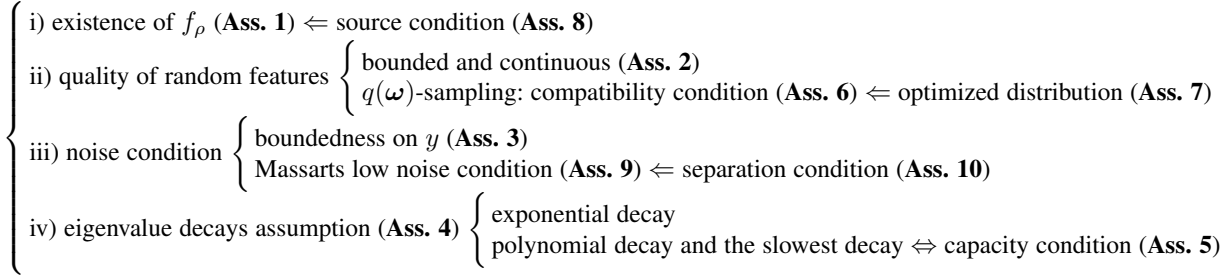


Figure 4. Relationship between the needed assumptions. The notation $A \Leftarrow B$ means that B is a stronger assumption than A.

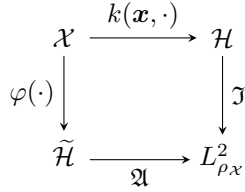


Figure 5. Maps between various spaces.

as $\Sigma = J J^*$ in terms of the inclusion operator $J : \mathcal{H} \rightarrow L^2_{\rho_X}$, $(Jf) = f$. Here J^* is the adjoint of J and is given by

$$J^* : L^2_{\rho_X} \rightarrow \mathcal{H}, (J^*f)(\cdot) = \int_{\mathcal{X}} k(\mathbf{x}, \cdot) f(\mathbf{x}) d\rho_{\mathcal{X}},$$

due to the self-adjoint property of the Hilbert spaces $L^2_{\rho_X}$ and \mathcal{H} [96]. With s random features, the inclusion operator J can be approximated by the operator $\mathfrak{A} : \tilde{\mathcal{H}} \rightarrow L^2_{\rho_X}$, $(\mathfrak{A}\beta) = \langle \varphi(\cdot), \beta \rangle_{\tilde{\mathcal{H}}}$, $\forall \beta \in \mathbb{R}^s$. Figure 5 presents the relationship between various spaces under different operators.

The integral operator Σ plays a significant role in characterizing the hypothesis space. In particular, the decay rate of the spectrum of Σ quantifies the capacity of the hypothesis space in which we search for the solution. This capacity in turn determines the number of random features required for accurate learning. Rudi and Rosasco [50] consider the following assumption on Σ .

Assumption 5 (Capacity condition [97], [98]). *Let $\lambda > 0$. There exist $Q > 0$ and $\gamma \in [0, 1]$ such that for any $\lambda > 0$, we have*

$$\begin{aligned} \mathcal{N}(\lambda) := \text{tr}((\Sigma + \lambda I)^{-1}\Sigma) &= \mathbb{E}_{\omega} \left\| (\Sigma + \lambda I)^{-1/2} \varphi(\mathbf{x}) \right\|_{L^2_{\rho_X}}^2 \\ &\leq Q^2 \lambda^{-\gamma}. \end{aligned} \quad (28)$$

The effective dimension $\mathcal{N}(\lambda)$ measures the “size” of the RKHS, and is in fact the operator form of d_K^{λ} in Eq. (23). Assumption 5 holds if the eigenvalues λ_i of Σ decay as $i^{-1/\gamma}$, which covers the polynomial decay and the slowest decay in Assumption 4 with $\gamma := 1/(2t)$. The case $\gamma = 0$ is the more benign situation, whereas $\gamma = 1$ is the worst case.

Quality of Random Features: Here we introduce several technical assumptions on the quality of random features. The leverage score in Eq. (22) admits the operator form

$$\mathcal{F}_{\infty}(\lambda) := \sup_{\omega} \left\| (\Sigma + \lambda I)^{-1/2} \varphi(\mathbf{x}) \right\|_{L^2_{\rho_X}}^2, \quad \forall \lambda > 0,$$

which is also called as the *maximum random features dimension* [50]. By definition we always have $\mathcal{N}(\lambda) \leq \mathcal{F}_{\infty}(\lambda)$. Roughly speaking, when the random features are “good”, it is easy to

control their leverage scores in terms of the decay of the spectrum of Σ . Further, fast learning rates using fewer random features can be achieved if the features are *compatible* with the data distribution in the following sense.

Assumption 6 (Compatibility condition [50]). *With the above definition of $\mathcal{F}_{\infty}(\lambda)$, assume that there exist $\varrho \in [0, 1]$, and $F > 0$ such that $\mathcal{F}_{\infty}(\lambda) \leq F\lambda^{-\varrho}$, $\forall \lambda > 0$.*

It always holds that $\mathcal{F}_{\infty}(\lambda) \leq \kappa^2 \lambda^{-1}$ when z is uniformly bounded by κ . Therefore, the worst case is $\varrho = 1$, which means that the random features are sampled in a problem independent way. The favorable case is $\varrho = \gamma$, which means that $\mathcal{N}(\lambda) \leq \mathcal{F}_{\infty}(\lambda) \leq \mathcal{O}(n^{-\alpha\gamma})$. In [15], the authors consider the following assumption.

Assumption 7 (Optimized distribution [15]). *The feature mapping $z(\omega, \mathbf{x})$ is called optimized if there is a small constant λ_0 such that for any $\lambda \leq \lambda_0$*

$$\mathcal{F}_{\infty}(\lambda) \leq \mathcal{N}(\lambda) = \sum_{i=1}^{\infty} \frac{\lambda_i(\Sigma)}{\lambda_i(\Sigma) + \lambda}.$$

Under the previous definitions, Assumption 7 holds only when $\mathcal{F}_{\infty}(\lambda) = \mathcal{N}(\lambda)$. This assumption is stronger than the compatibility condition in Assumption 6. Note that Assumption 7 is satisfied when sampling from the leverage score distribution $q(\omega)$.

Source condition on f_{ρ} : The following assumption states that f_{ρ} has some desirable regularity properties.

Assumption 8 (Source condition [50]). *There exist $1/2 \leq r \leq 1$ and $g \in L^2_{\rho_X}$ such that*

$$f_{\rho}(\mathbf{x}) = (\Sigma^r g)(\mathbf{x}) \quad \text{almost surely}.$$

Since the integral operator Σ is a compact positive operator on $L^2_{\rho_X}$, its r -th power Σ^r is well defined for any $r > 0$.⁴ Assumption 8 imposes a form of regularity/sparsity of f_{ρ} , which requires the expansion of f_{ρ} on the basis given by the integral operator Σ . Note that this assumption is more stringent than the existence of f_{ρ} in \mathcal{H} . The latter is equivalent to Assumption 8 with $r = \frac{1}{2}$ (the worst case), in which case $f_{\rho} \in \mathcal{H}$ need not have much regularity/sparsity.

Noise Condition: Sun et al. [15] consider the following two assumptions pertaining to the noisiness of the output/label.

Assumption 9 (Massart’s low noise condition [15]). *There exists $V \geq 2$ such that*

$$|\mathbb{E}_{(\mathbf{x}, y) \sim \rho}[y | \mathbf{x}]| \geq 2/V.$$

4. This assumption is also termed as the regularity condition. This more general condition (with $r > 0$) is often considered in approximation theory; see [99], [100].

Table 3
Comparison of learning rates and required random features for expected risk with the squared loss function.

sampling scheme	Results	key assumptions	eigenvalue decays	λ	learning rates	required s
	Theorem 1 in [50]	-	-	$n^{-\frac{1}{2}}$	$\mathcal{O}_p\left(n^{-\frac{1}{2}}\right)$	$s \geq \Omega(\sqrt{n} \log n)$
$\{\omega_i\}_{i=1}^s \sim p(\omega)$			i^{-2t}	$n^{-\frac{2t}{1+4rt}}$	$\mathcal{O}_p\left(n^{-\frac{4rt}{1+4rt}}\right)$	$s \geq \Omega(\frac{2t+2r-1}{1+4rt} \log n)$
	Theorem 2 in [50]	source condition	$1/i$	$n^{-\frac{1}{2r+1}}$	$\mathcal{O}_p\left(n^{-\frac{2r}{2r+1}}\right)$	$s \geq \Omega(n^{\frac{2r}{2r+1}} \log n)$
			$e^{-\frac{1}{c}i}$	$n^{-\frac{1}{2}}$	$\mathcal{O}_p\left(n^{-\frac{1}{2}}\right)$	$s \geq \Omega(\sqrt{n} \log \log n)$
	Corollary 2 in [16]	-	i^{-2t}	$n^{-\frac{1}{2}}$	$\mathcal{O}_p\left(n^{-\frac{1}{2}}\right)$	$s \geq \Omega(\sqrt{n} \log n)$
			$1/i$	$n^{-\frac{1}{2}}$	$\mathcal{O}_p\left(n^{-\frac{1}{2}}\right)$	$s \geq \Omega(\sqrt{n} \log n)$
$\{\omega_i\}_{i=1}^s \sim q(\omega)$		source condition; compatibility condition	i^{-2t}	$n^{-\frac{2t}{1+4rt}}$	$\mathcal{O}_q\left(n^{-\frac{4rt}{1+4rt}}\right)$	$s \geq \Omega(\frac{\varrho+(2r-1)(2t+1-2t\varrho)}{1+4rt} \log n)$
	Theorem 3 in [50]		$1/i$	$n^{-\frac{1}{2r+1}}$	$\mathcal{O}_q\left(n^{-\frac{2r}{2r+1}}\right)$	$s \geq \Omega(n^{\frac{2r}{2r+1}} \log n)$
			$e^{-\frac{1}{c}i}$	$n^{-\frac{1}{2}}$	$\mathcal{O}_q\left(n^{-\frac{1}{2}}\right)$	$s \geq \Omega(\log^2 n)$
	Corollary 1 in [16]	optimized distribution	i^{-2t}	$n^{-\frac{1}{2}}$	$\mathcal{O}_q\left(n^{-\frac{1}{2}}\right)$	$s \geq \Omega(n^{1/(4t)} \log n)$
			$1/i$	$n^{-\frac{1}{2}}$	$\mathcal{O}_q\left(n^{-\frac{1}{2}}\right)$	$s \geq \Omega(\sqrt{n} \log n)$

Assumption 10 (Separation condition [15]). *The points in \mathcal{X} can be collected into two sets according to their labels as follows*

$$\begin{aligned} X_1 &:= \{\mathbf{x} \in \mathcal{X} : \mathbb{E}[y|\mathbf{x}] > 0\}, \\ X_{-1} &:= \{\mathbf{x} \in \mathcal{X} : \mathbb{E}[y|\mathbf{x}] < 0\}. \end{aligned}$$

For $i \in \{\pm 1\}$, the distance of a point $\mathbf{x} \in X_i$ to the set X_{-i} is denoted by $\Delta(\mathbf{x})$. We say that the data distribution satisfies a separation condition if there exists $\Delta > 0$ such that $\rho_X(\Delta(\mathbf{x}) < c) = 0$.

The above two assumptions, both controlling the noise level in the labels, can be cast under into a unified framework [101] as follows. Define the regression function $\eta(\mathbf{x}) = \mathbb{E}[y|X = \mathbf{x}]$ in binary classification problems. The Massart's low noise condition means that there exists $h \in (0, 1]$ such that for $|\eta(\mathbf{x})| \geq h$ for all $\mathbf{x} \in \mathcal{X}$. Here h characterizes the level of noise in classification problems. If small h is small, then $\eta(\mathbf{x})$ is close to zero, in which case correct classification is difficult. Massart's condition can be extended to the following more flexible condition known as Tsybakov's low noise assumption [101]. This assumption stipulates that there exists a constant $C > 0$ such that for all sufficiently small $t > 0$, we have

$$\Pr(\{\mathbf{x} \in \mathcal{X} : |2\eta(\mathbf{x}) - 1| \leq t\}) \leq C \cdot t^q,$$

for some $q > 0$. The separation condition in Assumption 10 is an extreme case of the Tsybakovs noise assumption with $q = \infty$. It is clear that noise-free distributions satisfy this separation assumption, since the conditional probability η is bounded away from 1/2.

5.2.2 Squared loss in KRR

In this section, we review theoretical results on the generalization properties of KRR with squared loss and random features, for both the $p(\omega)$ -sampling (data-independent) and $q(\omega)$ -sampling (data-dependent) settings. Table 3 summarizes these results in terms of the key assumptions imposed, the learning rates, and the required number of random features.

We begin with the remarkable result by Rudi and Rosasco [50]. They are among the first to show that under some mild assumptions and appropriately chosen parameters, $\Omega(\sqrt{n} \log n)$ random features suffice for KRR to achieve minimax optimal rates. Below we present a general form of their result that holds for both $p(\omega)$ - and $q(\omega)$ -sampling under a flexible set of assumptions. This result pertains to the excessive risk $\mathcal{E}(\widetilde{f}_{\mathbf{z},\lambda}) - \mathcal{E}(f_\rho)$ (defined in Section 2.2) and the L^2 estimation error $\|\widetilde{f}_{\mathbf{z},\lambda} - f_\rho\|_{L_{\rho,\mathcal{X}}^2}^2 := \int_{\mathcal{X}} |\widetilde{f}_{\mathbf{z},\lambda}(\mathbf{x}) - f_\rho(\mathbf{x})|^2 d\rho_{\mathcal{X}}(\mathbf{x})$, which are equal under the squared loss of KRR.

Theorem 10 (Generalization bound; Theorem 3 in [50]). *Suppose that Assumption 8 (source condition) holds with $r \in [\frac{1}{2}, 1]$, Assumption 6 (compatibility) holds with $\varrho \in [0, 1]$, and Assumption 5 (capacity) holds with $\gamma \in [0, 1]$. Assume that $n \geq n_0$ and choose $\lambda := n^{\frac{1}{2r+\gamma}}$. If the number of random features satisfies*

$$s \geq c_0 n^{\frac{\alpha+(2r-1)(1+\gamma-\alpha)}{2r+\gamma}} \log \frac{108\kappa^2}{\lambda\delta},$$

then the excess risk of $\widetilde{f}_{\mathbf{z},\lambda}$ can be upper bounded as

$$\mathcal{E}(\widetilde{f}_{\mathbf{z},\lambda}) - \mathcal{E}(f_\rho) = \left\| \widetilde{f}_{\mathbf{z},\lambda} - f_\rho \right\|_{L_{\rho,\mathcal{X}}^2}^2 \leq c_1 \log^2 \frac{18}{\delta} n^{-\frac{2r}{2r+\gamma}},$$

where c_0, c_1 are constants independent of (n, λ, δ) , and n_0 does not depends on n, λ, f_ρ , or ρ .

Theorem 10 unifies several results in [50] that impose different assumptions. The simplest result is Theorem 1 in [50], which only requires the three basic Assumptions 1–3 on existence, boundedness and continuity, corresponding to the the worst case of Theorem 10 with $\varrho = \gamma = 1$ and $r = 1/2$. In this case, by choosing $\lambda = n^{-1/2}$, we require $\Omega(\sqrt{n} \log n)$ random features to achieve the minimax convergence rate $\mathcal{O}(n^{-1/2})$; also see Table 3.

A more refined result is given in Theorem 2 in [50], which accounts for the capacity of the RKHS and the regularity of f_ρ , as quantified by the parameters $\gamma \in [0, 1]$ (Assumption 5) and $r \in [\frac{1}{2}, 1]$ (Assumption 8), respectively. Under these conditions and

choosing $\lambda := n^{-\frac{1}{2r+\gamma}}$, we require $\Omega(n^{\frac{1+\gamma(2r-1)}{2r+\gamma}} \log n)$ random features to achieve the convergence rate $\mathcal{O}(n^{-\frac{2r}{2r+\gamma}})$. Note that $\gamma = 1$ is the worst case, where the eigenvalues of \mathbf{K} have the slowest decay, and $\gamma = 1/(2t) \in (0, 1)$ means that the eigenvalues follow a polynomial decay $\lambda_i \propto n^{1-2t}$. Table 3 presents this result with $\gamma := 1/(2t)$ for better comparison with the other results.

The above two results apply to the standard RFF setting with data-independent sampling. When $\{\omega_i\}_{i=1}^s$ are sampled from a data-dependent distribution satisfying the compatibility condition in Assumption 6 with $\varrho \in [0, 1]$, then Theorem 3 in [50] provide an improved result. In this case, by choosing $\lambda := n^{-\frac{1}{2r+\gamma}}$, we require $\Omega(n^{\frac{\varrho+(1+\gamma-\varrho)(2r-1)}{2r+\gamma}} \log n)$ random features to achieve the convergence rate $\mathcal{O}(n^{-\frac{2r}{2r+\gamma}})$.

If the compatibility condition is replaced by the stronger Assumption 7 (optimized distribution), satisfied by $q(\omega)$ -sampling, the work [16] derives an improved bound that is the sharpest to date. Below we state a general result from [16] that covers both $p(\omega)$ - and $q(\omega)$ -sampling.

Theorem 11 (Theorem 1 in [16]). *Suppose that the regularization parameter λ satisfies $0 \leq n\lambda \leq \lambda_1$. We consider two sampling schemes.*

- $\{\omega_i\}_{i=1}^s \sim p(\omega)$: if $s \geq (5z_0^2/\lambda) \log(16d_K^\lambda/\delta)$ and $|z(\omega, \mathbf{x})| \leq z_0$,
- $\{\omega_i\}_{i=1}^s \sim q(\omega)$: if $s \geq 5d_K^\lambda \log(16d_K^\lambda/\delta)$,

then for $0 < \delta < 1$, with probability $1 - \delta$, the excess risk of $\widetilde{f}_{\mathbf{z}, \lambda}$ can be upper bounded as

$$\|\widetilde{f}_{\mathbf{z}, \lambda} - f_\rho\|_{L_{\rho, \mathbf{x}}^2}^2 \leq 2\lambda + \mathcal{O}(1/\sqrt{n}) + \mathcal{E}(f_{\mathbf{z}, \lambda}) - \mathcal{E}(f_\rho), \quad (29)$$

where we recall that $\mathcal{E}(f_{\mathbf{z}, \lambda}) - \mathcal{E}(f_\rho)$ is the excess risk of standard KRR with an exact kernel (see Section 2).

For $p(\omega)$ -sampling, Theorem 11 improves on the results of [50] under the exponential and polynomial decays. Specifically, if $\{\omega_i\}_{i=1}^s \sim p(\omega)$, Theorem 11 requires $s \propto 1/\lambda \log d_K^\lambda$. Specialized to the exponential decay case, this result requires $\Omega(\sqrt{n} \log \log n)$ random features to achieve an $\mathcal{O}(n^{-1/2})$ learning rate, which is an improvement compared to [50] with $\Omega(\sqrt{n} \log n)$ random features.

For $q(\omega)$ -sampling, Theorem 11 shows that if $\lambda = n^{-1/2}$, then $s \propto d_K^\lambda \log d_K^\lambda$ random features is sufficient to incur no loss in the expected risk if KRR, with a minimax learning rate $\mathcal{O}(n^{-1/2})$. Corollaries of this result under three different regimes of eigenvalue decay are summarized in Table 3.

Carratino et al. [102] extend the result of [50] to the setting where KRR is solved by stochastic gradient descent (SGD). They show that under the basic Assumptions 1–3 and some mild conditions for SGD, $\Omega(\sqrt{n})$ random features suffice to achieve the minimax learning rate $\mathcal{O}(n^{-1/2})$. This result matches those for standard KRR with an exact kernel [103]. The above results can be improved if in addition the source condition in Assumption 8 holds, in which case $\Omega(n^{\frac{1+\alpha(2r-1)}{2r+\alpha}})$ random features suffice to achieve an $\mathcal{O}(n^{-\frac{2r}{2r+\alpha}})$ learning rate.

The work in [104] shows that if the randomized feature map is bounded (which is weaker than Assumption 2), then we have the following out-of-sample bound

$$\mathcal{E}(\widetilde{f}_{\mathbf{z}, \lambda}) - \mathcal{E}(f_{\mathbf{z}, \lambda}) \leq \mathcal{O}\left(\frac{1}{s\lambda}\right).$$

If we choose $\lambda := n^{-1/2}$, then $\Omega(n)$ random features are sufficient to ensure an $\mathcal{O}(n^{-1/2})$ rate in the out-of-sample bound.

5.2.3 Lipschitz continuous loss function

In this section, we consider loss functions ℓ that are Lipschitz continuous. Examples include the hinge loss in SVM and the cross-entropy loss in kernel logistic regression. Table 4 summarizes several existing results for such loss functions in terms of the learning rate and the required number of random features. We briefly discuss these results below and refer the readers to the cited work for the precise theorem statements.

If $\{\omega_i\}_{i=1}^s \sim p(\omega)$, i.e., under the standard RFF setting with data-independent sampling, we have the following results.

- Theorem 1 in [27] shows that the excess risk of $\widetilde{f}_{\mathbf{z}, \lambda}$ in Eq. (2) converges at a certain $\mathcal{O}(n^{-1/2})$ rate with $\Omega(n \log n)$ random features.
- Corollary 4 in [16] (Corollary 4) shows that with $\lambda \in \mathcal{O}(1/n)$ and $\Omega((1/\lambda) \log d_K^\lambda)$ random features, the excess risk of $\widetilde{f}_{\mathbf{z}, \lambda}$ can be upper bounded by

$$\mathcal{E}(\widetilde{f}_{\mathbf{z}, \lambda}) - \mathcal{E}(f_\rho) \leq \mathcal{O}(1/\sqrt{n}) + \mathcal{O}(\sqrt{\lambda}).$$

The above bound scales with $\sqrt{\lambda}$, which is different from the bound in Eq. (29) for the squared loss. Therefore, for Lipschitz continuous loss functions, we need to choose a smaller regularization parameter $\lambda \in \mathcal{O}(1/n)$ to achieve the same $\mathcal{O}(n^{-1/2})$ convergence rate. Also note that as before we can bound d_K^λ under the three types of eigenvalue decay.

If $\{\omega_i\}_{i=1}^s \sim q(\omega)$, i.e., under the data-dependent sampling setting, we have the following results.

- For SVM with random features, under the optimized distribution in Assumption 7 and the low noise condition in Assumption 9, Theorem 1 in [15] provides bounds on the learning rates and the required number of random features. This result is improved in Theorem 2 in [15] if we consider the stronger separation condition in Assumption 10. Details can be found in Table 4.
- In Section 4.5 in [49] and Corollary 3 in [16], it is shown that if Assumption 7 holds, then the excess risk of $\widetilde{f}_{\mathbf{z}, \lambda}$ converges at an $\mathcal{O}(n^{-1/2})$ rate with $\Omega(d_K^\lambda \log d_K^\lambda)$ random features, if we choose $\lambda \in \mathcal{O}(1/n)$.

5.3 Results for nonlinear component analysis

In addition to supervised learning problems such as classification and regression, random features can also be used in unsupervised learning, e.g., randomized nonlinear component analysis. Here we give an overview of the results for this problem.

The authors of [18] propose to use random features to approximate the kernel matrix in kernel Principal Component Analysis (KPCA) and kernel Canonical Correlation Analysis (KCCA). They show that the approximate kernel matrix converges to the true one in operator norm at a rate of $\mathcal{O}(n\sqrt{\log n}/s)$. More precisely, $s = \mathcal{O}((\log n)^2/\epsilon^2)$ suffices to ensure that $\|\widetilde{\mathbf{K}} - \mathbf{K}\|_2 \leq \epsilon n$ with the probability $1 - 1/n$. Their algorithm takes $\mathcal{O}(ns^2 + nsd)$ time to construct feature functions and $\mathcal{O}(s^2 + sd)$ space to store the feature functions and covariance matrix. Ghashami et al. [105] combine random features with matrix sketching for KPCA. For finding the top- ℓ principal components, they improve the time and space complexities to $\mathcal{O}(nsd + n\ell s)$ and $\mathcal{O}(sd + \ell s)$, respectively. Xie et al. [17] propose to use the doubly

Table 4
Comparison of learning rates and required random features for expected risk with a Lipschitz continuous loss function.

sampling scheme	Results	key assumptions	eigenvalue decay	λ	learning rates	required s
	Theorem 1 in [27]	-	-	-	$\mathcal{O}_p(n^{-\frac{1}{2}})$	$s \geq \Omega(n \log n)$
$\{\omega_i\}_{i=1}^s \sim p(\omega)$			$e^{-\frac{1}{c}i}$	$\frac{1}{n}$	$\mathcal{O}_p(n^{-\frac{1}{2}})$	$s \geq \Omega(n \log n)$
	Corollary 4 in [16]	-	i^{-2t}	$\frac{1}{n}$	$\mathcal{O}_p(n^{-\frac{1}{2}})$	$s \geq \Omega(n \log n)$
			$1/i$	$\frac{1}{n}$	$\mathcal{O}_p(n^{-\frac{1}{2}})$	$s \geq \Omega(n \log n)$
		low noise condition	$e^{-\frac{1}{c}i}$	$\frac{1}{n}$	$\mathcal{O}_q(\frac{1}{n} \log^{c+2} n)$	$s \geq \Omega(\log^c n \log \log^c n)$
	Theorem 1 in [15]	optimized distribution	i^{-2t}	$n^{-\frac{t}{1+t}}$	$\mathcal{O}_q(n^{-\frac{t}{1+t}} \log n)$	$s \geq \Omega(n^{\frac{1}{1+t}} \log n)$
			$1/i$	$\frac{1}{n}$	$\mathcal{O}_q(n^{-\frac{1}{2}})$	$s \geq \Omega(n \log n)$
$\{\omega_i\}_{i=1}^s \sim q(\omega)$	Theorem 2 in [15]	separation condition optimized distribution	$e^{-\frac{1}{c}i}$	n^{-2c^2}	$\mathcal{O}_q(\frac{1}{n} \log^{2c+1} n \log \log n)$	$s \geq \Omega(\log^{2c} n \log \log n)$
	Section 4.5 in [49]; Corollary 3 in [16]	optimized distribution	$e^{-\frac{1}{c}i}$	$\frac{1}{n}$	$\mathcal{O}_q(n^{-\frac{1}{2}})$	$s \geq \Omega(\log^2 n)$
			i^{-2t}	$\frac{1}{n}$	$\mathcal{O}_q(n^{-\frac{1}{2}})$	$s \geq \Omega(n^{1/(2t)} \log n)$
			$1/i$	$\frac{1}{n}$	$\mathcal{O}_q(n^{-\frac{1}{2}})$	$s \geq \Omega(n \log n)$

stochastic gradients scheme to accelerate KPCA. The authors of [106] investigate the statistical consistency of KPCA with random features. They show that the top- ℓ eigenspace of the empirical covariance matrix in \mathcal{H} converges to the covariance operator in \mathcal{H} at the rate of $\mathcal{O}(1/\sqrt{n} + 1/\sqrt{s})$. Therefore, $s \geq \Omega(n)$ random features are required to guarantee a $\mathcal{O}(1/\sqrt{n})$ rate. Ullah et al. [96] instead pose KPCA as a stochastic optimization problem and show that the empirical risk minimizer (ERM) in the random feature space converges in objective value at an $\mathcal{O}(1/\sqrt{n})$ with $\Omega(\ell\sqrt{n} \log n)$ random features.

Table 5
Dataset statistics.

datasets	d	#traing	#test	random split	scaling
<i>ijcnn1</i>	22	49,990	91,701	no	-
<i>EEG</i>	14	7,490	7,490	yes	mapstd
<i>cod-RNA</i>	8	59,535	157,413	no	mapstd
<i>covtype</i>	54	290,506	290,506	yes	minmax
<i>magic04</i>	10	9,510	9,510	yes	minmax
<i>letter</i>	16	12,000	6,000	no	minmax
<i>skin</i>	3	122,529	122,529	yes	minmax
<i>a8a</i>	123	22,696	9,865	no	minmax
<i>mushrooms</i>	112	4062	4062	yes	-
<i>spambase</i>	57	2301	2301	yes	minmax
<i>wilt</i>	5	4399	500	no	minmax
<i>wine-quality</i>	12	3249	3248	yes	mapstd
<i>MNIST</i>	784	60,000	10,000	no	minmax
<i>CIFAR-10</i>	3072	50,000	10,000	no	-

6 EXPERIMENTS

In this section, we empirically evaluate the kernel approximation and classification performance of representative random features algorithms on several benchmark datasets. All experiments are implemented in MATLAB and carried out on a PC with Intel® i7-8700K CPU (3.70 GHz) and 64 GB RAM.

6.1 Experimental settings

We choose the popular Gaussian kernel and the first-order arc-cosine kernel for experiments, where the kernel width σ in the Gaussian kernel is tuned by five-fold cross validation over the grid $\{0.01, 0.1, 1, 10\}$. For the subsequent classification task, the random feature mappings are used with two classifiers: the ridge linear regression (abbreviated as lr) with the squared loss, and the liblinear algorithm [107] (a linear classifier with the hinge loss). The regularization parameter λ in ridge linear regression and the balance parameter in liblinear are tuned via 5-fold inner cross validation on a grid of $\{10^{-8}, 10^{-6}, 10^{-4}, 10^{-3}, 10^{-2}, 0.05, 0.1, 0.5, 1, 5, 10\}$ and $\{0.01, 0.1, 1, 10, 100\}$, respectively. The random features dimension s in our experiments takes value in $\{2d, 4d, 8d, 16d, 32d\}$. We use $\|\mathbf{K} - \tilde{\mathbf{K}}\|_{\text{F}}/\|\mathbf{K}\|_{\text{F}}$ as the error metric for kernel approximation. A small error indicates a high approximation quality. To compute the approximation error, we randomly sample 1,000 data points to construct the sub-feature matrix and the sub-kernel matrix. All experiments are repeated 10 times and we report the average approximation error, average classification accuracy with their respective standard deviations as well as the time cost for generating random features.

We consider twelve non-image benchmark datasets⁵ as well as two representative image datasets. Table 5 gives an overview of these datasets including the number of feature dimension, training samples, test data, training/test split, and the normalization scheme. Some datasets include a training/test partition, denoted as “no” in the random split column. For the other datasets, we randomly pick half of the data for training and the rest for testing, denoted as “yes” in the random split column. There are two typical normalization schemes used in these datasets: “mapstd” and “minmax”. The “mapstd” scheme sets each sample’s mean to 0 and deviation to 1, while the “minmax” scheme is a standard min-max scaling operation mapping the samples to the bounded set $[0, 1]^d$. The two

5. These non-image datasets can be downloaded from <https://www.csie.ntu.edu.tw/~cjlin/libsvmtools/datasets/> or the UCI Machine Learning Repository (<https://archive.ics.uci.edu/ml/datasets.html>).

Table 6

Results statistics on twelve classification datasets. The best algorithm on each dataset is given in two cases: low dimensional (i.e., $s = 2d, 4d$) and high dimensional (i.e., $s = 16d, 32d$) according to approximation quality, test accuracy in linear regression or liblinear. The notation “-” means that there is no *statistically significant* difference in the performance of most algorithms.

datasets	approximation		lr		liblinear	
	low dim.	high dim.	low dim.	high dim.	low dim.	high dim.
<i>ijcnn1</i>	SSF	SORF, QMC, ORF	QMC	Fastfood	Fastfood	-
<i>EEG</i>	SSF	ORF	-	-	-	-
<i>cod-RNA</i>	SSF	-	-	-	-	-
<i>covtype</i>	ORF	-	-	-	-	-
<i>magic04</i>	SSF	SSF, ORF, QMC, ROM	-	-	-	-
<i>letter</i>	SSF	SSF, ORF	-	-	-	-
<i>skin</i>	SSF, ROM	QMC	-	-	-	-
<i>a8a</i>	-	-	SSF	-	SSF	-
<i>mushrooms</i>	-	-	Fastfood	-	Fastfood	-
<i>spambase</i>	ORF	ORF	-	-	-	-
<i>wilt</i>	SSF, ROM	ORF	-	SSF	-	-
<i>wine-quality</i>	SSF	SORF, QMC, ORF	-	-	-	-

image datasets are the *MNIST* handwritten digits dataset [108] and the *CIFAR10* natural image classification dataset [109], summarized in the last two rows in Table 5. The MNIST dataset contains 60,000 training samples and 10,000 test samples, each of which is a 28×28 gray-scale image of a handwritten digit from 0 to 9. Here the “minmax” normalization scheme means that each pixel value is divided by 255. The CIFAR10 dataset consists of 60,000 color images of size $32 \times 32 \times 3$ in 10 categories, with 50,000 for training and 10,000 for test.

We evaluate the following ten representative algorithms: RFF [12], ORF [36], SORF [36], ROM [65], Fastfood [31], SCRF [35], QMC [32], SSF [39], GQ [40], and LS-RFF [16]. These algorithms include both data-independent and data-dependent approaches and involve a variety of techniques including Monte Carlo and quasi-Monte Carlo sampling, quadrature rules, variance reduction, and computational speedup using structural/circulant matrices. We believe that the experiment results in this section provide a reasonably comprehensive comparison of these representative random features based algorithms.

6.2 Results for the Gaussian Kernel

Here we present the experimental results for the Gaussian kernel.

6.2.1 Classification results on non-image benchmark datasets

Figures 6, 10, and 11 show the approximation error for the Gaussian kernel, the time cost of generating randomized feature mappings, and the test accuracy yielded by linear regression and liblinear on the twelve datasets, respectively. (Figures 10 and 11 are deferred to Appendix A.) We see that as the number of random features increases, most algorithms achieve a smaller approximation error and a higher classification accuracy for both classifiers. We notice some interesting phenomena in terms of the relation between approximation quality and prediction performance, depending on whether the feature dimension is low (i.e., $s = 2d$ or $s = 4d$) or high (i.e., $s = 16d$ or $s = 32d$). In particular, the algorithms with the best kernel approximation performance are often different in the low-dimensional case and the high dimensional case. Therefore, no algorithm always dominate the others. On the other hand, while the

approximation quality of these algorithms varies, their prediction performance are often similar.

To better understand the above observations, we summarize the best performing algorithm on each dataset in terms of the approximation quality and classification accuracy in Table 6, where we distinguish the low dimension case (i.e., $s = 2d$ or $s = 4d$) and the high dimension case (i.e., $s = 16d$ or $s = 32d$). The notation “-” therein means that there is no *statistically significant* difference in the performance of most algorithms.

In terms of approximation error, we find that SSF achieves the best performance on most datasets in the low-dimensional case, while ORF often performs better than others in the high-dimensional case. Some possible explanations are as follows. SSF aims to generate asymptotically uniformly distributed points on the sphere \mathbb{S}^{d-1} . As such, a few points might be adequate, and additional points (i.e., a larger s) may have a small marginal benefit in variance reduction. Consequently, the approximation error of SSF sometimes stays almost the same with a larger number of random features, as can be observed in the *skin*, *spambase*, *wilt*, *magic04* and *ijcnn1* datasets. On the other hand, the expression for variance of ORF in Eq. (12) shows that ORF requires a high dimensional feature mapping to achieve significant variance reduction. This theoretical result is consistent with the numerical performance of ORF. Moreover, recall that the goal of using random features is to find a finite-dimensional (embedding) Hilbert space to approximate the original infinite-dimensional RKHS so as to preserve the inner product. To achieve this goal, both SSF and ORF are based on a similar principle, namely, generating random features that are as independent/complete as possible. Doing so allows one to use fewer random features to encode more information, which may explain the good performance of SSF and ORF.

In terms of prediction performance, we find that there is no significant difference between most algorithms. This means that a higher kernel approximation quality does not always translate to better classification performance. In fact, some methods, e.g., Fastfood, have inferior kernel approximation performance but achieve superior classification accuracy. Understanding this inconsistency between approximation quality and generalization performance is an important open problem; see the discussion in [14], [41], [48]. In principle, kernel approximation and prediction

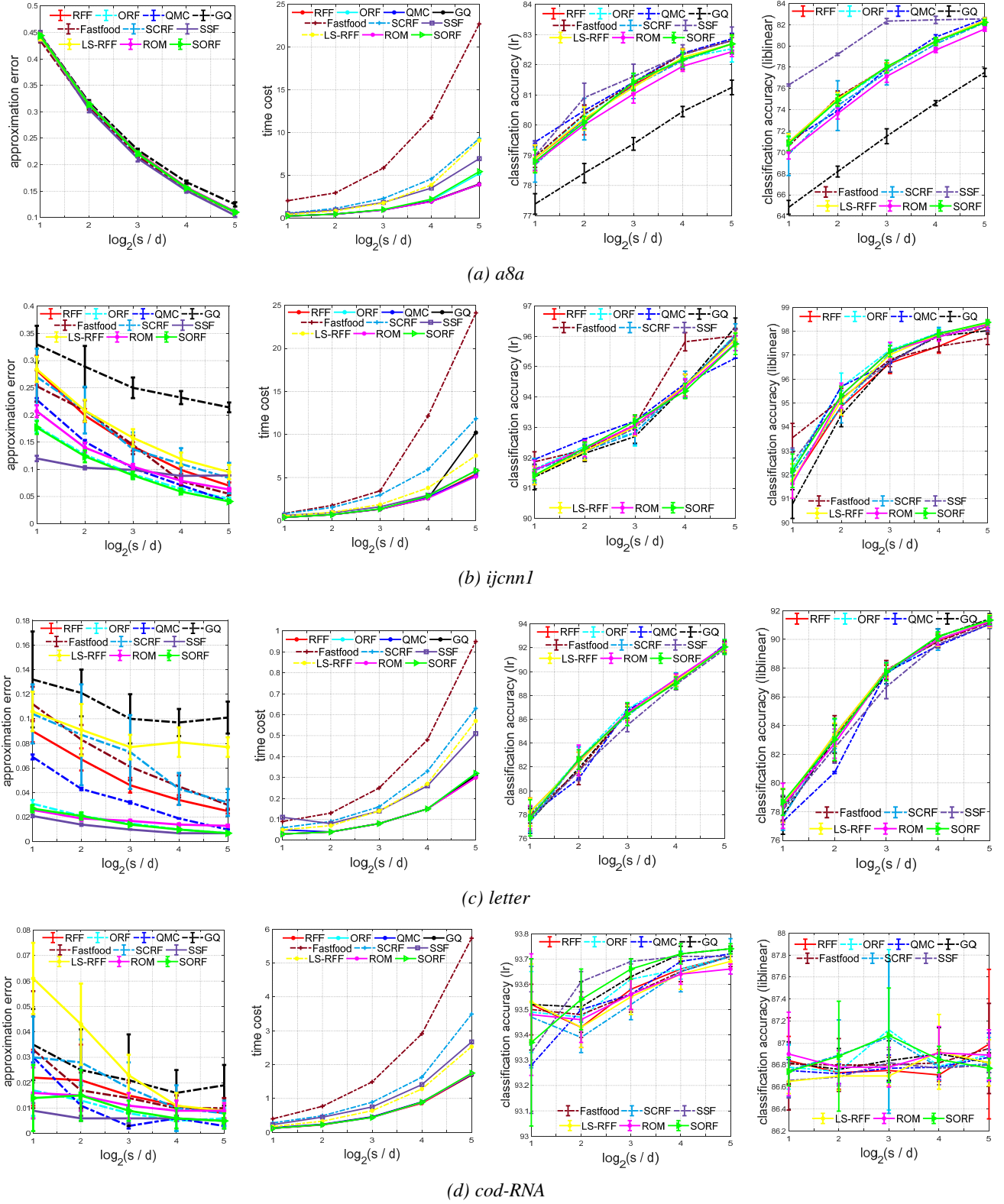


Figure 6. Results of various algorithms for the Gaussian kernel on the a8a, ijcn1, letter, cod-RNA datasets.

are two different goals. To be specific, kernel approximation aims to preserve the inner product in two Hilbert spaces, i.e., $\langle k(\mathbf{x}, \cdot), k(\mathbf{x}', \cdot) \rangle_{\mathcal{H}} \approx \langle \tilde{k}(\mathbf{x}, \cdot), \tilde{k}(\mathbf{x}', \cdot) \rangle_{\tilde{\mathcal{H}}}$. For prediction, taking

KRR as an example, we can decompose the excess error of $\tilde{f}_{\mathbf{z}, \lambda}$ as $\mathcal{E}(\tilde{f}_{\mathbf{z}, \lambda}) - \mathcal{E}(f_\rho) = [\mathcal{E}(f_{\mathbf{z}, \lambda}) - \mathcal{E}(f_\rho)] + [\mathcal{E}(\tilde{f}_{\mathbf{z}, \lambda}) - \mathcal{E}(f_{\mathbf{z}, \lambda})]$,

where we have $\tilde{f}_{\mathbf{z}, \lambda} = \sum_{i=1}^n \tilde{\alpha}_i \tilde{k}(\mathbf{x}, \cdot) \in \tilde{\mathcal{H}}$ and $f_{\mathbf{z}, \lambda} = \sum_{i=1}^n \alpha_i k(\mathbf{x}, \cdot) \in \mathcal{H}$ by the representer theorem. The first term on

the right hand is the excess risk of KRR, which is independent of the quality of kernel approximation. The second term on the right hand is the expected error difference between the original KRR and its random features approximation version. The preservation of the inner-product does not immediately guarantee that this term is small. In fact, there is no obvious definite relation between them (recall that $\tilde{\mathcal{H}}$ is not necessarily contained in \mathcal{H}).

In terms of time cost for generating the randomized feature mapping, we find that some algorithms that use structural/circulant information for acceleration (e.g., Fastfood, SSF, SORF, ROM, and SCRF) do not exhibit significant computational saving as suggested by theoretical analysis. One explanation is that depending on the specific algorithm implementation in MATLAB, directly sampling $W_{ij} \sim \mathcal{N}(0, \sigma^{-2})$ as in RFF need not be more time-consuming than generating a series of Hadamard/Walsh/Rademacher matrices, at least for the problem scale of our experiments.

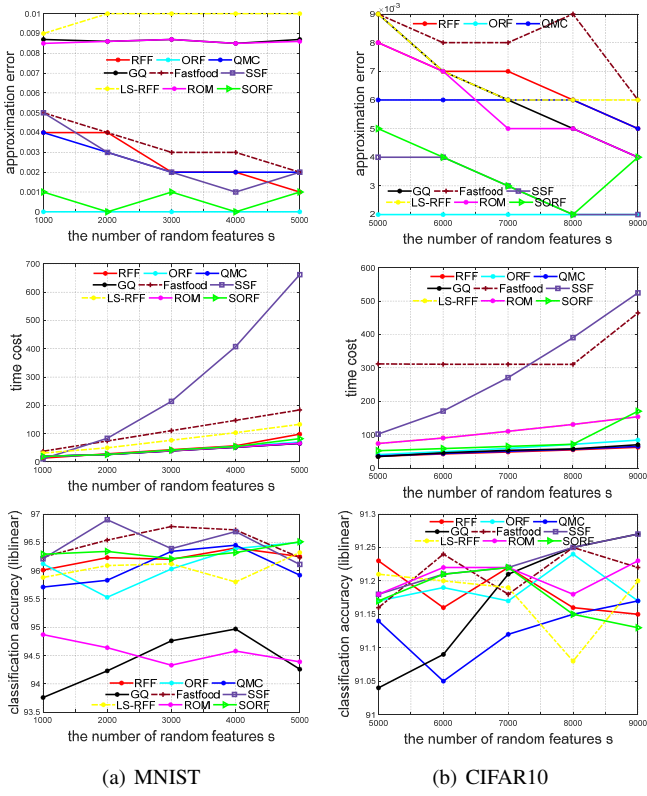


Figure 7. Approximation error, time cost, and test accuracy of random features based algorithms in liblinear on two image classification datasets.

6.2.2 Classification results on image datasets

Here we consider the MNIST and CIFAR10 datasets, on which we test various random features based algorithms (except SCRF⁶) for kernel approximation and then combine these algorithms with liblinear for image classification. In our experiment, we use the Gaussian kernel, whose kernel width σ is tuned by 5-fold cross validation over the grid $\sigma = [0.01, 0.1, 1, 10, 100]$. For the MNIST database, we directly use the original 784-dimensional feature as the data. For better performance on the CIFAR10 dataset, we use VGG16 with batch normalization [110] pre-trained on ImageNet [111] as a feature extractor. We fine-tune this model on

6. It requires s to be exponential in d in their implementation.

the CIFAR10 dataset with 240 epochs and a mini-batch size 64. The learning rate is initialized at 0.1 and then divided by 10 at the 120-th, 160-th, and 200-th epochs. For each color image, a 4096 dimensional feature vector is obtained from the output of the first fully-connected layer in this fine-tuned neural network.

Figure 7(a) shows the approximation error, the time cost, and the classification accuracy by liblinear across a range of $s = 1000$ to $s = 10,000$ random features on the MNIST database. We find that ORF yields the best approximation quality. On the other hand, while most algorithms achieve different approximation errors, there is no significant difference in the test accuracy, similarly to the results on non-image datasets. Similar results are observed on the CIFAR10 dataset with $s = 5000$ to $s = 12,000$ random features; see Figure 7(b).

6.3 Results for the Arc-cosine Kernel

Here we consider the first-order arc-cosine kernel and compare five algorithms including RFF [12], QMC [32], SSF [39], ROM [65], and SSR [41]. Note that several other algorithms, e.g., ORF, SORF, and Fastfood, are not applicable to arc-cosine kernels, which are rotation-invariant but not shift-invariant. Also note that Monte Carlo sampling (i.e., RFF) can still be used.

Figure 8 shows the results of the above five algorithms on four datasets *ijcnn1*, *letter*, *EEG*, and *cod-RNA*. It can be observed that in most cases SSF achieves a lower approximation error than the other approaches, especially when using low dimensional random features. When the number of random features increases to $s = 32d$, SSF, SSR, and QMC achieve similar approximation performance on the *letter*, *cod-RNA* datasets. In general, we find that the approximation performance and time cost of these algorithms on the arc-cosine kernel are similar to that on the Gaussian kernel, though the approximation error is often larger than that for the Gaussian kernel. In the term of classification accuracy, RFF achieves the similar generalization performance with SSR and SSF on the *ijcnn1*, *letter*, and *EEG* datasets. On the *cod-RNA* dataset, ROM performs significantly better than RFF when using lower dimensional random features. In general, the difference in test accuracy of most algorithms is relatively small compared to the difference in approximation quality.

7 TRENDS: RANDOM FEATURES IN DNNs

In the previous sections, we review random features based algorithms and their theoretical guarantees. It can be seen that these approaches are simple in formulation and effective in real-world large-scale problems. They also enjoy nice theoretical guarantees in kernel approximation and generalization properties. Recently, theoretical analysis of over-parameterized neural networks has attracted a lot of attention in the deep learning theory community, partly due to the observation of several intriguing phenomena, including capability of fitting random labels, strong generalization performance of overfitted classifiers [19], and double descent in the test error curve [20], [112]. Moreover, Belkin et al. [20], [113] point out that the above phenomena are not unique to deep networks but also exist in kernel methods. In Figure 9, we report the empirical training error, the test error, and the kernel approximation error of random features regression as a function of s/n on the *sonar* dataset⁷ and the MNIST dataset [108]. Even with n, d, s only in the hundreds, we can still observe that as s increases, the training error

7. <https://archive.ics.uci.edu/ml/datasets.html>.

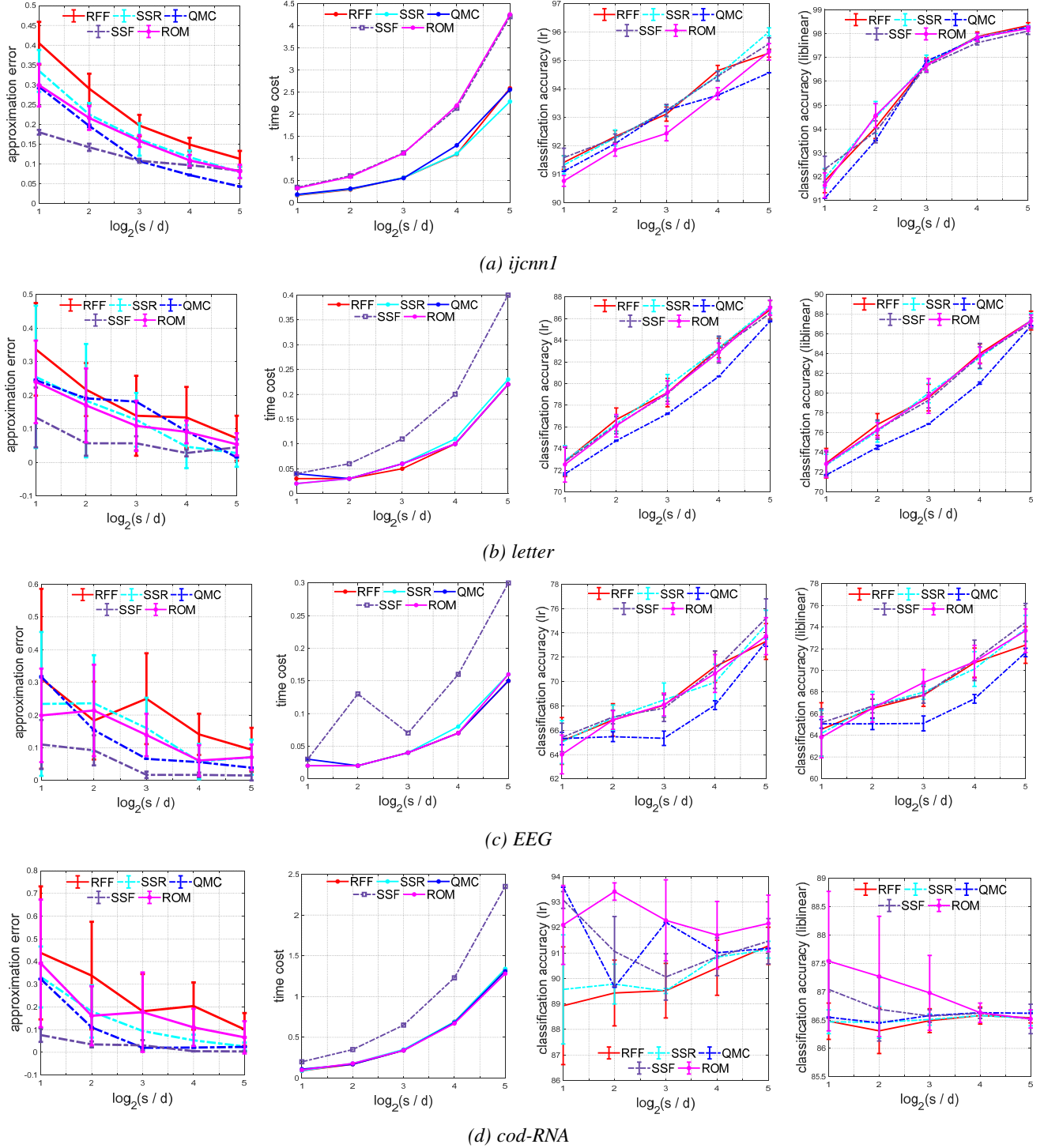


Figure 8. Results of various algorithms for the first-order arc-cosine kernel approximation on the *a8a*, *ijCNN1*, *letter*, *cod-RNA* datasets.

reduces to zero, the approximation error monotonously decreases, and the test error exhibits double descent.

The above observations have motivated researchers to build on the elegant theory of kernel methods/random features to provide an analysis of neural networks in the over-parameterized regime. This is a potentially fruitful research direction. Here we provide an overview of this topic and recent research trends that are related to random features. We remark upfront that the random features model is not the only way for analyzing DNNs. Many other approaches, with different points of views, have been proposed for deep learning

theory, but they are out of scope of this survey.

Below we briefly review the relations between random features and DNNs in Section 7.1, give an overview of recent work using random features to study double descent and NTK in Section 7.2, and discuss the gap between random feature models and DNNs in Section 7.3.

7.1 Relations between random features and DNNs

There is an interesting line of work showing insightful connections between kernel methods and over-parameterized neural networks;

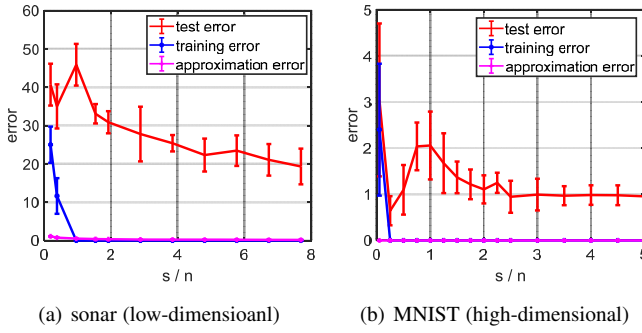


Figure 9. Training error, test error, and approximation error of random features regression with $\lambda = 10^{-8}$ on the *sonar* dataset with $n = 208$, $d = 60$ and the sub-set of MNIST (class 1 versus class 2) with $n = 200$, $d = 784$.

see below for several representative papers.

$$\left\{ \begin{array}{l} \text{weakly trained nets} \left\{ \begin{array}{l} \text{Gaussian process: [114], [115]} \\ \text{Random features model: [25], [116]} \end{array} \right. \\ \text{fully-trained nets: NTK [21], CNTK [24]} \end{array} \right.$$

The work [114] is among the first to point out this connection. There it is shown that a single-layer fully-connected neural network with *i.i.d.* random parameters is equivalent to a Gaussian process in the infinite-width limit. This equivalence between infinitely wide multi-layer networks and Gaussian processes is further explored in [115]. Daniely et al. [116], [117] show that under certain conditions and after the random initialization, SGD applied to over-parameterized neural networks is guaranteed to learn any function in the kernel space by updating the weights in the last layer. This procedure is similar to fitting a random features model. The work in [25] studies the training dynamics and generalization error bounds of a two-layer ReLU network with random initialization (i.e., a random features model) and gradient descent. Note that these results apply to *weakly-trained networks*, in which only the last (classification) layer is optimized and all other parameters are chosen randomly/fixed by a certain scheme. If a weakly-trained net uses fully-connected layers, it can be considered as a multi-layer random features model; moreover, several fully-connected blocks can be stacked via randomized feature mappings [118]. For fully-trained nets, in which all parameters are trained by gradient descent, it is shown in [21] that a fully-trained net is equivalent to a kernel regression predictor with a deterministic kernel called neural tangent kernel (NTK). Similarly, fully-trained nets with convolutional layers correspond to the convolutional neural tangent kernel (CNTK) [24]. Lee et al. [119] provide empirical verification for the theory of NTK by studying the linearization of neural nets and moreover prove that infinite width networks are actually linearized models.

We elaborate on the above results. Using random features in kernel methods such as KRR fits a linear model in RKHS. This model can be interpreted as a two-layer weakly-trained net, where the weights $\{\omega_i\}_{i=1}^s$ in the first layer are chosen randomly/fixed and only the output layer is optimized. As such, two-layer neural networks in the weakly-trained/fully-trained regimes are more amenable to theoretical analysis as compared to general arbitrary deep networks. The function class of a standard two-layer neural networks with s neurons (notation chosen to be consistent with the

number of random features) is given as follows [120]:

$$\mathcal{F}_{\text{NN},s} = \left\{ f(\mathbf{x}; \boldsymbol{\theta}) = \sum_{i=1}^s a_i \varphi(\langle \omega_i, \mathbf{x} \rangle) : a_i \in \mathbb{R}, \omega_i \in \mathbb{R}^d \right\},$$

where $\varphi(\cdot)$ is the active function and $\boldsymbol{\theta} := \{a_i, \omega_i\}_{i=1}^s$ is the network parameter, with ω_i and a_i being the weights of the input and output layers, respectively. Jacot et al. [21] point out that for highly over-parameterized networks, the network weights barely change from their random initialization; this is known as the lazy regime [121]. Accordingly, a nonlinear function $f_{\text{NN},s}(\mathbf{x}) \in \mathcal{F}_{\text{NN},s}$ can be approximated by its first order Taylor expansion around its initial weights $\boldsymbol{\theta}_0 := \{a_{0,i}, \omega_{0,i}\}_{i=1}^s$:

$$\begin{aligned} f_{\text{NN},s}(\mathbf{x}; \boldsymbol{\theta}) \approx f_{\text{NN},0}(\mathbf{x}; \boldsymbol{\theta}_0) + \sum_{i=1}^s (a_i - a_{0,i}) \varphi'(\langle \omega_{0,i}, \mathbf{x} \rangle) \\ + \sum_{i=1}^s a_{0,i} \langle \omega_i - \omega_{0,i}, \mathbf{x} \rangle \varphi'(\langle \omega_{0,i}, \mathbf{x} \rangle), \end{aligned}$$

where $f_{\text{NN},0}$ is the neural network at initialization and φ' is the derivative of the activation function φ . The function $f_{\text{NN},s} - f_{\text{NN},0}$ lies approximately in the space $\mathcal{F}_{\text{RF},s}(\mathbf{W}) \oplus \mathcal{F}_{\text{NTK},s}(\mathbf{W})$, where we define the function classes

$$\begin{aligned} \mathcal{F}_{\text{RF},s}(\mathbf{W}) &= \left\{ f_s(\mathbf{x}; \boldsymbol{\theta}) = \sum_{i=1}^s a_i \sigma(\langle \omega_i, \mathbf{x} \rangle) : a_i \in \mathbb{R} \right\}, \\ \mathcal{F}_{\text{NTK},s}(\mathbf{W}) &= \left\{ f_s(\mathbf{x}; \boldsymbol{\theta}) = \sum_{i=1}^s \sigma'(\langle \omega_i, \mathbf{x} \rangle) \langle \mathbf{a}_i, \mathbf{x} \rangle : \mathbf{a}_i \in \mathbb{R}^d \right\}. \end{aligned}$$

Here $\mathcal{F}_{\text{RF},s}(\mathbf{W})$ is referred to as the *random features model*, where the weights of the first/input layer are randomly chosen or fixed, and only the second/output layer is optimized. On the other hand, $\mathcal{F}_{\text{NTK},s}(\mathbf{W})$ corresponds to the first order term in the Taylor expansion with respect to the first layer weights. Both $\mathcal{F}_{\text{RF},s}(\mathbf{W})$ and $\mathcal{F}_{\text{NTK},s}(\mathbf{W})$ are finite-dimensional linear spaces, and minimizing the empirical risk over these spaces can be performed efficiently. Hence, in certain over-parameterized regimes, gradient descent applied to the neural model class $\mathcal{F}_{\text{NN},s}$ will converge to a model in $\mathcal{F}_{\text{RF},s}(\mathbf{W}) \oplus \mathcal{F}_{\text{NTK},s}(\mathbf{W})$. The gradient descent dynamics of such over-parameterized two-layer networks are characterized in [25], which shows that gradient descent converges at different rates for different types of labels.

Albeit simple, the random feature model $\mathcal{F}_{\text{RF},s}(\mathbf{W})$ is appealing in deep learning theory due to the following reasons. First, it can be regarded as a two-layer weakly-trained neural network and is closely related to the lazy regime of neural networks. Therefore, this model captures the learning dynamics of the last layer. Second, the randomness of the first layer weights mimics the random weight initialization commonly used in neural networks. Last and most importantly, the strong generalization performance of overfitted classifiers and the double descent phenomenon can also be observed in random features models. Such models have a solid theoretical foundation and hence provide a means to analyzing these phenomena. Similarly, the NTK model has also demonstrated success in providing a finer grained analysis of DNNs.

7.2 Analysis of DNNs using random features

Here we briefly overview the use of random features for analysis of over-parameterized neural networks.

7.2.1 Random features in double descent

The double descent phenomenon in risk curves [20] can be summarized as follows: i) as the model complexity increases, the training risk monotonically decreases; ii) in the under-parametrized regime, the test risk first decreases and then increases; once the model complexity passes a certain threshold into the over-parameterized regime, the test risk decreases again. It has been observed in [20] that this phenomenon is robust and holds for a variety of tasks, architectures, and optimization methods, including random features models, ResNet18 [122], standard 5-layer CNN, and transformers [123]. The double descent phenomenon can sometimes be quite complicated. For example, the bias and variance may show different tendency in the over-parameterized regime [124]. Moreover, the risk curve is not only a function of model size but also that of the number of epochs [20]. Some models even exhibit a risk curve with multiple descents [125].

Theoretical analysis on double descent often consider linear models with random data in the asymptotic [126] or non-asymptotic regimes [127]. An intuitive explanation of the double descent phenomenon is given in [128], which studies the condition number of the matrix $\frac{1}{d} \mathbf{X} \mathbf{X}^\top$ in a system of linear equations $\mathbf{X} \boldsymbol{\beta} = \mathbf{y}$ using the semi-circle law in random matrix theory [129], [130], [131]. They show that the condition number is the worst when $n = d$ and that kernel methods on i.i.d random data become well-conditioned in the $n \ll d$ case. Hastie et al. [132] use random matrix theory to study the asymptotic risks of ridge regression and minimum norm least-squares regression with random features. In particular, they show that as $n, d, s \rightarrow \infty$ with n/d being a constant and $s/n \rightarrow \psi_1 \in (0, \infty)$, the limiting variance increases when $\psi_2 \in (0, 1)$, decreases when $\psi_1 \in (1, \infty)$, and diverges when $\psi_1 \rightarrow 1$, which provides a theoretical explanation for the double descent phenomenon. On the other hand, Nakkiran et al. [133] show that adding ℓ_2 regularization in linear regression models fixes the ill-conditioning in the $n = d$ regime and thus effectively mitigates the double descent phenomenon. Moreover, with optimally-tuned regularization, ridge regression can achieve a test error that decrease monotonically in both the sample size and model size.

Apart from linear models, the random features model, corresponding to a weakly-trained two-layer net, is another model often used to demonstrate the double descent phenomenon. Belkin et al. [134] provide a precise analysis of this phenomenon for a one-dimensional version of the random features model. In a similar spirit, the authors of [135], [136] prove that the prediction errors of several models decrease monotonically with the number of random features in the over-parameterized regime. In particular, the work [135] considers the random features regression model over the sphere with ReLU activation, and shows that both the bias and variance have a peak at the interpolation threshold $s = n$ and diverge there when $\lambda \rightarrow 0$. This result pertains to the squared loss, and can be extended to show that gradient descent with cross-entropy loss and random features converges to the max-margin classifier in the over-parametrized regime [136]. A fine-grained analysis of the random features model is provided in [137], which quantitatively disentangle the contributions to the test error from different mechanisms, including the bias, various sources of variance of estimator, the data sampling procedure, the additive noise in the labels, and the initialization methods. The above results on the random features model provide the first step to further analysis of double descent in deep neural networks.

7.2.2 Random features in NTK

In an infinite-width neural network, under an appropriate initialization on weights, the network parameters are shown to stay close to their initialization during gradient descent training. In this case, the first-order Taylor expansion provides a good approximation, with the gradient converges as

$$\langle \nabla_{\boldsymbol{\theta}} f(\mathbf{x}; \boldsymbol{\theta}_0), \nabla_{\boldsymbol{\theta}} f(\mathbf{x}', \boldsymbol{\theta}_0) \rangle \rightarrow k(\mathbf{x}, \mathbf{x}'),$$

where the limiting kernel k is the so called neural tangent kernel. When using the squared loss and the ℓ_2 -regularizer, this network trained by gradient descent corresponds to kernel ridge regression with NTK [138].

Here we take a two-layer ReLU network as an example, i.e., $f(\mathbf{x}; \boldsymbol{\theta}) = \sqrt{\frac{2}{s}} \sum_{j=1}^s a_j \varphi(\boldsymbol{\omega}_j^\top \mathbf{x})$, where $\varphi(u) = \max(0, u)$ is the ReLU activation. Its corresponding NTK under the Gaussian initialization is then given by

$$k(\mathbf{x}, \mathbf{x}') := 2\mathbf{x}^\top \mathbf{x}' \int \mathcal{N}(\boldsymbol{\omega}; \mathbf{0}, \mathbf{I}_d) g_1(\boldsymbol{\omega}) d\boldsymbol{\omega} + 2 \int \mathcal{N}(\boldsymbol{\omega}; \mathbf{0}, \mathbf{I}_d) g_2(\boldsymbol{\omega}) d\boldsymbol{\omega},$$

where the integrand is $g_i(\boldsymbol{\omega}) = \phi(\boldsymbol{\omega}^\top \mathbf{x})^\top \phi(\boldsymbol{\omega}^\top \mathbf{x}')$, $i = 1, 2$ with $\phi(u) = 1\{u \geq 0\}$ in g_1 and $\phi(u) = \max\{0, u\}$ in g_2 [139]. The above NTK can also be represented as

$$k(\mathbf{x}, \mathbf{x}') = \|\mathbf{x}\|_2 \|\mathbf{x}'\|_2 \kappa \left(\frac{\langle \mathbf{x}, \mathbf{x}' \rangle}{\|\mathbf{x}\|_2 \|\mathbf{x}'\|_2} \right),$$

where $\kappa(u) = u\kappa_0(u) + \kappa_1(u)$, $\kappa_0(u)$ is the zero-order arc-cosine kernel and $\kappa_1(u)$ is the first-order arc-cosine kernel (see Section 2.3). The generalization errors of wide ReLU network with random initialization and SGD training is studied in [23].

Neural networks are typically trained using variants of (stochastic) gradient descent. The above framework suggests another way to train an over-parameterized wide neural network with the squared loss and ℓ_2 regularization: solve a kernel ridge regression with NTK, which can be done in closed form. For real-world datasets with a large amount of training data, regression with an exact kernel suffers from scalability issues. In this case, using random features based algorithms provide a potentially practical way of approximately computing the exact NTK [21] and CNTK [24]. However, if the random features are generated from practically sized nets, the empirical evidence in [24] indicates that the prediction performance significantly degrades. This issue is also related to the discussion in previous sections that good approximation of kernels does not necessarily guarantee good prediction performance.

7.3 Discussion: gaps and connections between random features and DNNs

As mentioned, random features models have been fruitfully used to analyze the double descent phenomenon. However, it is non-trivial to transfer results for these models to practical neural networks, which are typically deep but not too wide. There is still a substantial gap between existing theory based on random features and the modern practice of DNNs. For example, Ghorbani et al. [120] point out that as $n \rightarrow \infty$, a random features regression model can only fit the projection of the target function onto the space of degree- ℓ polynomials when $s = \Omega(d^{\ell+1-\delta})$ random features are used for some $\delta > 0$. More importantly, if the training data $\{\mathbf{x}_i\}_{i=1}^n$ are uniformly distributed over the d -dimensional sphere, and s, d are large with $s = \Omega(d)$, then the function space $\mathcal{F}_{\text{RF},s}(\mathbf{W})$ can only capture linear functions, whereas $\mathcal{F}_{\text{NTK},s}(\mathbf{W})$ can only capture

quadratic functions. In addition, Yehudai and Shamir [140] show that the random features model cannot efficiently approximate a single ReLU neuron as it requires the number of random features to be exponentially large in the feature dimension d . This is consistent with the classical result for kernel approximation in the under-parameterized regime: the random features model, QMC, and quadrature based methods require $s = \Omega(\exp(d))$ to achieve an ϵ approximation error [40]. Further, Ghorbani et al. [121] prove that both $\mathcal{F}_{\text{RF},s}(\mathbf{W})$ and $\mathcal{F}_{\text{NTK},s}(\mathbf{W})$ have limited approximation power in the lazy training scheme, whereas significant gain can be achieved by full training.

Admittedly, the above results may appear pessimistic. Nevertheless, random features is still a powerful tool for analyzing and understanding DNNs in certain regimes, and we believe its potential has yet to be fully exploited. Note that random features are strong and universal approximators [141] in the sense that the RKHSs induced by a broad class of random features are dense in the space of continuous functions. While the aforementioned results show that the number of required features may be exponential in the worst case, a more refined analysis can still provide useful insights for DNNs. In particular, in practical neural networks, the feature dimension d is often much smaller than the number of training data and the number of parameters (or neurons), i.e., $d \ll n \ll s$. It is therefore reasonable to consider the regime with $n, s \rightarrow \infty$ and d finite, rather than letting n, s, d all tend to infinity. Note that in this regime, classical random matrix theory may be insufficient due to the rank deficiency of the weight matrix \mathbf{W} . One potential way forward is to use the random features model to analyze DNNs *with pruning*. For example, the best paper [142] in the *Seventh International Conference on Learning Representations* (ICLR2019) put forward the following *Lottery Ticket Hypothesis*: a deep neural network with random initialization contains a small sub-network which, when trained in isolation, is able to compete with the performance of the original one. Malach et al. [22] provide a stronger claim that a randomly-initialized and sufficiently over-parameterized neural network contains a sub-network with nearly the same accuracy as the original one, without any further training. Their analysis demonstrates the equivalence between random features and the sub-network model. As such, the random features model is potentially useful for network pruning [143] in terms of, e.g., guiding the design of neurons pruning for accelerating computations, and understanding network pruning and the full DNNs.

8 CONCLUSION

In this survey, we systematically review random features based algorithms and their associated theoretical results. We also give an overview on the relations between random features and DNNs, survey the use of random features in DNNs, and discuss the limitations and potential of random features in the theory development for neural networks. Below we provide additional remarks and discuss several open problems that are of interest for future research.

- Experiments show that better kernel approximation does not directly translate to lower generalization errors. Current theoretical results based on error bounds of eigenvalues [83], [144] may be not sufficient to explain this phenomenon. We believe this issue deserves further in-depth study.
- Kernel learning via the spectral density is a popular direction [69], [71], which can be naturally combined with Generative

Adversarial Networks (GANs); see [67] for details. In this setting, one may associate the learned model with an implicit probability density that is flexible to characterize the relationships and similarities in the data. This is an interesting area for further research.

- The double descent phenomenon sometimes cannot be observed; see [145] for an example of two-layer neural networks. However, the existence of double descent appears robust in random features models. In this sense, random features may capture certain essential aspects of the mechanism of the double descent phenomenon. Current theoretical results, such as those in [135], may be extended to a more general setting with less restricted assumptions on the data distribution. Importantly, a line of work in [112], [124] points out that the risk in the double descent is not just a function of the number of features s but also depends on the number of epochs, and that the bias and variance may show different tendencies. Understanding these more delicate phenomena requires further investigation and refined analysis.
- There exist significant gaps between the random features model and practical neural networks, both in theory and empirically. Even for fitting simple quadratic or mixture models, the random features model cannot achieve a zero error with a finite number of neurons in general, while NTK and fully trained networks can [121]. Numerical experiments indicate that the prediction performance of NTK and CNTK may significantly degrade if the random features are generated from practically sized nets [24].
- In the standard setting, random Fourier features, QMC, and quadrature based rules often require $s = \Omega(\exp(d))$ features to achieve an ϵ approximation error. In the over-parameterized regime, this exponential dependence implies that the random features model needs exponential time to approximate/learn the target function [140]. This is actually a common problem in shallow networks (those with a single hidden layer), which require exponentially neurons in terms of d to represent a monomial function [146], [147]. Hence, a more refined analysis is needed to explain the polynomial-time learnability of deep neural networks observed in practice.
- Despite the limitations of existing theory, random features models are still useful for understanding and improving DNNs. For example, understanding the equivalence between the random features model and weight pruning in the Lottery Ticket Hypothesis [22], may be promising future directions.

We hope that this survey will stimulate further research on the above open problems.

APPENDIX A CLASSIFICATION RESULTS FOR THE GAUSSIAN KERNEL

Here we present the comparison between several random features based algorithms on the remaining eight classification datasets; see Figures 10 and 11, respectively.

REFERENCES

- [1] Bernhard Schölkopf and Alexander J. Smola, *Learning with kernels: support vector machines, regularization, optimization, and beyond*, MIT Press, 2003.

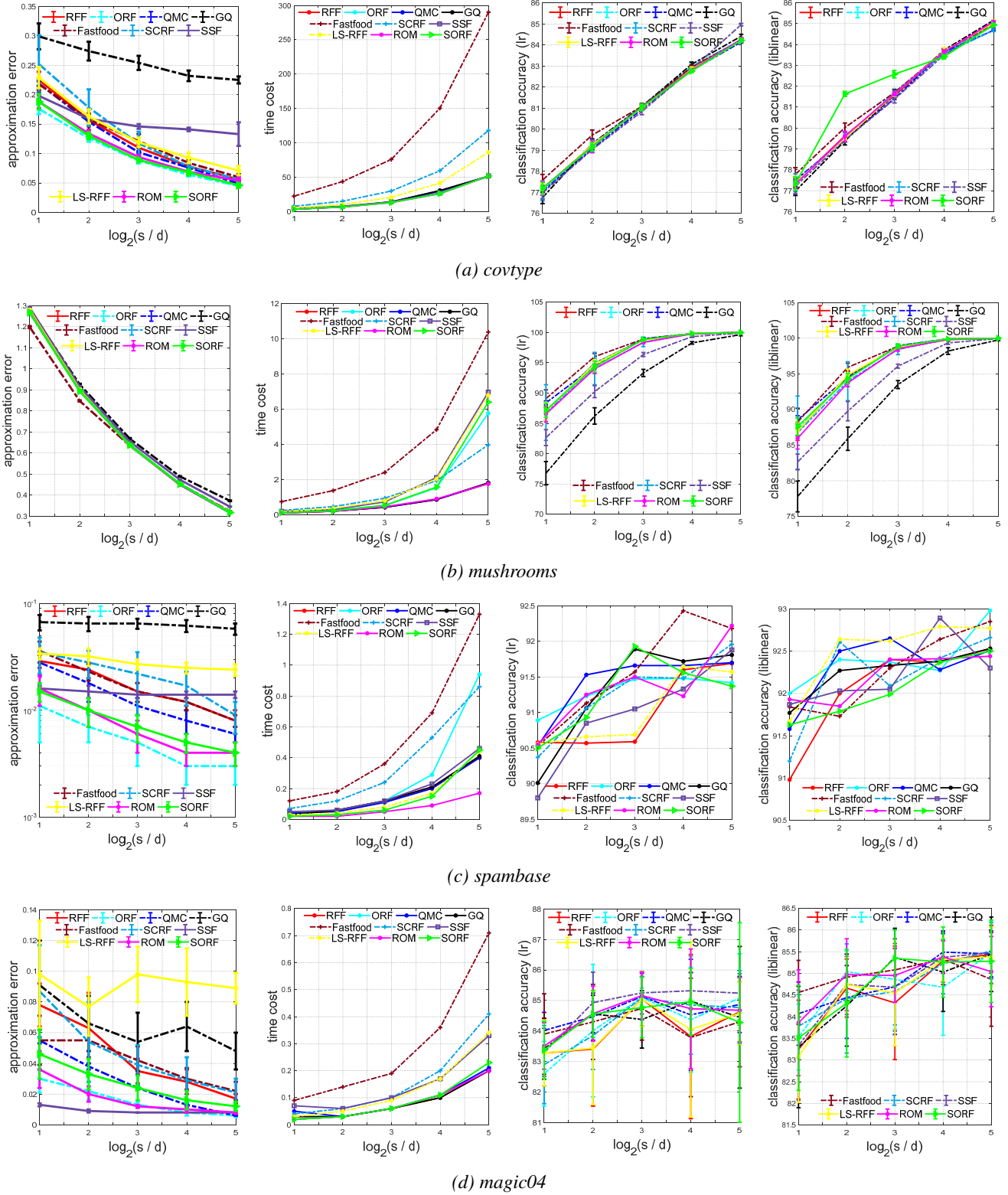


Figure 10. Results of various algorithms for the Gaussian kernel on the *covtype*, *mushrooms*, *spambase*, *magic04* datasets.

- [2] Johan A.K. Suykens, Tony Van Gestel, Jos De Brabanter, Bart De Moor, and Joos Vandewalle, *Least Squares Support Vector Machines*, World Scientific, 2002.
- [3] Mehran Kafai and Kave Eshghi, “CROification: accurate kernel classification with the efficiency of sparse linear SVM,” *IEEE Transactions on Pattern Analysis and Machine Intelligence*, vol. 41, no. 1, pp. 34–48, 2019.
- [4] Ji Zhu and Trevor Hastie, “Kernel logistic regression and the import

- vector machine,” *Journal of Computational and Graphical Statistics*, vol. 14, no. 1, pp. 185–205, 2002.
- [5] Harris Drucker, Christopher J.C. Burges, Linda Kaufman, Alex J. Smola, and Vladimir Vapnik, “Support vector regression machines,” in *Proceedings of Advances in Neural Information Processing Systems*, 1997, pp. 155–161.
- [6] Sebastian Mika, Bernhard Schölkopf, Alex J. Smola, Klaus-Robert Müller, Matthias Scholz, and Gunnar Rätsch, “Kernel PCA and de-

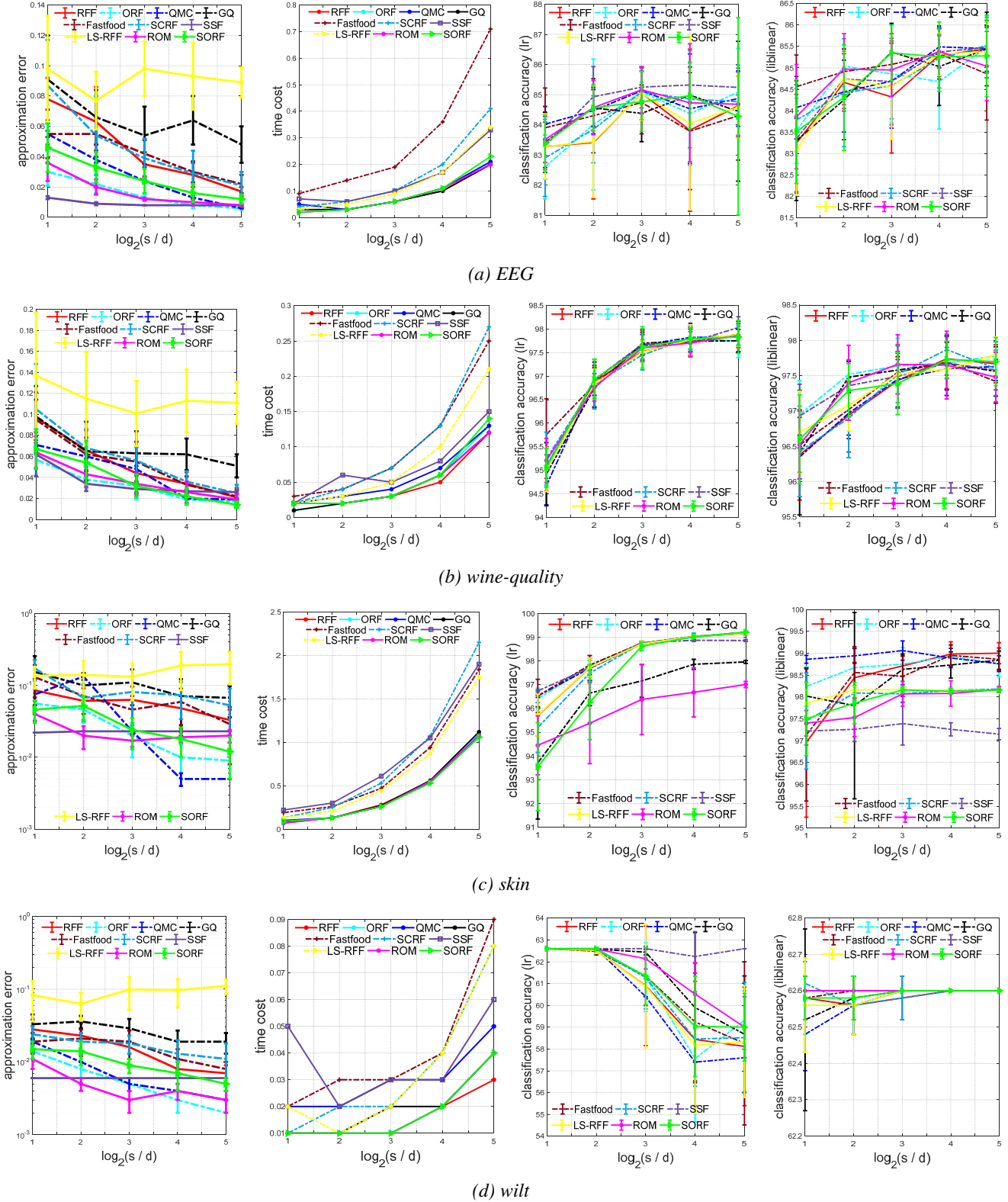


Figure 11. Results of various algorithms for the Gaussian kernel on the *EEG*, *wine-quality*, *skin*, *wilt* datasets.

noising in feature spaces,” in *Proceedings of Advances in Neural Information Processing Systems*, 1999, pp. 536–542.

[7] Inderjit S Dhillon, Yuqiang Guan, and Brian Kulis, “Kernel k-means: spectral clustering and normalized cuts,” in *Proceedings of ACM SIGKDD international conference on Knowledge discovery and data mining*. ACM, 2004, pp. 551–556.

[8] Cho-Jui Hsieh, Si Si, and Inderjit Dhillon, “A divide-and-conquer solver for kernel support vector machines,” in *Proceedings of the International Conference on Machine Learning*, 2014, pp. 566–574.

[9] Yuchen Zhang, John Duchi, and Martin Wainwright, “Divide and conquer kernel ridge regression,” in *Proceedings of Conference on Learning Theory*, 2013, pp. 592–617.

[10] Alex J. Smola and Bernhard Schölkopf, “Sparse greedy matrix approximation for machine learning,” in *Proceedings of the International*

Conference on Machine Learning, 2000, pp. 911–918.

[11] Christopher K.I. Williams and Matthias Seeger, “Using the Nyström method to speed up kernel machines,” in *Proceedings of Advances in Neural Information Processing Systems*, 2001, pp. 682–688.

[12] Ali Rahimi and Benjamin Recht, “Random features for large-scale kernel machines,” in *Proceedings of Advances in Neural Information Processing Systems*, 2007, pp. 1177–1184.

[13] Tianbao Yang, Yu Feng Li, Mehrdad Mahdavi, Rong Jin, and Zhi Hua Zhou, “Nyström method vs random Fourier features: a theoretical and empirical comparison,” in *Proceedings of Advances in Neural Information Processing Systems*, 2012, pp. 476–484.

[14] Jian Zhang, Avner May, Tri Dao, and Christopher Re, “Low-precision random Fourier features for memory-constrained kernel approximation,” in *Proceedings of the 22nd International Conference on Artificial Intelligence and Statistics*, 2019, pp. 1264–1274.

[15] Yitong Sun, Anna Gilbert, and Ambuj Tewari, “But how does it work in theory? Linear SVM with random features,” in *Proceedings of Advances in Neural Information Processing Systems*, 2018, pp. 3383–3392.

[16] Zhu Li, Jean-Francois Ton, Dino Oglic, and Dino Sejdinovic, “Towards a unified analysis of random Fourier features,” in *Proceedings of the 36th International Conference on Machine Learning*, 2019, pp. 3905–3914.

[17] Bo Xie, Yingyu Liang, and Le Song, “Scale up nonlinear component analysis with doubly stochastic gradients,” in *Proceedings of Advances in Neural Information Processing Systems*, 2015, pp. 2341–2349.

[18] David Lopez-Paz, Suvrit Sra, Alex J. Smola, Zoubin Ghahramani, and Bernhard Schölkopf, “Randomized nonlinear component analysis,” in *Proceedings of the International Conference on Machine Learning*, 2014, pp. 1359–1367.

[19] Chiyuan Zhang, Samy Bengio, Moritz Hardt, Benjamin Recht, and Oriol Vinyals, “Understanding deep learning requires rethinking generalization,” *arXiv preprint arXiv:1611.03530*, 2016.

[20] Mikhail Belkin, Daniel Hsu, Siyuan Ma, and Soumik Mandal, “Reconciling modern machine-learning practice and the classical bias-variance trade-off,” *Proceedings of the National Academy of Sciences*, vol. 116, no. 32, pp. 15849–15854, 2019.

[21] Arthur Jacot, Franck Gabriel, and Clément Hongler, “Neural tangent kernel: Convergence and generalization in neural networks,” in *Advances in neural information processing systems*, 2018, pp. 8571–8580.

[22] Eran Malach, Gilad Yehudai, Shai Shalev-Shwartz, and Ohad Shamir, “Proving the lottery ticket hypothesis: Pruning is all you need,” *arXiv preprint arXiv:2002.00585*, 2020.

[23] Yuan Cao and Quanquan Gu, “Generalization bounds of stochastic gradient descent for wide and deep neural networks,” in *Proceedings of Advances in Neural Information Processing Systems*, 2019, pp. 10835–10845.

[24] Sanjeev Arora, Simon S. Du, Wei Hu, Zhiyuan Li, Russ R. Salakhutdinov, and Ruosong Wang, “On exact computation with an infinitely wide neural net,” in *Proceedings of Advances in Neural Information Processing Systems*, 2019, pp. 8139–8148.

[25] Sanjeev Arora, Simon Du, Wei Hu, Zhiyuan Li, and Ruosong Wang, “Fine-grained analysis of optimization and generalization for overparameterized two-layer neural networks,” in *Proceedings of International Conference on Machine Learning*, 2019, pp. 322–332.

[26] Ziwei Ji and Matus Telgarsky, “Polylogarithmic width suffices for gradient descent to achieve arbitrarily small test error with shallow relu networks,” in *Proceedings of International Conference on Learning Representations*, 2020, pp. 1–8.

[27] Ali Rahimi and Benjamin Recht, “Weighted sums of random kitchen sinks: Replacing minimization with randomization in learning,” in *Proceedings of Advances in neural information processing systems*, 2009, pp. 1313–1320.

[28] Fuxin Li, Catalin Ionescu, and Cristian Sminchisescu, “Random Fourier approximations for skewed multiplicative histogram kernels,” in *Proceedings of Joint Pattern Recognition Symposium*. Springer, 2010, pp. 262–271.

[29] Purushottam Kar and Harish Karnick, “Random feature maps for dot product kernels,” in *Proceedings of the International Conference on Artificial Intelligence and Statistics*, 2012, pp. 583–591.

[30] Andrea Vedaldi and Andrew Zisserman, “Efficient additive kernels via explicit feature maps,” *IEEE Transactions on Pattern Analysis and Machine Intelligence*, vol. 34, no. 3, pp. 480–492, 2012.

[31] Quoc Le, Tamás Sarlós, and Alex J. Smola, “FastFood—approximating kernel expansions in loglinear time,” in *Proceedings of the International Conference on Machine Learning*, 2013, pp. 1–9.

[32] Jiyan Yang, Vikas Sindhwani, Haim Avron, and Michael Mahoney, “Quasi-Monte Carlo feature maps for shift-invariant kernels,” in *Proceedings of the International Conference on Machine Learning*, 2014, pp. 485–493.

[33] Bo Dai, Bo Xie, Niao He, Yingyu Liang, Anant Raj, Maria-Florina F Balcan, and Le Song, “Scalable kernel methods via doubly stochastic gradients,” in *Proceedings of Advances in Neural Information Processing Systems*, 2014, pp. 3041–3049.

[34] Jeffrey Pennington, Felix Xinnan X. Yu, and Sanjiv Kumar, “Spherical random features for polynomial kernels,” in *Proceedings of Advances in Neural Information Processing Systems*, 2015, pp. 1846–1854.

[35] Chang Feng, Qinghua Hu, and Shizhong Liao, “Random feature mapping with signed circulant matrix projection,” in *Proceedings of the Twenty-Fourth International Joint Conference on Artificial Intelligence*, 2015.

[36] Felix Xinnan Yu, Ananda Theertha Suresh, Krzysztof Choromanski, Daniel Holtmannrue, and Sanjiv Kumar, “Orthogonal random features,” in *Proceedings of Advances in Neural Information Processing Systems*, 2016, pp. 1975–1983.

[37] Krzysztof Choromanski and Vikas Sindhwani, “Recycling randomness with structure for sublinear time kernel expansions,” in *Proceedings of International Conference on Machine Learning*, 2016, pp. 2502–2510.

[38] Weiwei Shen, Zhihui Yang, and Jun Wang, “Random features for shift-invariant kernels with moment matching,” in *Proceedings of the Thirty-First AAAI Conference on Artificial Intelligence*, 2017.

[39] Yueming Lyu, “Spherical structured feature maps for kernel approximation,” in *Proceedings of the 34th International Conference on Machine Learning*. JMLR.org, 2017, pp. 2256–2264.

[40] Tri Dao, Christopher M. De Sa, and Christopher Ré, “Gaussian quadrature for kernel features,” in *Proceedings of Advances in neural information processing systems*, 2017, pp. 6107–6117.

[41] Marina Munkhoeva, Yermek Kapushev, Evgeny Burnaev, and Ivan Oseledets, “Quadrature-based features for kernel approximation,” in *Proceedings of Advances in Neural Information Processing Systems*, 2018, pp. 9147–9156.

[42] Shahin Shahrampour, Ahmad Beirami, and Vahid Tarokh, “On data-dependent random features for improved generalization in supervised learning,” in *Proceedings of Thirty-Second AAAI Conference on Artificial Intelligence*, 2018, pp. 4026–4033.

[43] Raj Agrawal, Trevor Campbell, Jonathan Huggins, and Tamara Broderick, “Data-dependent compression of random features for large-scale kernel approximation,” in *Proceedings of the 22nd International Conference on Artificial Intelligence and Statistics*, 2019, pp. 1822–1831.

[44] Fanghui Liu, Xiaolin Huang, Yudong Chen, Jie Yang, and Johan A.K. Suykens, “Random Fourier features via fast surrogate leverage weighted sampling,” in *Proceedings of Thirty-Fourth AAAI Conference on Artificial Intelligence*, 2020, pp. 4844–4851.

[45] Dougal J. Sutherland and Jeff Schneider, “On the error of random Fourier features,” in *Proceedings of the Thirty-First Conference on Uncertainty in Artificial Intelligence*, 2015, pp. 862–871.

[46] Bharath K. Sriperumbudur and Zoltán Szabó, “Optimal rates for random Fourier features,” in *Proceedings of Advances in Neural Information Processing Systems*, 2015, pp. 1144–1152.

[47] Jean Honorio and Yu-Jun Li, “The error probability of random Fourier features is dimensionality independent,” *arXiv preprint arXiv:1710.09953*, 2017.

[48] Haim Avron, Michael Kapralov, Cameron Musco, Christopher Musco, Ameya Velingker, and Amir Zandieh, “Random Fourier features for kernel ridge regression: Approximation bounds and statistical guarantees,” in *Proceedings of the 34th International Conference on Machine Learning-Volume 70*, 2017, pp. 253–262.

[49] Francis Bach, “On the equivalence between kernel quadrature rules and random feature expansions,” *Journal of Machine Learning Research*, vol. 18, no. 1, pp. 714–751, 2017.

[50] Alessandro Rudi and Lorenzo Rosasco, “Generalization properties of learning with random features,” in *Proceedings of Advances in Neural Information Processing Systems*, 2017, pp. 3215–3225.

[51] Ryoma Sato, Makoto Yamada, and Hisashi Kashima, “Random features strengthen graph neural networks,” *arXiv preprint arXiv:2002.03155*, 2020.

[52] Haim Avron, Vikas Sindhwani, Jiyan Yang, and Michael W. Mahoney, “Quasi-Monte Carlo feature maps for shift-invariant kernels,” *Journal of Machine Learning Research*, vol. 17, no. 1, pp. 4096–4133, 2016.

[53] Aman Sinha and John C. Duchi, “Learning kernels with random features,” in *Proceedings of Advances in Neural Information Processing Systems*, 2016, pp. 1298–1306.

[54] Alaa Saade, Francesco Caltagirone, Igor Carron, Laurent Daudet, Angélique Drémeau, Sylvain Gigan, and Florent Krzakala, “Random projections through multiple optical scattering: Approximating kernels at

the speed of light,” in *2016 IEEE International Conference on Acoustics, Speech and Signal Processing (ICASSP)*. IEEE, 2016, pp. 6215–6219.

[55] Ruben Ohana, Jonas Wacker, Jonathan Dong, Sébastien Marmin, Florent Krzakala, Maurizio Filippone, and Laurent Daudet, “Kernel computations from large-scale random features obtained by optical processing units,” *arXiv preprint arXiv:1910.09880*, 2019.

[56] Youngmin Cho and Lawrence K Saul, “Kernel methods for deep learning,” in *Advances in Neural Information Processing Systems*, 2009, pp. 342–350.

[57] Subhransu Maji, Alexander C Berg, and Jitendra Malik, “Efficient classification for additive kernel SVMs,” *IEEE Transactions on Pattern Analysis and Machine Intelligence*, vol. 35, no. 1, pp. 66–77, 2013.

[58] Fanghui Liu, Xiaolin Huang, Lei Shi, Jie Yang, and Johan A.K. Suykens, “A double-variational Bayesian framework in random Fourier features for indefinite kernels,” *IEEE Transactions on Neural Networks and Learning Systems*, 2019.

[59] Salomon Bochner, *Harmonic Analysis and the Theory of Probability*, Courier Corporation, 2005.

[60] Marc G. Genton, “Classes of kernels for machine learning: a statistics perspective,” *Journal of machine learning research*, vol. 2, no. Dec, pp. 299–312, 2001.

[61] Sami Remes, Markus Heinonen, and Samuel Kaski, “Non-stationary spectral kernels,” in *Proceedings of Advances in Neural Information Processing Systems*, 2017, pp. 4642–4651.

[62] Brian Bullins, Cyril Zhang, and Yi Zhang, “Not-so-random features,” in *Proceedings of International Conference on Learning Representations*, 2018.

[63] I. J. Schoenberg, “Positive definite functions on spheres,” *Duke Mathematical Journal*, vol. 9, no. 1, pp. 96–108, 1942.

[64] Ping Li, “Linearized GMM kernels and normalized random Fourier features,” in *Proceedings of the 23rd ACM SIGKDD International Conference on Knowledge Discovery and Data Mining*, 2017, pp. 315–324.

[65] Krzysztof M. Choromanski, Mark Rowland, and Adrian Weller, “The unreasonable effectiveness of structured random orthogonal embeddings,” in *Proceedings of Advances in Neural Information Processing Systems*, 2017, pp. 219–228.

[66] Wei-Cheng Chang, Chun-Liang Li, Yiming Yang, and Barnabás Póczos, “Data-driven random Fourier features using Stein effect,” in *Proceedings of the 26th International Joint Conference on Artificial Intelligence*, 2017, pp. 1497–1503.

[67] Chun-Liang Li, Wei-Cheng Chang, Youssef Mroueh, Yiming Yang, and Barnabás Póczos, “Implicit kernel learning,” in *Proceedings of the 22nd International Conference on Artificial Intelligence and Statistics*, 2019, pp. 2007–2016.

[68] Felix X. Yu, Sanjiv Kumar, Henry Rowley, and Shih Fu Chang, “Compact nonlinear maps and circulant extensions,” *arXiv preprint arXiv:1503.03893*, 2015.

[69] Andrew Gordon Wilson and Ryan Prescott Adams, “Gaussian process kernels for pattern discovery and extrapolation,” in *Proceedings of the International Conference on Machine Learning*, 2013, pp. 1067–1075.

[70] Zichao Yang, Andrew Wilson, Alex J. Smola, and Le Song, “À la carte–learning fast kernels,” in *Proceedings of Artificial Intelligence and Statistics*, 2015, pp. 1098–1106.

[71] Zheyang Shen, Markus Heinonen, and Samuel Kaski, “Harmonizable mixture kernels with variational Fourier features,” in *Proceedings of International Conference on Artificial Intelligence and Statistics*. PMLR, 2019.

[72] Junier B. Oliva, Avinava Dubey, Andrew G. Wilson, Barnabás Póczos, Jeff Schneider, and Eric P. Xing, “Bayesian nonparametric kernel learning,” in *Proceedings of the International Conference on Artificial Intelligence and Statistics*, 2016, pp. 1078–1086.

[73] Mariusz Bojarski, Anna Choromanska, Krzysztof Choromanski, Francois Fagan, Cedric Gouy-Pailler, Anne Morvan, Nouri Sakr, Tamas Sarlos, and Jamal Atif, “Structured adaptive and random spinners for fast machine learning computations,” in *Proceedings of Artificial Intelligence and Statistics*, 2017, pp. 1020–1029.

[74] Xiang Li, Bin Gu, Shuang Ao, Huaimin Wang, and Charles X. Ling, “Triply stochastic gradients on multiple kernel learning,” in *Proceedings of the Conference on Uncertainty in Artificial Intelligence*, 2017, pp. 1–9.

[75] Krzysztof Choromanski, Mark Rowland, Wenyu Chen, and Adrian Weller, “Unifying orthogonal Monte Carlo methods,” in *Proceedings of International Conference on Machine Learning*, 2019, pp. 1203–1212.

[76] Krzysztof Choromanski, Mark Rowland, Tamás Sarlós, Vikas Sindhwani, Richard Turner, and Adrian Weller, “The geometry of random features,” in *Proceedings of International Conference on Artificial Intelligence and Statistics*, 2018, pp. 1–9.

[77] Harald Niederreiter, *Random number generation and quasi-Monte Carlo methods*, vol. 63, SIAM, 1992.

[78] Johann S. Brauchart and Peter J. Grabner, “Distributing many points on spheres: minimal energy and designs,” *Journal of Complexity*, vol. 31, no. 3, pp. 293–326, 2015.

[79] Gwynne Evans, *Practical numerical integration*, Wiley New York, 1993.

[80] Alan Genz and John Monahan, “Stochastic integration rules for infinite regions,” *SIAM Journal on Scientific Computing*, vol. 19, no. 2, pp. 426–439, 1998.

[81] Florian Heiss and Viktor Winschel, “Likelihood approximation by numerical integration on sparse grids,” *Journal of Econometrics*, vol. 144, no. 1, pp. 62–80, 2008.

[82] Yinsong Wang and Shahin Shahrampour, “A general scoring rule for randomized kernel approximation with application to canonical correlation analysis,” *arXiv preprint arXiv:1910.05384*, 2019.

[83] Francis Bach, “Sharp analysis of low-rank kernel matrix approximations,” in *Proceedings of Conference on Learning Theory*, 2013, pp. 185–209.

[84] Hayata Yamasaki, Sathyawageeswar Subramanian, Sho Sonoda, and Masato Koashi, “Fast quantum algorithm for learning with optimized random features,” *arXiv preprint arXiv:2004.10756*, 2020.

[85] Corinna Cortes, Mehryar Mohri, and Afshin Rostamizadeh, “Two-stage learning kernel algorithms,” in *Proceedings of the International Conference on Machine Learning*, 2010, pp. 239–246.

[86] Trevor Campbell and Tamara Broderick, “Bayesian coreset construction via greedy iterative geodesic ascent,” in *Proceedings of International Conference on Machine Learning*, 2018, pp. 698–706.

[87] Trevor Campbell and Tamara Broderick, “Automated scalable Bayesian inference via Hilbert coresets,” *The Journal of Machine Learning Research*, vol. 20, no. 1, pp. 551–588, 2019.

[88] Raffay Hamid, Ying Xiao, Alex Gittens, and Dennis Decoste, “Compact random feature maps,” in *Proceedings of the International Conference on Machine Learning*, 2014, pp. 19–27.

[89] Jean-Francois Ton, Seth Flaxman, Dino Sejdinovic, and Samir Bhatt, “Spatial mapping with Gaussian processes and nonstationary Fourier features,” *Spatial statistics*, vol. 28, pp. 59–78, 2018.

[90] Ninh Pham and Rasmus Pagh, “Fast and scalable polynomial kernels via explicit feature maps,” in *Proceedings of ACM International Conference on Knowledge Discovery and Data Mining*, 2013, pp. 239–247.

[91] Kilian Weinberger, Anirban Dasgupta, John Langford, Alex J. Smola, and Josh Attenberg, “Feature hashing for large scale multitask learning,” in *Proceedings of the 26th International Conference on Machine Learning*, 2009, pp. 1113–1120.

[92] Subhransu Maji and Alexander C. Berg, “Max-margin additive classifiers for detection,” in *Proceedings of IEEE International Conference on Computer Vision*. IEEE, 2009, pp. 40–47.

[93] Ali Rahimi and Benjamin Recht, “Uniform approximation of functions with random bases,” in *Proceedings of the Annual Allerton Conference on Communication, Control, and Computing*. IEEE, 2008, pp. 555–561.

[94] Ingo Steinwart and Christmann Andreas, *Support Vector Machines*, Springer Science and Business Media, 2008.

[95] Gilles Blanchard and Nicole Krämer, “Optimal learning rates for kernel conjugate gradient regression,” in *Proceedings of Advances in Neural Information Processing Systems*, 2010, pp. 226–234.

[96] Enayat Ullah, Poorya Mianjy, Teodor Vanislavov Marinov, and Raman Arora, “Streaming kernel PCA with $\tilde{O}(\sqrt{n})$ random features,” in *Proceedings of Advances in Neural Information Processing Systems*, 2018, pp. 7311–7321.

[97] Felipe Cucker and Dingxuan Zhou, *Learning theory: an approximation theory viewpoint*, vol. 24, Cambridge University Press, 2007.

[98] Andrea Caponnetto and Ernesto De Vito, “Optimal rates for the regularized least-squares algorithm,” *Foundations of Computational Mathematics*, vol. 7, no. 3, pp. 331–368, 2007.

[99] Zheng-Chu Guo and Lei Shi, “Optimal rates for coefficient-based regularized regression,” *Applied and Computational Harmonic Analysis*, vol. 47, no. 3, pp. 662–701, 2019.

[100] Shao-Bo Lin, Xin Guo, and Ding-Xuan Zhou, “Distributed learning with regularized least squares,” *Journal of Machine Learning Research*, vol. 18, no. 1, pp. 3202–3232, 2017.

[101] Vladimir Koltchinskii, *Oracle Inequalities in Empirical Risk Minimization and Sparse Recovery Problems*, vol. 2033, Springer Science & Business Media, 2011.

[102] Luigi Carratino, Alessandro Rudi, and Lorenzo Rosasco, “Learning with SGD and random features,” in *Proceedings of Advances in Neural Information Processing Systems*, 2018, pp. 10212–10223.

[103] Ingo Steinwart and Clint Scovel, “Fast rates for support vector machines using Gaussian kernels,” *Annals of Statistics*, vol. 35, no. 2, pp. 575–607, 2007.

[104] Shusen Wang, “Simple and almost assumption-free out-of-sample bound for random feature mapping,” *arXiv preprint arXiv:1909.11207*, 2019.

[105] Mina Ghahami, Daniel J. Perry, and Jeff Phillips, “Streaming kernel principal component analysis,” in *Proceedings of Artificial intelligence and statistics*, 2016, pp. 1365–1374.

[106] Bharath Sriperumbudur and Nicholas Sterge, “Statistical consistency of kernel PCA with random features,” *arXiv preprint arXiv:1706.06296*, 2017.

[107] Rong-En Fan, Kai-Wei Chang, Cho-Jui Hsieh, Xiang-Rui Wang, and Chih-Jen Lin, “LIBLINEAR: a library for large linear classification,” *Journal of Machine Learning Research*, vol. 9, pp. 1871–1874, 2008.

[108] Yann Lecun, Leon Bottou, Yoshua Bengio, and Patrick Haffner, “Gradient-based learning applied to document recognition,” *Proceedings of the IEEE*, vol. 86, no. 11, pp. 2278–2324, 1998.

[109] Alex Krizhevsky and Geoffrey Hinton, “Learning multiple layers of features from tiny images,” *Technical report, University of Toronto*, 2009.

[110] Sergey Ioffe and Christian Szegedy, “Batch normalization: accelerating deep network training by reducing internal covariate shift,” in *Proceedings of the International Conference on Machine Learning*, 2015, pp. 448–456.

[111] Jia Deng, Wei Dong, Richard Socher, Li Jia Li, Kai Li, and Fei Fei Li, “Imagenet: A large-scale hierarchical image database,” in *Proceedings of the IEEE Conference on Computer Vision and Pattern Recognition*, 2009, pp. 248–255.

[112] Preetum Nakkiran, Gal Kaplun, Yamini Bansal, Tristan Yang, Boaz Barak, and Ilya Sutskever, “Deep double descent: Where bigger models and more data hurt,” in *Proceedings of International Conference on Learning Representations*, 2019.

[113] Mikhail Belkin, Siyuan Ma, and Soumik Mandal, “To understand deep learning we need to understand kernel learning,” in *Proceedings of International Conference on Machine Learning*, 2018, pp. 541–549.

[114] Christopher K.I. Williams, “Computing with infinite networks,” in *Proceedings of Advances in Neural Information Processing Systems*, 1997, pp. 295–301.

[115] Jaehoon Lee, Yasaman Bahri, Roman Novak, Samuel S Schoenholz, Jeffrey Pennington, and Jascha Sohl-Dickstein, “Deep neural networks as Gaussian Processes,” in *Proceedings of International Conference on Learning Representations*, 2018.

[116] Amit Daniely, “SGD learns the conjugate kernel class of the network,” in *Proceedings of Advances in Neural Information Processing Systems*, 2017, pp. 2422–2430.

[117] Amit Daniely, Roy Frostig, and Yoram Singer, “Toward deeper understanding of neural networks: The power of initialization and a dual view on expressivity,” in *Proceedings of Advances In Neural Information Processing Systems*, 2016, pp. 2253–2261.

[118] Siamak Mehrkanoon and Johan A.K. Suykens, “Deep hybrid neural-kernel networks using random Fourier features,” *Neurocomputing*, vol. 298, pp. 46–54, 2018.

[119] Jaehoon Lee, Lechao Xiao, Samuel Schoenholz, Yasaman Bahri, Roman Novak, Jascha Sohl-Dickstein, and Jeffrey Pennington, “Wide neural networks of any depth evolve as linear models under gradient descent,” in *Proceedings of Advances in Neural Information Processing Systems*, 2019, pp. 8570–8581.

[120] Behrooz Ghorbani, Song Mei, Theodor Misiakiewicz, and Andrea Montanari, “Linearized two-layers neural networks in high dimension,” *arXiv preprint arXiv:1904.12191*, 2019.

[121] Behrooz Ghorbani, Song Mei, Theodor Misiakiewicz, and Andrea Montanari, “Limitations of lazy training of two-layers neural network,” in *Proceedings of Advances in Neural Information Processing Systems*, 2019, pp. 9108–9118.

[122] Kaiming He, Xiangyu Zhang, Shaoqing Ren, and Jian Sun, “Identity mappings in deep residual networks,” in *Proceedings of European conference on computer vision*. Springer, 2016, pp. 630–645.

[123] Ashish Vaswani, Noam Shazeer, Niki Parmar, Jakob Uszkoreit, Llion Jones, Aidan N Gomez, Łukasz Kaiser, and Illia Polosukhin, “Attention is all you need,” in *Proceedings of Advances in Neural Information Processing Systems*, 2017, pp. 5998–6008.

[124] Zitong Yang, Yaodong Yu, Chong You, Jacob Steinhardt, and Yi Ma, “Rethinking bias-variance trade-off for generalization of neural networks,” *arXiv preprint arXiv:2002.11328*, 2020.

[125] Tengyuan Liang, Alexander Rakhlin, and Xiyu Zhai, “On the risk of minimum-norm interpolants and restricted lower isometry of kernels,” *arXiv preprint arXiv:1908.10292*, 2019.

[126] Ganesh Kini and Christos Thrampoulidis, “Analytic study of double descent in binary classification: The impact of loss,” *arXiv preprint arXiv:2001.11572*, 2020.

[127] Peter L. Bartlett, Philip M. Long, Gábor Lugosi, and Alexander Tsigler, “Benign overfitting in linear regression,” *Proceedings of the National Academy of Sciences*, 2020.

[128] Tomaso Poggio, Gil Kur, and Andrzej Banburski, “Double descent in the condition number,” *arXiv preprint arXiv:1912.06190*, 2019.

[129] Terence Tao, *Topics in random matrix theory*, American Mathematical Society, 2012.

[130] Cosme Louart, Zhenyu Liao, and Romain Couillet, “A random matrix approach to neural networks,” *The Annals of Applied Probability*, vol. 28, no. 2, pp. 1190–1248, 2018.

[131] Zhenyu Liao and Romain Couillet, “On the spectrum of random features maps of high dimensional data,” in *Proceedings of the International Conference on Machine Learning*, 2018, pp. 3063–3071.

[132] Trevor Hastie, Andrea Montanari, Saharon Rosset, and Ryan J. Tibshirani, “Surprises in high-dimensional ridgeless least squares interpolation,” *arXiv preprint arXiv:1903.08560*, 2019.

[133] Preetum Nakkiran, Prayaag Venkat, Sham Kakade, and Tengyu Ma, “Optimal regularization can mitigate double descent,” *arXiv preprint arXiv:2003.01897*, 2020.

[134] Mikhail Belkin, Daniel Hsu, and Ji Xu, “Two models of double descent for weak features,” *arXiv preprint arXiv:1903.07571*, 2019.

[135] Song Mei and Andrea Montanari, “The generalization error of random features regression: Precise asymptotics and double descent curve,” *arXiv preprint arXiv:1908.05355*, 2019.

[136] Andrea Montanari, Feng Ruan, Youngtak Sohn, and Jun Yan, “The generalization error of max-margin linear classifiers: High-dimensional asymptotics in the overparametrized regime,” *arXiv preprint arXiv:1911.01544*, 2019.

[137] Stéphane d’Ascoli, Maria Refinetti, Giulio Biroli, and Florent Krzakala, “Double trouble in double descent: Bias and variance(s) in the lazy regime,” *arXiv preprint arXiv:2003.01054*, 2020.

[138] Wei Hu, Zhiyuan Li, and Dingli Yu, “Simple and effective regularization methods for training on noisily labeled data with generalization guarantee,” in *Proceedings of International Conference on Learning Representations*, 2020, pp. 1–8.

[139] Alberto Bietti and Julien Mairal, “On the inductive bias of neural tangent kernels,” in *Proceedings of Advances in Neural Information Processing Systems*, 2019, pp. 12873–12884.

[140] Gilad Yehudai and Ohad Shamir, “On the power and limitations of random features for understanding neural networks,” in *Proceedings of Advances in Neural Information Processing Systems*, 2019, pp. 6594–6604.

[141] Yitong Sun, Anna Gilbert, and Ambuj Tewari, “On the approximation properties of random ReLU features,” *arXiv preprint arXiv:1810.04374*, 2018.

[142] Jonathan Frankle and Michael Carbin, “The lottery ticket hypothesis: Finding sparse, trainable neural networks,” in *Proceedings of International Conference on Learning Representations*, 2019.

[143] Hengyuan Hu, Rui Peng, Yu-Wing Tai, and Chi-Keung Tang, “Network trimming: A data-driven neuron pruning approach towards efficient deep architectures,” *arXiv preprint arXiv:1607.03250*, 2016.

[144] Mikio L. Braun, “Accurate error bounds for the eigenvalues of the kernel matrix,” *Journal of Machine Learning Research*, vol. 7, no. Nov, pp. 2303–2328, 2006.

[145] Jimmy Ba, Murat A. Erdogdu, Taiji Suzuki, Denny Wu, and Tianzong Zhang, “Generalization of two-layer neural networks: an asymptotic viewpoint,” in *Proceedings of Advances in Neural Information Processing Systems*, 2020, pp. 1–8.

[146] Henry W. Lin, Max Tegmark, and David Rolnick, “Why does deep and cheap learning work so well?,” *Journal of Statistical Physics*, vol. 168, no. 6, pp. 1223–1247, 2017.

[147] David Rolnick and Max Tegmark, “The power of deeper networks for expressing natural functions,” in *Proceedings of International Conference on Learning Representations*, 2018, pp. 1–9.